The effect of UVA irradiation on the DNA damage response in a human keratinocyte cell line

Matthew Eastham

Division of Biomedical and Life Sciences

Faculty of Health and Medicine

Lancaster University

Thesis submitted for the degree of Master of Science by Research

November 2016

Declaration

I declare that this thesis is my own work and has not been submitted in part, or as a whole, for the award of a higher degree of qualification at this university or elsewhere.

Matthew Eastham

Acknowledgements

First of all I would like to express my sincere gratitude to my supervisor Dr. Sarah Allinson for her continuous support during my MSc by research studies, for her patience when things were not going according to plan, for motivating me to continue and for being a source of knowledge and great inspiration. Her guidance helped me in developing as an independent student who is confident in their ability, and for this I will be forever grateful.

Secondly, I would like to thank other members of lab A27 at Lancaster University, in particular Dr. Harriet Steel, who was always made herself available to provide advice and was always prepared to teach me new techniques. Everyone in the lab provided a warm environment and I thank them for their input during weekly lab meetings and for providing stimulating discussions, regardless of the topic at hand.

Last but by no means least, I would like to thank my family and friends, especially my parents who had to cope with during times of stress and fatigue, especially throughout the process of writing up this thesis.

Abbreviations

64PPs	6-4 pyrimidine-pyrimidone photoproducts
8-oxoG	8-Oxoguanine
9-1-1	Rad9-Hus1-Rad1 complex
ATM	Ataxia telangiectasia mutated
ATR	Ataxia telangiectasia and Rad3 related
BER	Base excision repair
CPD	Cyclobutate pyrimidine dimer
DDR	DNA damage response
DMEM	Dulbecco's Modified Eagle's Medium
DSB	Double strand break
EdU	5-ethynyl-2'-deoxyuridine
GG-NER	Global-genomic NER
MRN	Mre11, Rad50 and Nbs1
MTT	3-(4,5-dimethylthiazol-2-yl)2-5-diphenyltetrazolium bromide
NER	Nucleotide excision repair
NHEJ	Non-homologous end joining
PBS	Phosphate buffered saline
PI3K	Phosphoinositide 3-kinase
PIKK	Phosphatidylinositol 3-kinase-related kinase
RPA	Replication protein A
ROS	Reactive oxygen species
SSB	Single strand break
TC-NER	Transcription coupled NER
TLS	Translesion synthesis
UVR	Ultraviolet radiation
XP	Xeroderma Pigmentosum
XTT	(2,3-bis-(2-methoxy-4-nitro-5-sulphophenyl)-2H-tetrazolium-5-carboxanilide)

Contents

List of Figures

List of tables

Abstract

The DNA damage response (DDR) recognises different types of DNA damage and initiates signalling pathways to bring about cell cycle arrest so the appropriate repair mechanisms can be activated, or to bring about cell death when the damage is unrepairable. DNA damage surveillance and repair pathways play an important role in protecting skin cells against the carcinogenic effects of ultraviolet radiation (UVR). In this research project, HaCaTs were used to investigate the direct and indirect effects of UVA irradiation on the DDR. Independent inhibition of ATM and ATR prior to irradiation with 50 kJ m^{-2} UVA caused cell survival to decrease in a dose-dependent manner over that seen where HaCaTs were irradiated in the absence of inhibitor pre-treatment, suggesting the involvement of ATM and ATR in processing UVA-induced lesions. The same observation was not seen when the dosage was increased to 100 kJ m^{-2}. Western blot and immunofluorescence studies found that γH2AX activation peaked between 1 and 4h following irradiation with 100 kJ m^{-2} UVA. Chk2 phosphorylation peaked immediately following UVA irradiation. Inhibition of ATM prior to UVA exposure resulted in a temporal decoupling of H2AX and Chk2 phosphorylation with peak γH2AX activation occurring at a later timepoint whilst p-Chk2 activation was unchanged, implying that UVA-induced Chk2 phosphorylation may not be entirely ATM-dependent. The UVA-induced bystander effect was also investigated. γH2AX activation in bystander cells increased at 48h over that seen at 24h when these cells were co-cultured with UVA-irradiated cells. A dose-dependent UVA-induced bystander response was observed following 1 week co-incubation as determined by clonogenic survival assays, which was not the case at 48h. These data suggest that the rate at which damage signals are released from irradiated cells decreased over time in a dose-dependent manner.

1. Introduction

Genomic integrity is constantly threatened by both exogenous sources, such as ultraviolet radiation, ionising radiation and toxins, and endogenous sources, which primarily consist of oxygen free radicals generated during mitochondrial respiration (Droge, 2002). The importance of maintaining such integrity is highlighted by the fact that the potential genomic alterations, such as DNA mutations or chromosomal rearrangements, are the primary causes of numerous diseases, which include both hereditary disorders and cancer (Sadikovic et al., 2008). Cancer is one of the leading causes of death worldwide and is the collective term used to describe a group of diseases characterised by abnormal, uncontrolled cell growth with the ability for such cells to metastasise and spread to other areas of the body. Thus, eukaryotic cells possess signalling networks that ensure the preservation of genomic integrity by detecting DNA damage and generating signals to bring about their repair. Collectively, these signalling networks make up the DNA damage response, which function to prevent deleterious mutations from occurring (Sulli et al., 2012). The aim of this literature review is to outline the DNA damage response in the context of damage that has been associated with skin cancer, one of the most common cancer types (Dubas and Ingraffea, 2013). It will discuss how ultraviolet radiation contributes to DNA damage, with emphasis on the understudied UVA wavelength region, and how it impacts the DNA damage response.

I. Skin Cancer

Skin cancer is the most common form of human malignancy with its global incidence steadily increasing for the past several decades, particularly amongst light-skinned populations (Dubas and Ingraffea, 2013). This steady increase has been attributed to a number of factors such as cheaper international travel, increasingly relaxed attitudes towards sunbathing, increased recreational use of sunbeds and ozone layer depletion (Wehner et al., 2014). All these factors share in common that they contribute towards increased exposure to ultraviolet radiation (UVR). The major source of UVR is solar radiation. Due to the earth's atmosphere absorbing the UVC waveband and most of the UVB waveband, UVR reaching the earth's surface consists of 90-95% UVA (315-400 nm) with the rest being UVB (280-315 nm).

An increased desire to acquire tans for fashion and cosmetic purposes has contributed to the development of a large artificial tanning industry, particularly in

western countries where a significant proportion of residents have pale skin. Tanning beds are sources of both UVB and UVA. Radiation within the whole UV spectrum is associated with skin cancer and as a result tanning beds increase the risk of both nonmelanoma skin cancer and cutaneous malignant melanoma (Nilsen et al., 2016). Sunbeds can differ in the ratio of UVB to UVA they emit. In the past, the majority of sunbeds emitted less UVB and therefore more UVA, as UVB-rich sunbeds caused intermittent overexposures and risk of acute sunburns (WWW, WHO | Sunbeds). Solar radiation exposure has been found to result in a specific mutation fingerprint due to pyrimidine dimer generation in DNA, which was originally attributed to UVB. However, exposure to UVA alone generated the same mutation fingerprint in the skin of mice (Ikehata et al., 2008). Additionally, the same mutation spectra generated by UVB (C to T transition mutations following pyrimidine dimer generation) in the *TP53* gene in both the skin tumours of hairless mice and in humans were found to be induced by UVA (Runger and Kappes, 2008) (Agar et al., 2004). As such, in 2009 the full spectrum of UVR was categorised as carcinogenic to humans (El Ghissassi et al., 2009). Consequently, many sunbed manufacturers are returning to producing sunbeds with a UVR output similar to natural sunlight (WWW, WHO | Sunbeds). However, a relatively recent study revealed that many sunbeds in the UK emit UVR levels that exceed British and European safety limits (Tierney et al., 2015, Tierney et al., 2013).

Skin cancers are divided based on the skin cell type from which they originate, with strong epidemiological and molecular evidence between each type and UVR exposure. Non-melanoma skin cancers (NMSC), of which basal cell carcinoma (BCC) and squamous cell carcinoma (SCC) are the two most common subtypes, arise from keratinocytes. Together these NMSCs make up the majority of all skin cancers. Basal cell carcinomas, which originate from keratinocytes located within the basal layer of the epidermis, make up 80-85% of all NMSCs and are the most common form of malignancy amongst light-skinned populations. BCCs rarely invade other organs, whereas SCCs (5-10% of NMSCs), which arise from squamous epithelial cells within the skin's epidermis, are more likely to metastasise and lead to death. Although mortality rates are low, NMSCs contribute towards physical and psychological consequences, particularly due to most NMSCs occurring on highly visible areas, such as the face and neck (Narayanan et al., 2010) (Lomas et al., 2012).

On the other hand, cutaneous malignant melanoma, which arises from melanocytes, account for the majority of skin cancer deaths, 55,000 deaths per year, despite

making up less than 10% of skin cancer cases (Ferlay et al., 2015). Cutaneous malignant melanoma incidence rates are highest within regions consisting of mainly light-skinned populations. Melanocytes are the melanin-producing cells, which are responsible for pigmentation and photoprotection. Two main types of melanin pigments are produced, brown/black eumelanin, which is photoprotective as it provides UVR attenuation, and red pheomelanin (Lo and Fisher, 2014). The importance of melanin in UVR protection is highlighted by the genetic disorder albinism, whereby patients have hypopigmentation of the skin, hair and eyes due to the loss of cutaneous melanin pigment production and as a result have a predisposition to the harmful effects of UVR such as photophobia, extreme sun sensitivity and increased risk of skin cancer development (Witkop, 1989). In contrast, melanin, particularly pheomelanin is also known to act as a photosensitiser that generates active oxygen species upon UV irradiation.

II. Ultraviolet radiation

The full spectrum of UVR can be divided into three wavebands: UVA (315-400 nm); UVB (280-315 nm) and UVC (200-280 nm) (Figure 1.1). Each waveband of UVR has been demonstrated as being able to contribute towards DNA damage. Solar radiation is the main source of UVR to which humans are exposed. UVC does not contribute to solar photocarcinogenesis as the earth's atmosphere can completely absorb the waveband. The terrestrial UVR humans are exposed to vary slightly depending on geo-orbital and environmental factors, such as latitude, season, time of day and ozone layer thickness (Battie et al., 2014). The atmosphere can efficiently attenuate the majority of UVB, whilst all the UVA component of solar radiation is able to penetrate the atmosphere. Consequently, UVR reaching the earth's surface consists of approximately 90-95% UVA with UVB making up the remainder, (El Ghissassi et al., 2009). Due to this, another factor thought to be contributing towards increased incidences or NMSC and CMM is ozone layer depletion. It is well established that various industrial halogenated chemicals including chlorofluorocarbons (CFCs) and methyl bromide, while inert at ambient temperatures on Earth's surface, react with ozone in the extremely cold polar stratosphere, contributing towards its depletion, particularly in late winter and early spring (WWW, WHO | Climate change and human health – risks and responses. Summary). Due to this, it is estimated through the modelling of future ozone levels and UVR exposures that by 2050, a European

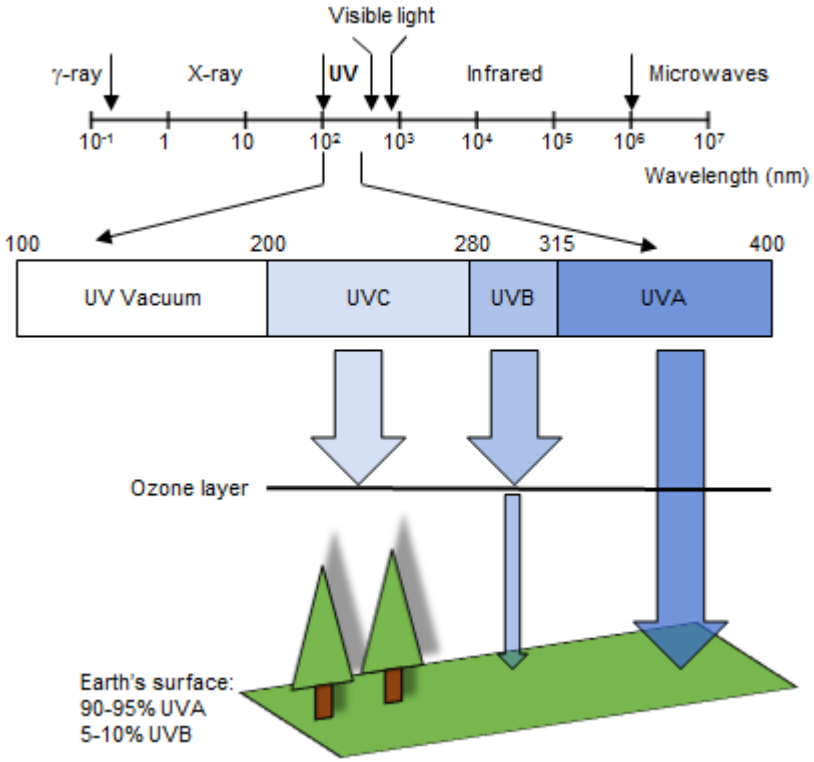

Figure 1.1. Spectrum of ultraviolet radiation

Ultraviolet radiation is a component of electromagnetic radiation with a wavelength of 100-400 nm. Ultraviolet radiation is split into three wavebands, UVC (200-280 nm), UVB (280-315 nm) and UVA (315-400nm). Ultraviolet radiation that reaches the earth's surface consists of 90-95% UVA and 5-10% UVB as all of the UVC component and 90-95% of the UVB component is absorbed by the earth's atmosphere

population living at approximately 45 degrees north will have an approximate 5% excess of skin cancer incidence.

UVA can penetrate glass, which UVB cannot. Consequently, high UVA exposure is possible within buildings and vehicles (Tewari et al., 2013). UVB is also less effective at penetrating and reaching the deeper layers of the skin than UVA. This was demonstrated by Tewari et al. (2013), where both types of UVB-induce DNA damage were shown to be attenuated with increasing skin depth, which was attributed to UVB absorbing chromophores in the skin. In contrast, they observed UVA to be less well absorbed by the upper layer of the epidermis with increasing amounts of DNA lesions generated by UVA seen with increasing skin depth. They suggest that this may occur due to UVA photons scattering in a forward or backward direction within the epidermis. Back scattering within the epidermis allows for increased opportunities for chromophores within the skin to absorb the photons whilst forward scattering

increases the number of photons reaching the upper layers of the dermis (Tewari et al., 2013). It is well established that both UVA and UVB can produce different types of DNA damages, which can lead to the generation of harmful mutations and consequently photocarcinogenesis. However, the theoretical mechanisms by which they do so are thought to differ.

Understanding the biological consequences of these UV-induced lesions requires an understanding of the generated photoproducts. Initial insights into UV-induced DNA damage came over 50 years ago, with the discovery that UVC can promote the dimerization of adjacent thymine residues, which was later shown to be a major DNA lesion generated upon UVB and solar irradiation (Cadet et al., 2012, Beukers and Berends, 1960). Since then, increased research has led to the understanding that UVB induces DNA damage via a direct mechanism. DNA bases are highly conjugated chromophores, with a peak absorbance of 260 nm. As a result, they can absorb within the UVR spectrum and can readily absorb UVB photons (280-315 nm) (Sutherland and Griffin, 1981). Photoexcitation by UVB can lead to the formation of covalent bonds between adjacent pyrimidines, of which there are two types, cyclobutane pyrimidine dimers (CPDs) and 6-4 pyrimidine-pyrimidone photoproducts (6-4PPs). These lesions significantly distort the structure of DNA, preventing the progression of replication and transcription as well as being mutagenic (Freeman et al., 1986, Sutherland et al., 1980).

However, despite making up the majority of the terrestrial UVR we are exposed to, the mechanism by which UVA induces DNA damage is less well understood, with both direct and indirect mechanisms being proposed. UVA cannot be directly absorbed by DNA bases as the waveband falls outside the absorption spectrum for them. Despite this, there are numerous studies that have demonstrated that UVA is still able to generate CPDs (but not 6-4PPs) (Tewari et al., 2013, Freeman et al., 1987). Consequently, it is thought that UVA-induced CPD formation occurs via an indirect pathway with macromolecules other than DNA functioning as UVA photosensitisers. It is theorised that this indirect mechanism involves the formation of reactive oxygen species (ROS), which can damage numerous cellular biomolecules, including DNA bases through the process of oxidation. This theory explains why UVA exposure leads to the generation of oxidised bases such as 8-oxoguanine, the most common type of DNA lesion resulting from base oxidation by ROS (Kielbassa et al., 1997, Kvam and Tyrrell, 1997). However, recent studies have demonstrated the ability of UVA to generate CPDs in isolated, purified genomic DNA, implying that

UVA also has the potential to generate DNA damage directly (Jiang et al., 2009, Mouret et al., 2006a).

III. Pyrimidine Dimers

As mentioned previously, both UVA and UVB are able to induce DNA damage by generating pyrimidine dimer photoproducts, of which there are two main species cyclobutane pyrimidine dimers and 6-4 pyrimidine-pyrimidone photoproducts (Figure 1.2). CPDs occur at a higher frequency than 6-4PPs, as demonstrated by experiments involving transfected mouse cell lines or transgenic mice that ubiquitously express CPD-photolyase, 6-4PP-photolyase, or both (Jans et al., 2005, You et al., 2001). Photolyases are repair enzymes that bind to CPDs or 6-4PPs in a lesion-dependent manner and rapidly repair the damage by splitting the dimers back to undamaged bases in a light-dependent manner. Placental mammals have undergone an evolutionary loss of these repair enzymes and therefore must rely on the nucleotide excision repair pathway to repair UV-induced lesions. Both studies were able to use these photolyase enzymes to identify CPDs as the main pyrimidine dimer photoproduct generated following UV exposure. One explanation for why this may be the case is that 6-4PPs are efficiently removed and repaired by NER (Sinha and Hader, 2002). 6-4PPs can be photoisomerised by wavelengths longer than 290 nm to form related Dewar isomers, which are highly mutagenic and poorly repaired (Lee et al., 2000). Both CPDs and 6-4PPs are formed from the covalent cross-linking of adjacent pyrimidine bases.

CPDs are generated in a [2+2] photocycloaddition reaction between the C5-C6 double bonds of adjacent pyrimidine bases, leading to the formation of a cyclobutane ring (Schreier et al., 2007). Sequence context has been demonstrated to be a factor impacting the distribution of UVB-induced CPDs, with TT dimers occurring most frequently and CC occurring least frequently (Douki and Cadet, 2001). Appropriate orientations of the reacting double bonds are required for the photocycloaddition reaction to occur. Usually, such as in reactions between two ethylene molecules, the reaction yields multiple stereoisomers. However, due to DNA backbone constraints, only a single CPD isomer is formed following exposure to UVR, in both naked and cellular DNA (Schreier et al., 2007). 6-4PPs are also generated via [2+2] cycloaddition reactions, however, these lesions are generated via the reaction occurring between the C5-C6 double bond of the 5’-end pyrimidine base and the C4 carbonyl group of a 3’-end pyrimidine residue (Cadet et al., 2012).

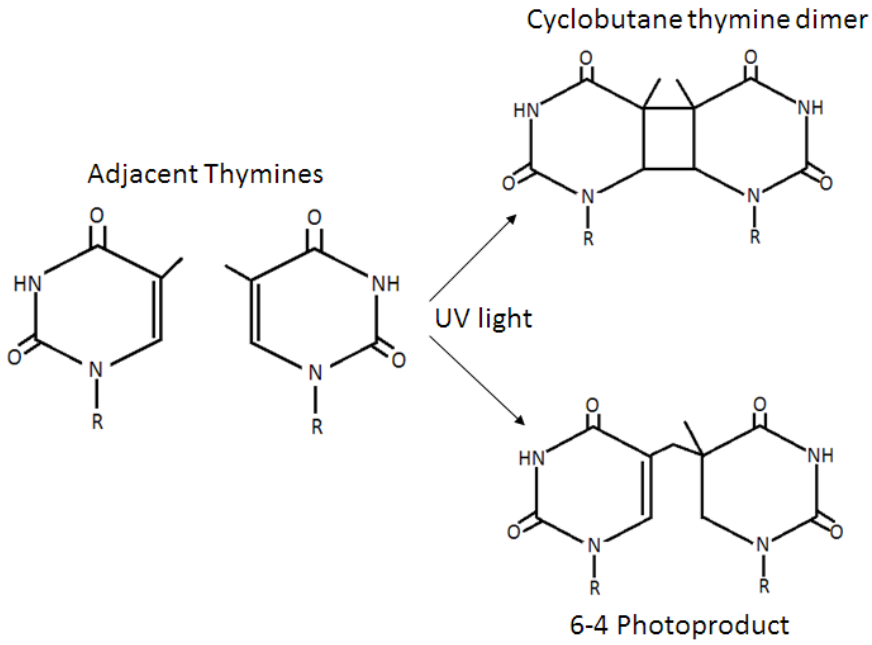

Figure 1.2. Pyrimidine dimer formation

UVA and UVB radiation are both able to induce DNA damage by generating pyrimidine dimer photoproducts, which consist of two main species, cyclobutane pyrimidine dimers (CPDs) and 6-4 pyrimidine-pyrimidone photoproducts (6-4 PPs). CPDs are generated in a [2+2] photocycloaddition reaction between the C5-C6 double bonds of adjacent pyrimidine bases, generating a cyclobutane ring. 6-4PPs are generated via [2+2] cycloaddition reactions between the C5-C6 double bond of the 5'end pyrimidine base and the C4 carbonyl group of the 3'-end pyrimidine base. The figure represents the formation of thymine photodimers following photocycloaddition reactions between adjacent thymine residues.

The mutation signature generated following UV-induced pyrimidine dimer formation is characterised by cytosine (C) to thymine (T) transitions, and although rare, CC to TT tandem base substitutions can also occur (Setlow, 1974). These substitutions are generated following the hydrolytic deamination of cytosine- and 5-methylcytosine-containing lesions to produce uracil and thymidine residues, respectively. Consequently, two adjacent cytosine bases are considered mutation hotspots for UVA and UVB irradiation (Ravanat et al., 2001b). The importance of this mutation signature in contributing towards skin cancer is highlighted by the *TP53* gene, whereby C to T transitions represent approximately 35% of p53 mutations, localised to several mutation hotspots (Tornaletti and Pfeifer, 1995).

Whilst CPDs and 6-4PPs have been well documented as being DNA base photoproducts of UVB irradiation, UVA has also been established as being able to form pyrimidine dimers. The ability of UVA to generate CPDs was initially

demonstrated in bacteria (Tyrrell, 1973). Following this, as well as being able to generate oxidative lesions, CPDs were detected in UVA-irradiated human skin, although it was estimated that UVA was 10^4-10^5-fold less effective than UVB at generating CPDs (Freeman et al., 1989, Burren et al., 1998). Interestingly, despite being less effective at generating CPDs, there is evidence to suggest that pyrimidine dimers generated by UVA are more mutagenic than those induced by UVB. It was hypothesised that the increased mutation rate seen for UVA-induced pyrimidine dimers is due to the mechanism by which the cells process the DNA damage (Runger et al., 2012). Cell cycle regulation, DNA repair and apoptosis induction in primary human fibroblasts following equimutagenic doses of UVA and UVB-irradiation were compared. It was found that cell cycle arrest regulated, in part, by the activation of p53, was prolonged and more prominent in UVB-irradiated cells than UVA.

UVA cannot be directly absorbed by DNA bases and as a result, it was generally believed that its mutagenic effect does not occur through dipyrimidine photoproduct formation. For this reason, it was previously believed that UVA-induced damage was ROS-dependent (Ravanat et al., 2001b). However, two studies in 1999 demonstrated that UVA exposure can directly lead to the generation of CPDs (Douki et al., 1999, Kuluncsics et al., 1999). Despite being less effective than UVB, CPDs have since been demonstrated as being the predominant lesions generated by UVA in rodent skin cells, cultured mammalian cells and in whole human skin (Courdavault et al., 2004, Douki et al., 2003, Mouret et al., 2006b). Comparing the ratio of UVA-induced CPDs to 8-oxoguanine, the most common DNA lesion generated from oxidative damage, revealed CPD levels to be approximately 5-fold higher, with slight variation depending on the cell type (Mouret et al., 2012). Interestingly, a CPD:8-oxoguanine ratio of 1.4 was observed in melanocytes, indicating that this cell type possesses a mechanism that contributes towards increased oxidative stress. Despite this, the possibility that the decreased ratio arose due to decreased generation of CPDs needs to be considered. When comparing the levels of CPDs and 6-4PPs in the epidermis and dermis in skin biopsies, which had been taken immediately following irradiation with equivalent doses of UVA or UVB, not only was it demonstrated that UVB-induced lesions were attenuated with increasing skin depth but also that UVA-induced CPD levels were highest at the basal layers of the epidermis (Tewari et al., 2013, Tewari et al., 2012). These studies, as with the majority of studies looking at the ability of UVA to generate 6-4PPs suggest that UVA is unable to generate such lesions (Mouret et al., 2010). One suggestion for why this occurs is that these lesions

are repaired very efficiently, even during the irradiation period. Support for this was provided when 6-4PPs were observed in cell lines deficient in components for nucleotide excision repair (Cortat et al., 2013). Interestingly, despite being unable to generate 6-4PPs, UVA has been shown to be more efficient at inducing the photo-isomerisation of these to Dewar isomers (Courdavault et al., 2005).

Regardless of whether they were generated from UVA or UVB irradiation, pyrimidine dimers introduce distortions into the structure of DNA that prevent replication by preventing replicative DNA polymerases from passing them (Horsfall and Lawrence, 1994). These lesions are recognised by components of the nucleotide excision repair pathway (NER), a pathway with two mechanisms for the detection of DNA damage; transcription coupled repair, which detects lesions in transcribed regions of the genome and global genome repair, which detects lesions across the entire genome (Batty and Wood, 2000). The importance of global genome NER in the repair of UVR-induced damage is highlighted by Cockayne's syndrome where patients possess mutations in transcription coupled repair genes. Patients with this disorder possess neurological abnormalities but do not have a predisposition to skin cancer development, as patients still possess functioning ggNER (Murray et al., 2016).

NER is fairly efficient at removing pyrimidine dimers and similar lesions before they are replicated, however, in the event that NER is unable to complete the repair, cells possess other mechanisms to help prevent mutagenic outcomes. One such mechanism is known as translesion DNA synthesis (TLS), whereby specialised DNA polymerases known as TLS polymerases are able to use lesions as templates in order to bypass DNA lesions by incorporating nucleotides opposite the lesion (Waters et al., 2009). It is proposed that TLS polymerases carry out their function by ignoring conventional Watson-Crick base pairing rules, which would be expected to be error-prone. However, the TLS polymerase specific for CPDs, DNA polymerase η (Polη) is able to prevent the generation of mutations with relative efficiency, as seen with the process being non-mutagenic for T-T dimers, which make up the majority of UVA- and UVB-induced pyrimidine dimers (Masutani et al., 2000). However, in the event that cytosine residues within dimers are deaminated to uracil residues, the mechanism of action for Polη means C to T and CC to TT transitions, which make up the UV signature for both UVA and UVB, are possible outcomes (Biertumpfel et al., 2010, Ikehata and Ono, 2011).

For a long time it had been suggested that the pyrimidine dimer signature produced following UVA irradiation was photosensitiser mediated. However, recent studies

examining the damage spectra generated by UVA on isolated DNA revealed that CPDs are generated with similar distributions to those observed in keratinocytes. The generation of CPDs in the absence of photosensitisers suggests that UVA produces these lesions directly. Although this is a large step forward in resolving the controversy regarding the origin of UVA-induced CPDs, the exact mechanism by which is does so remains to be elucidated (Jiang et al., 2009). Potential insight was provided in 2010 when the formation of all four possible CPD bipyrimidine dimer products were compared in the context of UVA irradiated cells, isolated genomic DNA and an oligonucleotide duplex sequence (dA(20):dT(20)) (Mouret et al., 2010). The relative frequencies of the lesions to each other was similar in the three types of samples, providing support for UVA possessing a direct photochemical mechanism. They suggested that, although the individual bases are unable to absorb UVA directly, that the double-stranded structure of DNA increases the capacity for the bases to absorb UVA photons. Whether or not ssDNA sequences produce similar mutation spectra needs to be considered.

It is important to note that whilst the majority of lesions within DNA generated following UVA exposure are CPDs and that there is emerging evidence for this being mediated via a direct mechanism, one cannot rule out the role of photosensitisers and other types of DNA damage in UVA-induced mutagenesis. This has been demonstrated by the fact that by lowering the dose of UVA caused increased cytotoxicity, which was attributed to increased DNA damage via increase ROS-mediated oxidation and lipid peroxidation (Shorrocks et al., 2008). The importance of understanding the role of various dose rates and how they contribute towards UVA-induced DNA damage has real world importance as UVA dosages vary considerably with geographical location, time of day and the use of different sunscreens. Understanding the indirect mechanism by which photosensitisers contribute towards UVA-induced mutagenesis is therefore also required alongside knowledge of UVA's direct mechanisms of action.

IV. Oxidative DNA base damage

As mentioned earlier, although there are implications for DNA duplexes absorbing UVA directly, the UVA waveband of UVR falls outside of the absorption spectrum for individual DNA bases. UVA however can be directly absorbed by endogenous photosensitisers such as riboflavin, flavins, porphyrins and also melanin (Cadet et al., 2015). Absorption of UVA photons by these cellular biomolecules leads to the

generation of reactive oxygen species (ROS), which include hydrogen peroxide, hydroxyl radicals and singlet oxygen. The photoexcitation of these molecules occurs via one of two reactions, known simply as type 1 and type 2 photosensitisation reactions (Figure 1.3). The ROS generated via these reactions are the molecules responsible for generating DNA damage.

In the type 1 photoexcitation reaction, the excited photosensitiser reacts directly with a target molecule in its vicinity (Cadet et al., 2015). This results in electron abstraction from the molecule, producing a pair of charged radicals. The anion photosensitiser radicals are oxidised back to their neutral state by reaction with oxygen. The cation radical, within an aqueous environment, can then undergo either deprotonation and/or hydration reactions. In either case, neutral radicals are generated, which can go on to react with molecular oxygen or O_2^-, generating peroxyl radicals, intermediates that can yield final oxidation products through additional reactions.

The type 2 photoexcitation reaction, on the other hand, involves the energy transfer from the excited photosensitiser to molecular oxygen. The excited oxygen ($^1O_2$) can react according to three main mechanisms, of which the ene-reaction that yields hydroperoxides is the most important in terms of generating DNA damage (Greer, 2006). A side reaction of this process involves charge transfer with oxygen, generating O_2^-. Dismutation of two superoxide ions catalysed by superoxide dismutase generates hydrogen peroxide. H_2O_2 oxidises ferric ions to yield hydroxyl radicals (Finkel and Holbrook, 2000). Both types of reaction are therefore similar in that they result in the generation of ROS, particularly singlet oxygen ($^1O_2$) and hydroxyl radicals (•OH), which can damage a range of cellular biomolecules, such as DNA.

The exact nature of the photosensitisers involved in UVA-mediated oxidative DNA damage is unclear, with flavins, porphyrins and even melanin proposed as being endogenous photosensitisers for UVA (Wondrak et al., 2006). The differences in the properties of the excited states of the different photosensitisers means that there is likely more than one potential pathway for generating oxidative damage. ROS can generate a number of different DNA lesions. ROS-mediated oxidation can occur at all four bases, but occurs most frequently at guanine bases, which are oxidised at high rates due to their higher oxidation rates, with the most frequently generated DNA damage of this type being 8-oxoguanine (8-oxoG) (Steenken and Jovanovic, 1997).

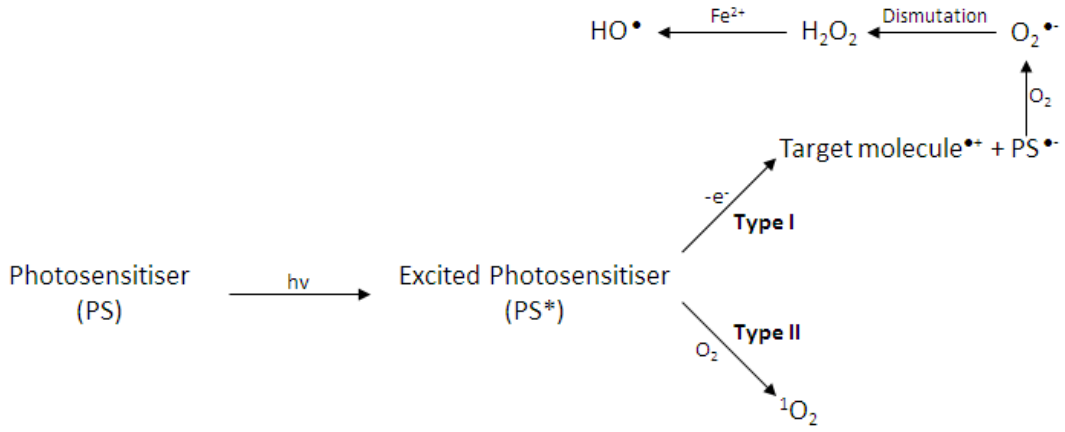

Figure 1.3 Type I and type II photosensitisation reactions

In photosensitisation reactions, a sensitiser absorbs a photon and becomes excited. Endogenous photosensitisers include cytochromes, flavins, riboflavins, porphyrins and melanin. Absorption of photons by these photosensitisers leads to the generation of reactive oxygen species (ROS), such as hydrogen peroxide, hydroxyl radicals and singlet oxygen. In the type I reaction, the excited photosensitiser reacts with a target molecule in its vicinity whilst in the type II reaction, energy is transferred from the excited photosensitiser to molecular oxygen. Both types of reaction result in the production of ROS that can damage a range of cellular biomolecules, such as DNA.

8-oxoG is well established as being a product of UVA irradiation, as demonstrated in cultured cells and in skin (Mouret et al., 2006b, Rosen et al., 1996). The generation of 8-oxoG via $^1O_2$ begins with the conversion of guanine to 4,8-endoperoxide via a $^1O_2$-mediated Diels Alder [4+2] photocycloaddition reaction. The resulting intermediate product is able to rearrange within dsDNA, forming 8-hydroxyperoxyguanine, which is then further reduced to 8-oxoG (Sheu et al., 2002, Ravanat et al., 2001a). •OH, in contrast to $^1O_2$ does not specifically target DNA bases, but reacts with all components of DNA (Cadet et al., 1999). When •OH reacts with purines, a C8-hydroxylated radical is generated, which then gives rise to 8-oxoG along with degradation products of adenine (Cadet et al., 2012). •OH can also react with pyrimidines at the C5-C6 double bond to generate oxidative lesions of adenine and thymine.

Although CPDs are the predominant lesion generated by UVA exposure, the importance of oxidative damage still needs to be acknowledged when considering the UVA-mutagenic signature, particularly within melanocytes where the ratio of CPDs to 8-oxoG lesions is much smaller when compared to other cells types (Mouret et al., 2012). Analysis of the mutagenic potential of 8-oxoG lesions demonstrated that the predominant mutation is a G:C to T:A transversion (Yasui et al., 2014). There

have been controversies in the past in regards to the UVA mutagenic signature. A number of groups have studied the pattern of mutations induced by UVA in cultured cells, but there have been some differences between the reported mutation spectra (Besaratinia et al., 2004, Robert et al., 1996). One of the mutations observed most frequently was the otherwise rare T to G transversion that was determined to be too unique as to be rarely induced by other conditions within the studies. Furthermore, this transversion was mainly found following exposure of Chinese hamster ovary cells to UVA but not to UVB, hence this mutation was designated as the UVA fingerprint (Huang et al., 2009). The same fingerprint was detected in a study involving human skin tumours, with particular bias towards the basal epidermal layer and the dermis (Agar et al., 2004). This raises questions in regards to how 8-oxoG contributes towards UVA-induced mutagenesis as this oxidation product is understood to induce G to T mutations, which are rarely observed following UVA exposure (Rochette et al., 2003, Sage et al., 1996).

Oxidation of DNA bases to generate lesions such as 8-oxoG is not unique to UVR and other forms of radiation. ROS are constantly being generated endogenously as by-products of oxidative metabolism within the mitochondria and as a result, DNA bases are constantly under pressure of oxidation. Consequently, cells have evolved effective defences against oxidative damage through the process of base excision repair (BER), initiated when DNA glycosylases recognise and remove the damaged bases. Due to the number of base alterations possible through oxidation and other processes such as deamination and alkylation, there are multiple DNA glycosylases available, each possessing selective binding sites specific to particular types of base modifications (Kim and Wilson, 2012). The DNA glycosylase responsible for the recognition and removal of 8-oxoG is OGG1. Indirect indication for the UVA-induced oxidative stress came when it was demonstrated through confocal microscopy that hOGG1 was recruited to the nuclear matrix from a nucleoplasmic localisation following UVA irradiation (Campalans et al., 2007). Furthermore, two years prior to this, an investigation into how multiple yeast mutants were affected by UVA exposure was conducted. Here it was shown that all of the major DNA damage repair pathways, of which BER is included, were able to protect yeast from the lethal action of UVA. OGG1 DNA glycosylase was shown to be very efficient at preventing UVA-induced mutagenesis (Kozmin et al., 2005). Interestingly, the use of anti-hOGG1 immunohistochemical staining of frozen sections from human skin found that hOGG1 was expressed at highest levels in the upper region of the epidermis, with lowest levels seen in the basal cells (Javeri et al., 2008). This has implications in

carcinogenesis as basal cell carcinoma arises from these proliferating basal cells. The lower levels of the DNA repair enzyme OGG1 in these cells may account for the accumulation of UVA-induced oxidative damage and therefore increased mutagenesis (Halliday et al., 2011).

As well as having implications in NMSC carcinogenesis, oxidative damage also has implications in melanoma skin cancer. Melanocytes are located in the stratum basale of the skin's epidermis and therefore have lower levels of OGG1 than cells located in the upper layers of the epidermis (Javeri et al., 2008). Similar repair rates for oxidative modifications of purine bases were observed in human skin fibroblasts and melanoma cells under normal conditions and following UVA irradiation. However, the repair of these modifications was severely compromised in glutathione-depleted cells following UVA irradiation for both cell types, suggesting that the base excision repair of oxidative purine modifications is vulnerable to oxidative stress, which is not the case for pyrimidine dimers (Eiberger et al., 2008). Also, whilst CPDs were found to be the most frequently generated lesion by UVA irradiation for keratinocytes, 8-oxoG has been shown to be more readily induced by UVA exposure in melanocytes compared to keratinocytes (Mouret et al., 2012). This is consistent with the suggestion that a factor affecting the distribution of UVA-induced lesions is cell type-specific. Evidence for melanocytes being more susceptible than other cell types for UVA-induced oxidative damage has been provided in both cultured cells and in pigmented mice (Noonan et al., 2012, Wang et al., 2010). The possible importance of UVA-induced oxidative damage is supported by evidence that the second most common type of mutation seen in melanomas are G to T transversions, implying that 8-oxoG has a large role in melanomagenesis (Pleasance et al., 2010). The increased frequency of lesions that occur via photosensitisation reactions within melanocytes suggests a role for melanin pigments in the generation of these lesions.

Initial suggestions for the role of melanin as a photosensitiser in the induction of DNA damage came in 1993. Here, the induction of malignant melanoma was investigated in heavily pigmented hybrids of the genus *Xiphophorus,* which are highly sensitive to melanoma induction following single UV exposures. It was found that melanoma induction had particular sensitivity at 365, 405 and 436 nm, wavelengths that are not directly absorbed by DNA, and correspond in part with the UVA waveband of UVR. It was interpreted that photons of these wavelengths were absorbed by melanin and that melanoma induction is mediated by wavelengths within the UVA region (Setlow et al., 1993). At the time, the ability to apply these findings to human melanoma skin cancers was questionable as whether or not this fish model was suitable for human

melanomas was not fully understood. Re-evaluation of the methodology and model used has since discredited the findings from this study, with it now being accepted that only UVB is able to induce melanoma formation in this particular model (Mitchell et al., 2010). However, since then, a number of studies have been conducted, investigating the role of melanin as a photosensitiser in UVA-induced mutagenesis.

The two types of melanin, eumelanin and pheomelanin are derived from a common precursor, dopaquinone (Wondrak et al., 2006). Most melanin pigments in skin tissues are mixtures of eumelanin and pheomelanin with melanocytes of light-skinned individuals primarily producing pheomelanin. Pheomelanin has a limited capacity to absorb UVR and the limited photoprotection provided by pheomelanin explains why the incidence of skin cancer is increased amongst light-skinned populations. Noonan et al. (2012) studied melanoma induction by UVA and UVB in mice, whose melanin consisted of >90% eumelanin. They found that UVA melanoma induction was melanin dependent whilst UVB melanoma induction occurred in a pigment-independent manner. A suggested mechanism for how melanin functions as a photosensitiser in melanomagenesis came in 2015. Here it was shown that CPDs, that are typically generated picoseconds following UV exposure, were still being generated 3 hours following UVA irradiation within melanocytes (Premi et al., 2015). These so-called “dark CPDs” constitute the majority of CPDs seen in melanocytes following UV exposure. UVR is known to upregulate the nitric oxide synthase iNOS, NADPH oxidase (NOX) and enzymes involved in melanin synthesis, resulting in sustained generation of nitric oxide (NO•) and superoxide ($\bullet O_2^-$) radicals. UVA exposure results in increased generation of these radicals causing increased peroxynitrite ($ONOO^-$) generation. The increased levels of $ONOO^-$ causes melanin degradation, producing fragments that are able to pass into the nucleus. Electrons within these fragments can be excited to a quantum triplet state, which has the same energy as UV photons and can induce CPDs by energy transfer to DNA. These studies are significant as they indicate melanin to not only play protective roles against skin carcinogenesis but also in promoting carcinogenesis.

V. Double strand breaks

The ability for UVR to generate base modifications has been well established, however, it is also important to consider the capacity for UVR to induce both single-strand (SSB) and double-strand breaks (DSBs). The ability for UVR to generate single-strand breaks as minor classes of DNA damage has been demonstrated in a

number of cases, including experiments involving exposure of human keratinocytes to UVA (Wischermann et al., 2008). SSBs are repaired efficiently and do not significantly contribute to mutation formation, whilst DSBs are highly mutagenic and carcinogenic as they induce genomic instability by promoting the generation of deletions and insertions (Rizzo et al., 2011). UVB has been established as being able to induce the formation of DSBs with suggestions that it occurs following the collapse of replication forks at unrepaired CPDs, which are readily generated by UVB (Garinis et al., 2005). The ability of UVA to induce DSB formation however is debated.

DSBs can be repaired through either homologous recombination or non-homologous end joining (NHEJ) with activation of the former occurring through the Fanconi anaemia (FA)/BRCA pathway. In investigating UVA-induced DSB formation, Rizzo et al (2011) studied the activation of this pathway in primary skin fibroblasts following exposure to different doses of UVA at various times following irradiation. They found that UVA was unable to activate this pathway, unlike ionising radiation and UVB, suggesting that UVA does not induce DSBs. They supported this with evidence that UVA did not induce DSBs through investigation of γH2AX nuclear foci formation, which is considered to be a biomarker of DSB formation. Despite this however, there is an abundance of evidence to suggest that UVA can induce DSBs, although the exact mechanism by which this occurs remains to be elucidated.

Contrary to the findings by Rizzo et al (2011), a number of other studies have found UVA irradiation is able to induce γH2AX formation. Whilst Rizzo et al. were unable to detect γH2AX formation at doses of 400 kJ m^{-2}, a dose-dependent increase in γH2AX generation was observed up to 160 kJ m^{-2} in JB6 cells (Lu et al., 2006). Determining whether the γH2AX nuclear foci formed are due to UVA-induced DSB formation or not is difficult to determine, as γH2AX can also be activated via different forms of damage via the DNA damage response or independent of DNA damage, such as through heat shock. Additional evidence for DSB generation by UVA exposure came when components of both the error-prone NHEJ and homologous recombination were investigated following UVA exposure. Components exclusive to the individual pathways and components involved in both were compared. XRCC4, DNA-PK and Ku70 were used as representative of NHEJ, Rad51 and Rad52 were used for homologous recombination and Mre11 and Rad50, which are involved in the detection of DSBs, were used as representatives of both pathways. It was found that in G_2 cells, in which both repair pathways are active, the repair pathways cooperate to repair the same DSBs following UVA exposure (Rapp and Greulich, 2004). This is

supported by evidence that cell lines deficient in DSB repair pathways were sensitive to UVA and formed increased chromosome damage following DSB formation (Fell et al., 2002).

Although providing evidence that UVA exposure can lead to the formation of DSBs, these studies do not provide any indication regarding the exact mechanism by which they do so. A recent paper proposed that UVA-induced DSBs result from the repair of clustered oxidative DNA damages (Greinert et al., 2012). It has been demonstrated for other types of radiation and chemical toxins that DNA lesions generated by oxidising agents are converted into DSBs during their repair, whereby both DNA strands are incised simultaneously in close proximity (Gulston et al., 2004). UVA photons possess insufficient energy to induce covalent bond breakages directly and so DSBs must be generated by UVA indirectly. Greinert et al. (2012) detected DSBs immediately following UVA exposure through the use of neutral Comet assays and γH2AX formation. The use of the antioxidant Naringin prior to irradiation prevented DSB formation, indicating that ROS, which as previously mentioned are readily generated by UVA, are involved in DSB formation. Consequently, it was interpreted that the mechanism for UVA-induced DSB formation is similar to that of other types of radiation in that it occurs via the clustering of oxidative lesions followed by their repair.

VI. The bystander effect

The radiation-induced bystander effect, which was first discovered in 1954, refers to the phenomenon whereby nonirradiated cells exhibit the characteristics of irradiated cells due to signals received from nearby irradiated cells (Parsons et al., 1954). The characteristic events that occur in these nonirradiated cells appear mainly as cell-damaging effects such as apoptosis induction, cytogenic damage and activation of the DNA damage response and repair pathways. The bystander effect has been well established for ionising radiation (Rzeszowska-Wolny et al., 2009, Prise et al., 2003). UVA and UVB have also been found to be able to induce bystander effects, but the exact mechanism by which they do so remains to be elucidated (Dahle et al., 2005). For example, does the bystander effect occur by signals passing from an irradiated cell to an unirradiated cell via intracellular junctions, such as gap junctions, or does it occur through paracrine signalling?

In one study, human keratinocytes and fibroblasts were exposed to UVA or UVB irradiation and were co-cultured with unirradiated cells, with the differentially treated populations separated by a medium-permeable insert, meaning the cells were not in direct contact with each other (Whiteside and McMillan, 2009). Here, they observed that irradiation with 100 kJ m^{-2} UVA was able to induce a bystander effect as determined by reduced clonogenic survival of the unirradiated cells, whilst similarly toxic doses up to 0.4 kJ m^{-2} UVB did not have the same outcome. Using a similar co-culture method with human dermal fibroblasts, a study using considerably increased doses of UVB (up to 10 kJ m^{-2}) and decreased doses of UVA (up to 20 kJ m^{-2}) found that both UVB and UVA caused a dose-dependent decrease in survival and increase in apoptosis in the bystander cells (Widel et al., 2014). The study also investigated the roles of ROS and interleukins 6 and 8 (IL-6 and IL-8). Increased levels of ROS and IL-6 were detected within the bystander cells and within the media of the irradiated cells, implicating a role for these in generating the bystander effect following UVB or UVA irradiation. Further evidence for the role of ROS in the UVR-induced bystander effect came with studies involving melanocytes. Here, although melanocytes appeared to be more resistant that keratinocytes or fibroblasts to the direct effects of UVA, melanocytes were found to be more susceptible to the bystander effect following co-culturing with UVA-irradiated keratinocytes or fibroblasts (Redmond et al., 2014).

It would be expected that the ROS involved in the UVA-induced bystander effect are generated from type 1 and type 2 photosensitisation reactions, however, there is also some evidence to suggest that the UVA excitation of dermal extracellular matrix protein chromophores could possible give rise to ROS that participate in generating the bystander effect (Wondrak et al., 2006). The most abundant potential target for UV photons in human skin are chromophores associated with skin structural proteins, which include keratin, collagen and elastin. An example of the potential role of these in ROS generation was seen when collagen and elastin were found to be active photosensitisers for UV-driven generation of H_2O_2 (Wondrak et al., 2003).

VII. Skin cancer mutational signatures

All cancers possess somatic mutations, of which a certain subset, known as driver mutations are responsible for inducing cancer development by inducing uncontrolled cell growth. Additional information can be provided about how specific cancers arise by analysing the spectrum of mutations that occur. In the context of skin cancer,

sufficient information is available in regards to the mechanisms by which the components of UVR contribute to the generation of different DNA damage lesions. However, the damage needs to be understood in the context of UVR carcinogenesis by examining how the generated lesions affect specific genes and the outcomes this has on carcinogenesis. Catalogues of somatic mutations provide great insight into the forces that shape the particular cancer's genome. For example, Pleasance et al. (2010) used next generation sequencing to sequence the genomes of a malignant melanoma and a lymphoblastoid cell line from the same person, providing a catalogue of somatic mutations from an individual cancer. The dominant mutational signature found, C to T transition, reflected DNA damage that arises following UVR exposure.

There are a number of genes, usually either proto-oncogenes or tumour suppressor genes, which are frequently mutated across the many different types of cancer. One of the most frequently mutated genes in human cancer is *TP53* (Olivier et al., 2010). CPDs generated by both UVB and UVA account for the major UV signature mutation of C to T transitions or CC to TT tandem mutations, which account for approximately 35% of p53 mutations, localised to several mutational hotspots (Tornaletti and Pfeifer, 1995). These mutations have been found in the *TP53* gene in both BCCs and SCCs (Rady et al., 1992, Brash et al., 1991). Early studies suggested that more than 90% of SCCs and more than 50% of BCCs possessed *TP53* mutations, however, it is now thought that the frequency is approximately 50% of all skin cancer but that the frequency is over 90% in skin cancers of xeroderma pigmentosum patients (Boukamp, 2005).

BCCs have also been shown to contain UVR-induced mutations in *PTCH*, which is a member of the hedgehog-patched-smoothened pathway, which is deregulated in more than 70% of BCCs (Brash, 2015). The *PTCH* tumour suppressor gene was discovered following studies looking at the autosomal dominant disorder nevoid basal cell carcinoma (NBCC) syndrome, which is characterised by multiple BCCs at an early age (Kimonis et al., 1997). Additionally, novel mutations in the promoter region of the telomerase reverse transcriptase gene (*TERT*), which had previously been observed in up to 71% of cutaneous malignant melanoma cases were also demonstrated to occur in 50-78% of NMSC cases, following C to T or CC to TT mutations as a result of UVR exposure (Griewank et al., 2013). These mutations result in increased *TERT* expression due to an increased number of ETS/TCF transcription factor binding sites. Telomerase is a ribonucleoprotein that is responsible for adding telomeric sequences, TTAGGG hexamers, to the ends of

chromosomes in order to maintain telomeres (Horn et al., 2013). Telomeres shorten progressively over multiple cell generations and eventually lose the ability to protect the ends of chromosomes from end-to-end fusions which threaten cell viability. The increased expression of TERT serves to maintain telomere lengths and therefore contributes to one of the hallmarks of cancer by enabling replicative immortality (Hanahan and Weinberg, 2011).

Melanomas, as well as NMSC, show preferential mutational signatures towards particular driving mutations. The best-studied and most common mutation that occurs in melanomas is the oncogenic mutation of *BRAF*, occurring in approximately 44% of melanomas (Davies et al., 2002). The majority of mutations are V600E point mutations that arise following a T to A transversion. *BRAF* encodes a serine/threonine kinase downstream of Ras in the RAS/RAF/MAPK pathway (Thomas et al., 2004). It has been demonstrated in vitro and in vivo that this point mutation alone results in senescence and in order to induce tumour formation, additional genetic alterations are required (Patton et al., 2005). The *CDKN2A* locus, at which two distinct tumour suppressors, $p16^{INK4a}$ and $p14^{ARF}$ are encoded by alternative reading frames, has also been shown to be frequently mutated in melanoma (Sharpless and Chin, 2003). Numerous studied have linked the loss of $p16^{INK4a}$ and melanoma and now a recent study has implicated the loss of $p14^{ARF}$ with assisting the V600E point mutated *BRAF* in inducing melanomagenesis (Luo et al., 2013). The group proposed that this occurred as the two mutations synergise to inhibit NER via epigenetic repression of XPC. Another study has also suggested that $BRAF^{V600E}$ can contribute to melanomagenesis via cooperation with mutated *TP53* (Viros et al., 2014).

In addition to *BRAF* mutations, oncogenic RAS mutations comprise another subset of mutations that are frequently present in cancer. RAS, a small GTP-binding protein, activates a number of effector proteins such as phosphoinositide 3-kinase (PI3K), RAF protein kinases in order to regulate signalling pathways responsible for controlling proliferation, senescence and cell survival. Mammals possess three *RAS* genes, *HRAS, KRAS* and *NRAS*. The proteins these encode serve overlapping but non-identical functions and promote oncogenesis once mutationally activated at codon 12, 13 or 61 (Prior et al., 2012). Despite the high degree of similarity among isoforms, each isoform displays a preference towards particular cancer types. *NRAS* is second most frequently mutated gene in melanoma, occurring in approximately 18% of melanoma cases, with more than 80% of mutations occurring at glutamine 61 (Pedersen et al., 2014). In contrast, *KRAS* and *HRAS* account for 2% and 1% of

melanoma cases, respectively. As with *BRAF*, multiple studies employing transgenic mouse models have shown that oncogenic NRAS can only induce melanomagenesis if tumour suppressor genes were also deleted.

The requirement of additional mutations in tumour suppressor genes and proto-oncogenes in order for BRAF and NRAS to induce melanomagenesis demonstrates the importance of additional driver mutations in melanoma. As a result, the advancement of genome sequencing technologies to identify new driver mutations in melanoma has significant importance. An example of such a driver mutation discovered by this method is *PREX2*, a PTEN-interacting protein and negative regulator of PTEN, which was found to have a mutation frequency of approximately 14% in a study of 107 melanomas (Berger et al., 2012).

VIII. Defects in the repair of UV-induced damage in skin cancer predisposition

The mechanisms by which UVB and UVA, as well as other endogenous and exogenous damaging agents, are able to induce a variety of DNA lesions with the potential to generate different mutations, highlights the need for signalling pathways that both recognise the damage sites and activate pathways that lead to the repair of these lesions. The significant importance of such pathways is exemplified by genetic disorders in which components of DNA repair pathways or pathways upstream of these are deficient in activity or absent altogether and can result in the patient possessing predispositions to particular disease outcomes. An excellent example of this in regards to skin cancer is in the genetic disorder Xeroderma pigmentosum.

Xeroderma pigmentosum (XP) is a group of related autosomal recessive inherited disorders, clinically characterised by early onset development of skin cancer, particularly in sun-exposed skin (Satokata et al., 1992). XP was the first syndrome in which cellular defects in DNA processing pathways were associated with a clinical phenotype (Cleaver, 1968). Skin is normal in affected newborns, but prominent sunburn reactions can occur during infancy. From early childhood, XP patients are highly likely to develop multiple skin tumours, both non-melanoma and melanomas, as well as experience premature skin aging and pigmentary changes (Nikolaou et al., 2012). A median onset age of 8-9 years is seen in patients who are not protected from sun exposure. Compared with the remaining population, XP patients have a 10,000-fold increase in NMSC incidence and a 2,000-fold increase in melanoma (Menck and Munford, 2014).

XP has been classified into eight different complementation groups, XP-A through to XP-G, and XP variants (XP-V), with each group corresponding to mutations in eight different genes. Seven of the genes, which account for groups XP-A through XP-G are involved in the repair of DNA lesions via NER. XP-V patients are NER proficient and are able to remove generated lesions but are unable to replicate DNA following UV exposure as they are deficient in translesion synthesis (Menck and Munford, 2014). XP-C, in complex with RAD23b, is responsible for DNA damage recognition in GG-NER, whilst the remaining XP genes, with the exception of XP-V, are common to both GG-NER and TC-NER. XP patients are therefore at increased risk of developing skin cancers as they are inefficient at recognising and removing pyrimidine dimers generated by both UVB and UVA exposure. As a result, the characteristic C to T transitions and CC to TT tandem base substitutions that make up the mutation signature of UV-induced pyrimidine dimers occur more frequently.

There are some discrete clinical characteristics between the different complementation groups, for example, XP-A patients may also have some neurological impairment whilst XP-C patients are at a particular risk of developing melanomas (Yang et al., 2007, Lynch et al., 1984). Interestingly, it has been shown that proteins involved in GG-NER damage recognition play a crucial role in deciding a cell's fate by triggering the initiation of the repair pathway or by signalling apoptosis (Stoyanova et al., 2009). Consequently, if the GG-NER pathway was defective, neither DNA repair or apoptosis initiation can occur, generating cancer cells that cannot undergo apoptosis and contains high levels of UV-induced mutations (Pleasance et al., 2010). A recent paper has demonstrated that GG-NER is deficient in melanoma cells following UVA exposure (Murray et al., 2016). Pathogenic mutations in components of GG-NER (XP-C) lead to XP whilst mutations in TC-NER components, such as ERCC8 and ERCC6 result in Cockayne's syndrome, which is characterised by neuronal abnormalities but no increased incidence of skin cancer. The involvement of XP-C in GG-NER and the understanding that GG-NER is deficient in melanomas following UVA exposure explains why patients of the complementation group XP-C have an increased incidence of melanoma skin cancer.

IX. The DNA damage response

Genome injury, not only from DNA lesions generated following UV exposure but also other genotoxic stress sources to which all living organisms are constantly exposed to, must be repaired to prevent the mutational outcomes that can occur. In order to

preserve the information that DNA encodes, cells must detect the damage and propagate signals to ensure the correct repair pathways are initiated. This is accomplished through a cascade of mechanisms that together encompass the DNA damage response (DDR), which can detect the variety of potential lesions and manage the frequency at which they are generated. The DDR can be divided into multiple distinct but functionally similar pathways, largely depending on the type of DNA lesion being detected and repaired (Lord and Ashworth, 2012). The pathway to be activated following lesion detection is determined by the activation of PI3K-like kinases (PIKKs) family proteins, which include ataxia-telangiectasia mutated (ATM), ataxia-telangiectasia and Rad3-related (ATR) and DNA-dependent protein kinase catalytic subunit (DNA-PKcs), which are responsible for phosphorylating various components of the DDR in order to coordinate cell cycle arrest and DNA repair pathway activation (Sulli et al., 2012) (Figure 1.4). In the event that the damage cannot be repaired, the DDR is able to induce cell death through either apoptosis or cellular senescence.

The DDR comprises two main DNA damage sensors, the MRE11-RAD50-NBS1 (MRN) complex, which detects DSBs, and replication protein A (RPA) and the RAD9 RAD1-HUS1 (9-1-1) complex, which detects replication stress by recognising stalled replication forks. The NBS1 component of the MRN complex has been demonstrated as being dispensable for the binding of the whole complex to DSBs (Mirzoeva and Petrini, 2001). MRE11/RAD50 binds to DNA as a heterotetramer that tethers the broken ends of DSBs, due to two DNA-binding motifs possessed by MRE11 (van den Bosch et al., 2003, de Jager et al., 2001). The architecture of the MRN complex is altered upon DNA binding, generating a parallel orientation of the coiled-coils of RAD50 to create a configuration that favours intercomplex association (Lavin, 2007). MRE11 possesses both endonuclease and exonuclease activity which are stimulated by association with RAD50 and activated upon binding to DSBs. MRN then resects DSBs, generating short 3’-ssDNA tails that are immediately coated by RPA (Huhn et al., 2013). This process of DSB resection is required for homologous recombination but not for NHEJ and therefore serves as an important step in determining how DSBs are repaired (Polo and Jackson, 2011). In the same manner that RPA detects regions of ssDNA generated by MRN resection, RPA is responsible for detecting stalled replication forks following replicative stress by again detecting regions of ssDNA. In these cases, RPA then recruits the 9-1-1 complex to activate a different pathway of the DDR. Following lesion recognition, the MRN complex and the 9-1-1

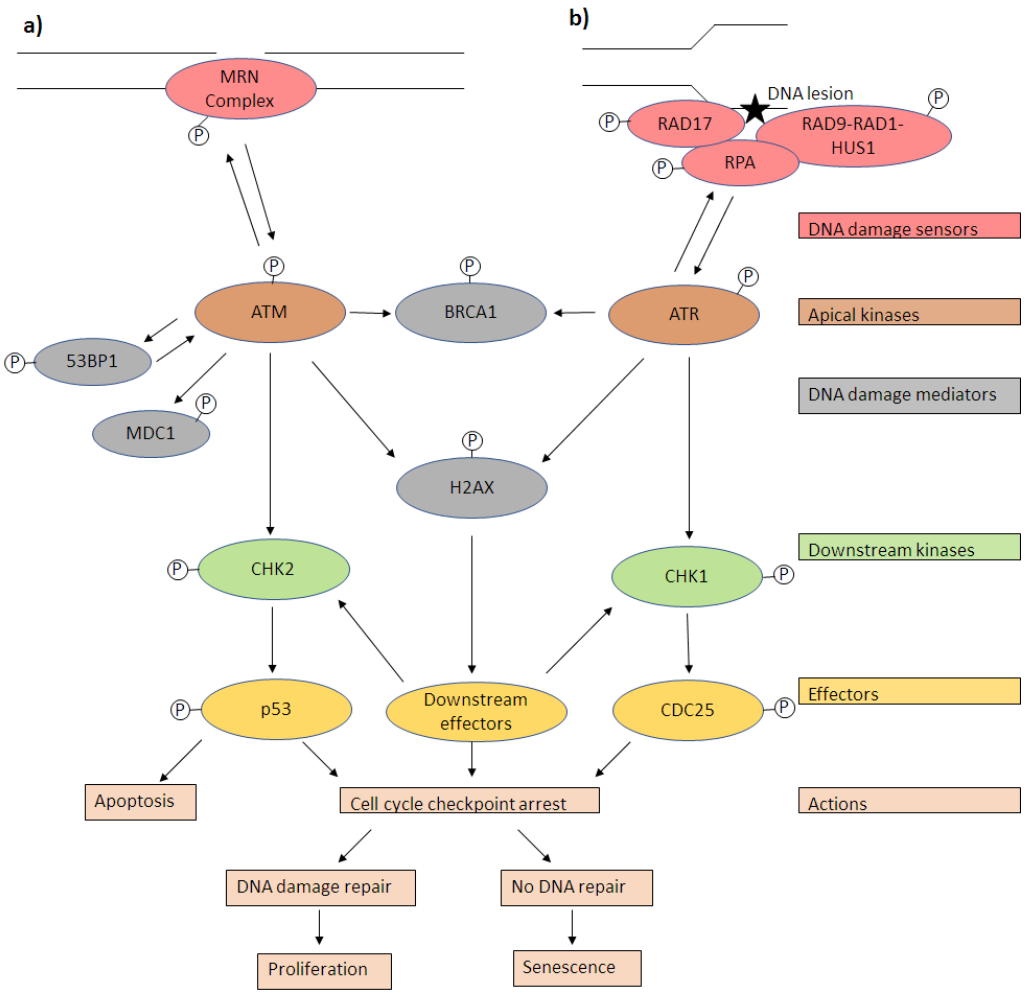

Figure 1.4. The DNA damage response

The DNA damage response (DDR) encompasses a cascade of reactions responsible for detecting different types of DNA damage and then signalling for their repair following cell cycle arrest. Two main DNA damage sensors are involved in the pathway, the MRN complex (a), which recognises DNA double strand breaks (DSBs); and RPA and the 9-1-1 complex (b), which together are responsible for recognising stalled replication forks generated by replication stress. The DNA damage sensors recruit the apical kinases ATM and ATR, via the MRN and 9-1-1 complex, respectively. ATM and ATR can phosphorylate a number of DNA damage mediators such as the histone variant H2AX at Ser139 to generate γH2AX, in the region proximal to the detected lesion. ATM can phosphorylate 53BP1 and MDC1, which form a positive feedback loop by enhancing ATM accumulation and activity to sustain DDR signalling. Eventually, DDR signalling pathways lead to the engagement of the diffusible kinases Chk2, which is phosphorylated by ATM, and Chk1, which is phosphorylated by ATR. These downstream kinases can then phosphorylate a number of effector proteins such as p53 and CDC25 phosphatases. The effectors are then responsible for propagating the actions of the DDR such as inducing cell cycle arrest so that the DNA lesions can be repaired before the proliferation resumes. However, in the event that the damage cannot be repaired, the DDR can induce cellular senescence or apoptosis.

complex recruit and activate the two large protein kinases ATM and ATR, respectively.

Whilst the NBS1 complex is not needed for the binding of the MRN complex to DSBs, it is required for the binding of ATM to the complex as indicated by cells expressing a truncated form of NBS1 lacking its 20 C-terminal residues (Falck et al., 2005). Experiments have shown that ATM recruitment to NBS1 requires that the MRN complex is DNA-bound. Ionising radiation treatment of soluble extracts containing ATM and MRN did not enhance complex formation, whilst addition of dsDNA oligonucleotides from untreated cells to the extracts resulted in increased NBS1-ATM association. Activation of ATM by interaction with MRN results in the autophosphorylation of ATM at Ser1981. Single-stranded DNA generated at stalled replication forks or following dsDNA resection by MRN is recognised and bound by RPA, which generates a signal for ATR recruitment via its partner protein ATR-interacting protein (ATRIP) (Cortez et al., 2001). ATR kinase activity is boosted by recruitment of both the 9-1-1 complex by RPA and by topoisomerase-II-binding protein 1 (TOPBP1) (d'Adda di Fagagna, 2008). Once activated, the two kinases are able to phosphorylate multiple targets, some of which are common to both ATM and ATR, in order to further propagate the DDR.

One important component of the DDR that is a common target for both ATM and ATR is the histone variant H2AX. The kinases phosphorylate H2AX at Ser139 to generate γH2AX, foci of which are rapidly generated at DSB sites and are thought to be required for further recruitment of repair factors. This positive feedback loop, to which mediator of DNA-damage checkpoint 1 (MDC1) and p53-binding protein 1 (53BP1) are crucial, causes the recruitment of additional ATM in order to amplify ATM activity, resulting in the spread of γH2AX along the chromatin (Lou et al., 2003, Abraham, 2002). For a while, γH2AX was classified as a biomarker for DSB formation, with studies demonstrating that DSB formation via ionising radiation or cytotoxic agents causes rapid H2AX phosphorylation (Kuo and Yang, 2008). However, whilst it is true that DSB formation is complemented by γH2AX formation, not all γH2AX formation can be attributed to DSBs as other forms of DNA lesions, such as stalled replication forks, can also generate γH2AX (Cleaver et al., 2011, Cleaver, 2011). Following DNA damage repair, the foci are disassembled, which is attributed to the actions of chromatin remodelling machinery and also dedicated phosphatases, which dephosphorylate γH2AX (Downey and Durocher, 2006).

H2AX is just one of hundreds of targets of the apical kinases ATM and ATR. Two of the most important and best studied targets are the diffusible protein kinases Chk2 and Chk1, which are specifically targeted by ATM and ATR, respectively. These targets function to reduce cyclin dependent kinase (CDK) activity by various mechanisms, including those mediated by the transcription factor p53 and cell-division cycle 25 (CDC25) (Jackson and Bartek, 2009). Inhibition of this activity helps to bring about cell cycle arrest at the various cell cycle checkpoints. ATM is able to directly phosphorylate p53 at Ser15, which enhances the activity of p53 as a transcription factor (Banin et al., 1998). Chk2 is able to phosphorylate p53 at Ser20, which interferes with the p53-MDM2 interaction, causing the complex to dissociate. MDM2 is an ubiquitin ligase and targets p53 for proteasome-mediated degradation (Ryan et al., 2001). This dissociation and the enhancement of p53 activity allows it to induce the transcription of p21, a CDK inhibitor, which results in cell cycle arrest (Deng et al., 1995). Chk1 is responsible for phosphorylating the checkpoint phosphatase CDC25, which marks it for degradation. Normally, CDC25 functions to dephosphorylate and maintain the activity of CDK2 and CDK1. CDK2 governs the G1-S transition and S phase progression whilst CDK1 governs transition from G2 into mitosis (Falck et al., 2002). Therefore, DNA-damage induced CDC25 inactivation prevents cell-cycle checkpoint transition and results in cell cycle arrest. ATM, ATR, Chk2 and Chk1 also activate a number of targets involved in activating the various DNA damage repair pathways, with different targets activated depending on the type of lesion to be repaired.

X. UVR and the DNA damage response

As with all exogenous and endogenous damaging agents, studying the mechanics of the DDR in response to these agents can provide significant insight into the mechanisms by which they generate damage and how their repair is initiated. UVR is no exception and a number of research groups have looked at both UVB and UVA and how the DDR is affected by them. One of the initial stages of the DDR is the activation and recruitment of ATM and ATR following the detection of different DNA lesions by the MRN and 9-1-1 complexes, respectively. UVA and UVB have been shown by several studies to be able to increase the levels of both ATM and ATR, suggesting that both DSBs and replication stress are involved in the DNA damaging mechanisms of UVR (Ray et al., 2016, Girard et al., 2008). A key target for ATM and ATR and thus a key component in the DDR is the histone variant H2AX. Its

phosphorylation on serine 139 to yield γH2AX, is associated with DSB repair and other lesions formed following UVR exposure (Barnes et al., 2010).

In 2010, Barnes et al. demonstrated that γH2AX can be used as an accurate biomarker for detecting genotoxic stress caused by UV-irradiation both in vitro, in both keratinocyte cell culture and within an artificial epidermis, as well as in vivo in human skin. They showed that apparently stress-free keratinocytes activated γH2AX as a result of damage from endogenous sources, especially within S phase, but this activation increased following exposure to 0.1 kJ m^{-2} UVB with maximum activation seen 2 h post exposure and baseline levels returning at 24h. A dose of 0.2 kJ m^{-2} however resulted in much greater activation with maximum activation at 8 h post exposure. Similar results were observed following application of the same doses of UVB to an artificial epidermis, which demonstrated a significant increase in signal throughout the entire epidermis 2 h post irradiation. An even higher signal intensity seen for the higher dose, with a maximum reached at 8 h post exposure. In vivo investigations in four volunteers showed that 24 h post irradiation, the majority of the epidermal and dermal cells had intense pan-nuclear staining for γH2AX. They also found a correlation of UVB-induced phosphorylation of both H2AX and p53.

The involvement of γH2AX in the UVR-induced DDR was both supported and expanded upon by investigations into DNA damage of mice skin following UVA and UVB irradiation at physiological doses in mice skin (Svobodová et al., 2012). A significant dose dependent increase in γH2AX positive cells was seen in the basal layer and entire epidermis following UVB at both 2 kJ m^{-2} and 8 kJ m^{-2} at both 4 h and 24 h post irradiation. UVA at doses of 100 and 200 kJ m^{-2} did not stimulate γH2AX formation, which was in agreement with other papers that sunburn cells are not produced following UVA irradiation (Takeuchi et al., 2004, Lavker and Kaidbey, 1997). However, there are inconsistencies in the research regarding the ability of UVA to induce γH2AX formation, as other studies have shown that UVA can induce γH2AX formation (Stixova et al., 2014, Wischermann et al., 2008). Wischermann et al. (2008) used UVA doses of 100 to 600 kJ m^{-2} and observed a dose-dependent increase in the number of γH2AX foci generated following UVA exposure.

Another key player in the DDR is the transcription factor p53, which has been termed the ‘guardian of the genome,’ due to its important function as a tumour suppressor and cell-cycle regulator (Menendez et al., 2009). The importance of p53 in the DDR following UVR exposure is highlighted by evidence that mice which possess a *p53* knockout are hyerpsensitive to the induction of skin cancers by UVR exposure (Jiang

et al., 1999). In comparing how DDR component activation in primary human skin cells differ following exposure to UVA or UVB irradiation, Runger et al. (2012), using the same physiological and equimutagenic doses (100-300 J m^{-2} UVB, 100-300 kJ m^{-2} UVA) found that UVB was more prominent at inducing p53-mediated cell cycle arrest than UVA. This was due to UVB being able to cause phosphorylation of p53 at Ser15 more efficiently than UVA. Similar doses applied to mice skin by Svobodova et al. (2012) observed similar increases in phospho-p53, again with the increase being more apparent in UVB treated mice. The increased p53-mediated cell cycle arrest seen following UVB could explain why lesions generated by UVA have greater toxicity and mutagenic potential, due to the decreased time available for the lesions to be repaired.

Recent studies have reported that signal transducer and activator of transcription 3 (STAT3) is required for efficient repair of UV-induced DNA lesions by modulating the ATM-Chk2 and ATR-Chk1 interactions (Liao et al., 2015, Barry et al., 2010). A431 human epidermoid cancer cells exposed to UVR showed that STAT3 enhanced activation of ATR at both mRNA and protein levels and regulated ATR activity following DNA damage. STAT3 is also responsible for downregulating the transcription of microRNA-383. This miRNA is itself able to suppress ATR activation and so these results taken together suggests that STAT3 regulates ATR activation of of expression via miRNA. This provides increasing evidence for the role of miRNAs, which are critical regulators of gene expression, in the DDR. The miRNA was found to target the 3'-untranslated region of ATR mRNA, downregulating ATR activation, whilst STAT3 functions to downregulate the miRNA-383 promoter. Alternatively, there is evidence that miRNA expression following UVR exposure can result in enhancement of the DDR (Pothof et al., 2009). Here, silencing of essential components of the miRNA processing pathway, such as Dicer and Ago2, compromised cell survival and checkpoint response following UV exposure. Furthermore, it has been demonstrated that UVA and UVB irradiation of human primary keratincoytes differentially regulates the expression of several cellular miRNAs (Kraemer et al., 2013). They demonstrated miRNAs expressed specifically following either UVB or UVA irradiation, such as miR-23b, a human keratinocyte differentiation marker, which was up-regulated following UVA irradiation.

A recent study has provided insight into the DDR of human melanocytes following UV irradiation. MC1R, a G protein-coupled receptor important in human pigmentation diversity, was shown to be activated by α-melanocortin following UVR exposure (Swope et al., 2014). This leads to enhancement of CPD repair by upregulation of

XPC, the enzyme responsible for the detection of DNA lesions in NER, and increased UV-induction of ATM and ATR, ultimately leading to increased levels of γH2AX. The *MC1R* gene confers melanoma susceptibility, with some of its alleles being strongly associated with red hair phenotype and therefore increased risk of melanoma. Expression of two of these alleles, either hetereozygously or homozygously resulted in loss of function of MC1R in melanocytes and compromised DNA repair capacity.

Understanding how the different components of UVR effect the mechanics of the DDR holds significant importance for understanding how the lesions are generated and repaired. Despite making up 90-95% of the terrestrial UVR we are exposed to, much less is understood about how UVA contributes to carcinogenesis in comparison to UVB. This research project therefore aims to look at how environmentally relevant doses of UVA impact the DNA damage response, with particular emphasis on how the DDR changes over time following UVA exposure, providing insight into how the DDR remains activated when cells are no longer exposed to UVA irradiation. The project will also consider the role of the UVA-induced bystander effect on DDR activation. Considering how directly irradiated cells can influence the DDR in nearby cells which received no irradiation is important due to the fact that not all cells within the skin will absorb UVR, but can still become damaged due to signals received through the radiation-induced bystander effect.

2. Materials and Methods

I. Media and Buffers

Table 2.1

Buffer/Media Name	Components	pH
Lonza BioWhittaker™ Dulbecco's Modified Eagle's Medium w/ 4.5 g/L Glucose w/ L-glutamine and phenol red	Supplemented with 10% FCS and 100 U/ml penicillin and 100 μg/ml steptomycin (Gibco)	7-7.4
Lonza BioWhittaker™ Dulbecco's Modified Eagle's Medium w/ 4.5 g/L Glucose w/o L-glutamine and phenol red	Supplemented with 10% FCS and 4 mM L-glutamine (Gibco)	7-7.4
10X TGS	250 mM Tris (Melford), 1.92 M glycine (Melford), 1% SDS	8.3
10X TBST	10X TBS solution (Melford) contains 0.25 M Tris, 1.37 M NaCl, 0.027 M KCl. 1X TBS solution contains 0.1% Tween-20 (Sigma)	7.6
RIPA++ buffer	25 mM Tris, 150 mM NaCl, 0.1% SDS, 0.5% sodium deoxycholate, 1% Triton X 100. Supplemented with Roche cOmplete™ Mini, EDTA-free protease inhibitor cocktail tablets and Roche PhosSTOP phosphatase inhibitor cocktail tablets	7.4
Semi-dry transfer buffer	7.2 g Trisma base (Sigma), 0.44 g CAPs (Sigma) 20 ml ethanol (Fisher), 0.4 ml 10% w/v SDS (Melford**)** up to 200 ml milli-Q H_2O	

II. Antibodies

Table 2.2

Antibody	Concentration used	Supplier
Histone H2AX (pSer139) Mouse monoclonal antibody	Western blot 1:2000 Immunofluorescence 1:400	EpiGentek (A-0466-200)
Phospho-Chk2 (Thr68) Rabbit monoclonal antibody	Western blot 1:2000	Cell signalling technologies (from cell cycle/checkpoint antibody sampler kit) (9917T)
Purified mouse anti-actin Ab-5 monocolonal antibody	Western blot 1:2000	BD Bioscience (612656)
Sheep anti-mouse IgG (HRP) polyclonal secondary antibody	Western blot 1:4000	Abcam (ab6808)
Goat anti-rabbit IgG (HRP) polyclonal secondary antibody	Western blot 1:4000	Abcam (ab9721)
Alexa Fluor 488 goat anti-mouse IgG	Immunofluorescence 1:1000	Life technologies (A-11001)

III. Cell culture

HaCaT keratinocytes were cultured in 75 cm^2 cell culture flasks in 20 ml DMEM supplemented w/ 4.5 g/L glucose w/ L-glutamine and phenol red (Lonza, Table 2.1) and grown at 37^{o}C 5% CO_2. The cells were passaged when 80% confluency was reached. The media was removed from the culture cells and the cells washed once with PBS, using at least the same volume of PBS as culture media. Cells were treated with 12 ml of 0.5 mM EDTA (Invitrogen) in PBS and incubated at 37^{o}C 5% CO_2 for 12 min. This helps to detach the desmosomes. The PBS-EDTA was removed and 1 ml 0.25% trypsin-EDTA (1X) (Gibco) was added. The cells were incubated at 37^{o}C 5% CO_2 until they had detached. The trypsinisation reaction was neutralised by addition of 2 ml supplemented DMEM. The cells were pelleted by centrifugation at 5000 x g 5 min. The supernatant was removed and the cells resuspended in DMEM. For experiments where cells were to be irradiated, cells were resuspended in phenol

red free DMEM. Cell counts were performed and the required volume prepared according to the assay or experiment to be performed.

IV. Ultraviolet A irradiation

In this experiment, UVA doses up to 100 kJ m^{-2}, which represents an environmentally relevant dose, were used. Cells were seeded into different types of culture dishes at densities suitable for the experimental demands and were grown until attachment. All irradiations were performed in DMEM supplemented with FCS and L-glutamine and did not contain phenol red as it can function as a photosensitiser (Table 2.1). UVA irradiation was performed using seven Phillips TLR 36W tubes. Wavelengths below 320 nm were filtered out using Mylar film. The UVA output was measuring using a double monochromator spectroadiometer (Model SR911-PC, Macam Photometrics, UK) with peak output measured at 365 nm.

V. Inhibitor and drug treatments

Various compounds that inhibit different components of the DNA damage response or induced DNA damage were used. For each inhibitor, cells were pretreated for 1 h prior to irradiation with UVA. ATM inhibitor (Ku-60019, Selleckchem) and ATR inhibitor (VE-821, Selleckchem) were used at concentrations up to 1.0 μM, depending on the experiment being carried out. PI3K inhibitor (LY294002, Cell guidance systems) was used at a concentration of 50 μM. Mirin (CAS 299953-00-7, Santa Cruz) an inhibitor of the MRN complex, was used at a concentration of 100 μM.

VI. Cell viability assays

The effect of UVA in conjunction with inhibitor treatments on cell viability was monitored by MTT and XTT assays, colourimetric assays for assessing cell metabolic activity. In both cases, HaCaT cells were seeded in 96-well plates at a density of 5000 cells/well in a total volume of 100 μl phenol red free DMEM per well. Cells to be irradiated with UVA were seeded on separate 96-well plates. The cells were treated with various DNA damage response component inhibitors in triplicate and incubated at 37°C 5% CO_2 for 1 h before UVA exposure. Following UVA irradiation, the plates were incubated at 37°C 5% CO_2 for 24 h.

Next, for the MTT cell viability assay, 20 μl 5 mg/ml MTT solution was added to each well and plates incubated at 37ºC 5% CO_2 for 3 h. A triplicate set of control wells containing MTT only was included. The media was carefully removed without disturbing the cells and without rinsing with PBS. Formazan crystals in each well were dissolved in 150 μl DMSO. Cells were agitated on an orbital shaker for 15 min and absorbance measured at 540 nm.

The XTT cell viability assay was performed using the Biotium XTT cell viability kit. 25 μl activated XTT solution (which gives a broader dynamic range of detection versus 50 μl activated solution) was added to the medium in each well. The plates were incubated for 3 h at 37ºC 5% CO_2. The absorbance signal of the wells were measured at a wavelength of 490 nm whilst background absorbances were measured at 630 nm. Absorbances were measured using a BioTek ELx808 absorbance microplate reader.

VII. Western blot analysis

For obtaining protein extracts, HaCaT cells were seeded at 3 x 10^6 cells per 60 mm cell culture dish and grown until 70-80% confluent prior to UVA irradiation. Following irradiation, the media was removed and the cells washed with 1X PBS. Residual PBS was removed using an aspirator. Total protein extracts were obtained by addition of 150 μl RIPA++ (contains protease and phosphatase inhibitors; Table 2.1) and harvesting with a cell scraper before being transferred to microcentrifuge tubes. Cells were harvested on ice at various points post irradiation according to the demands of the experiment. Cellular debris was pelleted by centrifugation at 13,000 rpm for 10 min at 4ºC. Protein concentrations were determined via Bradford assay using RIPA++ to generate a blank and various concentrations up to 1 mg/ml BSA (Sigma-Aldrich) were used to generate a standard curve. The samples were normalised to each other and the volumes required for 10 mg of each sample was determined. The volume was made up to 10 μl with 1X PBS and samples boiled for 10 min in 3X SDS loading buffer (188 mM Tris-Cl (pH 6.8), 3% SDS, 30% glycerol, 0.01% bromophenol blue, 15% β-mercaptoethanol). Protein extracts were electrophoresed in 1X TGS running buffer (Table 1) on a 4-15% gradient TGX gel (Bio-Rad) at 200V. Using a semidry transfer at 63 mA constant (per gel) for 2 h, the proteins were blotted on to Immobilon-P polyvinylidene difluoride membrane (Sigma-Aldrich). Prior to transfer, the PVDF the membrane was activated by addition of methanol, which was then

removed and excess washed off. After blocking with 5% w/v non-fat milk in 1X TBST, membranes was incubated with primary antibody (Table 2.2), which was diluted in 5% milk in 1X TBST. Prior to incubation with the secondary antibody, the membrane was washed three times with 1X TBST. The membrane was then washed five times with 1X TBST and the antibodies detected using Pierce ECL Plus western blotting substrate (Thermo Scientific). Western blot images were taken using a Bio-Rad ChemiDoc™ MP system.

VIII. Immunofluorescence

For immunofluorescence experiments, 2 x 10^5 cells were seeded onto 15 mm coverslips, which were contained within 35 mm cell culture dishes. Following UVA irradiation, cells were washed once with 1X PBS and fixed with 4% PFA at room temperature for 20 min. For experiments where replicating cells were to be detected, a Click-iT® EdU Alexa Fluor 555 Imaging kit (C10339, Invitrogen) was used to label replicating cells. 10 μM EdU (component A) was added at 1:1000 to the coverslip and incubated for 1 h prior to fixation. Cells were fixed at various points following irradiation to comply with demands of the experiment. After fixation, cells were washed three times in PBS and then permeabalised in 0.5% Triton X 100 in PBS at room temperature for 10 min. The permeabilisation buffer was removed and the coverslips washed three times in 1X PBS. 500 μL of Click-iT reaction cocktail per coverslip was prepared according to the instructions provided by the kit. The plates were incubated for 30 min at room temperature, protected from the light. All subsequent incubation steps were carried out with the samples protected from the light. The coverslips were washed three times in PBS and were transferred onto labelled Para film in a humidified chamber. Fresh 3% BSA in PBS was used to block the fixed cells for 1 h at room temperature. The coverslips were incubated for 1 h in γH2AX primary antibody (Table 2.2) at a concentration of 1:400 in 3% BSA in PBS. The coverslips were washed three times in 1X PBS prior to 1 h incubation with the anti-mouse Alexa fluor 488 secondary antibody, 1:1000 in 3% BSA in 1X PBS (Table 2.2). Following incubation with the secondary antibody, coverslips were washed five times in PBS and rinsed with ddH_2O. Excess water was removed from the coverslips and they were then mounted onto slides using Vectashield mounting medium containing DAPI (Vector Labs). Once dried, the slides were sealed with clear nail varnish and stored at 4°C, shielded from light ready for visualisation by microscopy using a Zeiss LSM 880 confocal microscope. Zen from Zeiss was used to generate

images and measure the intensity of the AlexaFluor 488 signal in order to quantify γH2AX activation. Categorical scatter graphs used to display data from each analysed nucleus was generated using Graphpad Prism 7.

IX. Bystander effect experiments

To investigate the ability of UVA to induce the radiation-induced bystander effect, irradiated and nonirradiated cells were co-incubated in six well dishes, with a sterile insert separating the two cell populations by a 1-μm-pore membrane (Greiner bio-one) to allow diffusion of medium components between the two populations. The experimental design is outlined below in Figure 2.1a. The mechanism by which signals pass between the separate cell populations is shown in Figure 2.1b. The co-culture method used does not require collection and transfer of conditioned media between cell populations, providing an improvement over some previous methods used to investigate the radiation-induced bystander effect. The model allows partial simulation of the skin environment to be made as it allows investigation of paracrine signalling between differentially treated feeder and bystander cells to be investigated. This would be the case within the skin as not all cells would directly absorb UVA radiation.

HaCaT cells were seeded at a density of 5000 cells/insert in 1 ml phenol red free DMEM (Table 2.1) and were incubated in six-well plates with each well containing 2 ml phenol red free DMEM. These would be the irradiated cells. For experiments where immunofluorescence was to be carried out, coverslips were placed in the wells of separate six-well plates and HaCaT cells seeded at a density of 1×10^5 cells/well in 2 ml phenol red DMEM. For experiments where clonogenic analysis was to be carried out, cells were seeded at a density of 200 cells/well in 2 ml phenol red DMEM. These would be the nonirradiated bystander cells. Phenol red is a photosensitiser, therefore, phenol red and antibiotic free medium was used for the irradiated cells. Phenol red medium was used for the bystander cells to prevent infection following extended periods of incubation, as the medium is supplemented with penicillin and streptomycin. Inserts which were to be irradiated with UVA or different doses of UVA were incubated in separate six-well plates. Immediately prior to irradiation, the nonirradiated control inserts were transferred to six-well plates containing the nonirradiated bystander cells and following irradiation with UVA, the irradiated inserts were transferred to six-well plates containing the bystander cells.

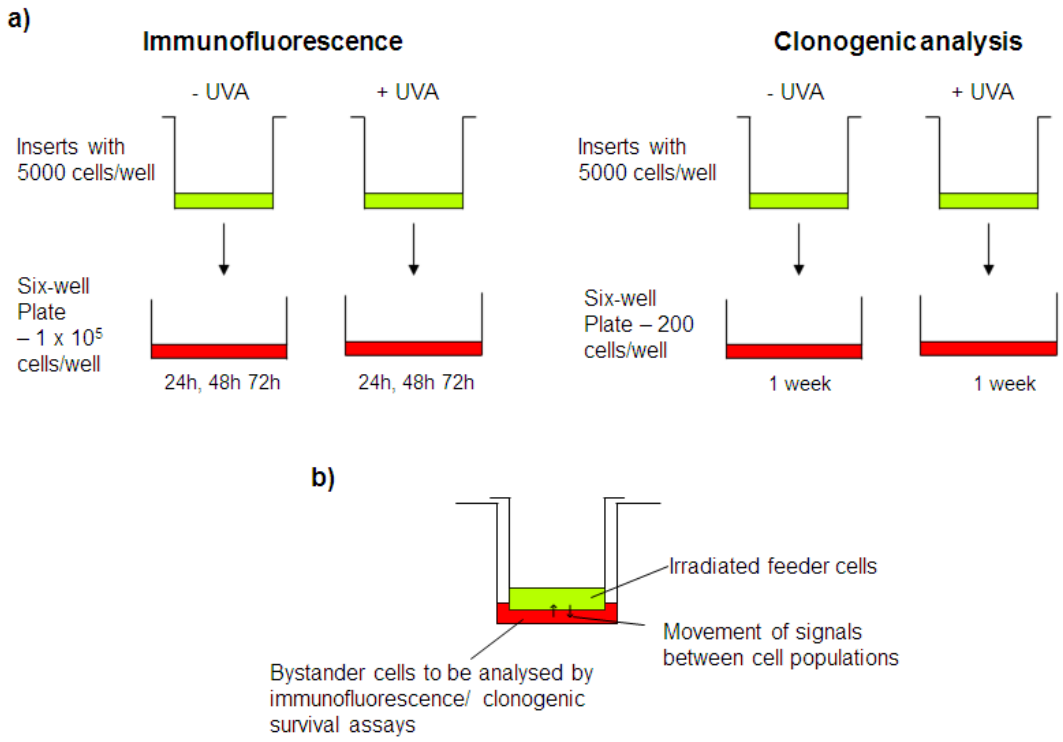

Figure 2.1. Bystander effect experimental design

(a) HaCaT keratinocytes to be irradiated were seeded at a density of 5000 cells/insert. The bystander cells were seeded at densities of either 1 x 10^5 cells/well for immunofluorescence, in which the wells also contained a coverslip, or 200 cells/well for clonogenics. Post-irradiation, the inserts were transferred to the six-well plates containing the bystander cells. Control inserts containing cells that had not received any irradiation were transferred prior to any irradiations. The plates containing both the inserts and bystander cells were incubated according to the experimental demands. (b) Example of the co-culture system used to induce the bystander effect following the transfer of the inserts containing the irradiated cells to the six-well plates containing the bystander

The plates were incubated at 37ºC 5% CO_2 and bystander cells processed according to the experimental demands.

X. Clonogenic analysis

The UVA-induced bystander effect was investigated using clonogenic survival assays. HaCaT cells were seeded in inserts at a density of 5000 cell/well and the bystander cells seeded at a density of 200 cell/well in six-well plates. Each experimental condition was set up in triplicate. Prior to irradiation, the nonirradiated control inserts were transferred to six well plates. The remaining inserts were

irradiated with 12.5, 25, 50 and 100 kJ m^{-2} UVA and then immediately transferred to six well plates containing the bystander cells and incubated at 37^{o}C and 5% CO_2. After seven days, the resulting colonies were fixed in 70% ethanol (Fisher) with 20 min incubation at room temperature and stained with 5% Giemsa (Fluka) through 20 min incubation at room temperature. The stain was removed to waste and the wells washed with water and left to air dry. For each well, the number of colonies was determined and mean percentage survival calculated relative to the nonirradiated controls.

3. Results

Ultraviolet radiation is composed of different waveband components, UVA, UVB and UVC. The main source of UVR is solar radiation and the atmosphere is able to absorb all of the UVC waveband, 90-95% of the UVB waveband whilst the UVA waveband is not absorbed. Consequently, the terrestrial UVR that we are exposed to from the sun consists of 90-95% UVA with the remainder being UVB. Both wavebands can damage cellular biomolecules, which includes DNA, and the resulting lesions can lead to mutations that can contribute towards carcinogenesis. Although both wavebands damage DNA, the theoretical mechanisms by which they do so are thought to differ, with direct absorbance of UVB by bases leading to the generation of pyrimidine dimers the accepted mechanism for UVB. On the other hand, the mechanism by which UVA generates DNA damage remains debatable, with both direct and indirect mechanisms proposed. In each case however, the generated lesions are detected by the DNA damage response, a cascade of reactions that connect the detection of the lesions with the initiation of repair following cell cycle arrest. Despite making up the vast majority of terrestrial UVR, the effect of UVA on the DNA damage response is relatively understudied in comparison to UVB. This research project therefore aims to provide further insight into how the DNA damage response is affected by UVA in both directly irradiated cells and nonirradiated, bystander cells.

I. UVA irradiation induces a dose-dependent decrease in cell survival in HaCaT keratinocytes

The DDR is responsible, through a number of complexes and mechanisms, for recognising different types of DNA damage sites and initiating numerous signalling pathways in order to bring about cell cycle arrest. This then allows for the appropriate repair mechanisms to be activated before the cell cycle can resume. However, in cases in which the damage cannot be repaired, the DDR is able to bring about cell death by either inducing senescence or apoptosis. Measuring cell viability, of which there are numerous assays and methods available, is a good way of measuring how a mutagen, in this case UVA, affects cell viability. Consequently, this can provide some initial insight into how UVA is able to activate the DDR and bring about cell death.

The XTT cell viability assay was conducted to determine cell viability following irradiation with various dosages of UVA. Doses up to 100 kJ m^{-2} were used. 100 kJ m^{-2} is an environmentally relevant dose and reflects the range observed following an hour's exposure in subtropical regions in summer months (Whiteside and McMillan, 2009). HaCaT keratinocytes were seeded at low density in triplicate in 96-well plates and were exposed to different dosages of UVA. The mean percentage survival was calculated relative to nonirradiated controls. As shown by Figure 3.1, in which mean survival was calculated based on the results of three separate experiments, cell viability gradually decreased with an increase in UVA radiation dose from 0 to 100 kJ m^{-2}, with a mean percentage survival of 39% ($p = 0.001$) seen with the highest dose used. There was no significant difference in cell survival between cells which were exposed to 25 kJ m^{-2} UVA and those which were exposed to 50 kJ m^{-2} UVA ($p = 0.578$) but there was a significant decrease in cell survival seen when increasing UVA exposure from 50 to 100 kJ m^{-2} ($p = 0.018$).

II. Inhibition of ATM and ATR caused decreased cell viability following irradiation with 50 kJ m^{-2} UVA

The DNA damage response comprises different DNA damage sensors, which are responsible for detecting different types of generated lesions. Whilst the MRN complex recognises DSBs, the 9-1-1 complex and RPA cooperate to detect stalled replication forks. To evaluate the role of the different arms of the DDR in responding to UVA, cell viability following UVA irradiation was investigated in conjunction with inhibition of different components of the DDR. An MTT cell viability assay was used to investigate how inhibition of ATM, which is downstream of the MRN complex, and ATR, which is downstream of the 9-1-1 complex, affected cell survival following irradiation with 50 kJ m^{-2} UVA. Ku-60019 (IC_{50} = 6.3 nM) was used as the ATM inhibitor whilst VE-821 (IC_{50} = 26 nM) was used as the ATR inhibitor The inhibitors are highly selective and specific for their targets with minimal cross reactivity against related PIKKs. Concentrations up to 1 μM of each inhibitor were used and HaCaT keratinocytes seeded at low density in triplicate in 96-well plates as before were pre-treated with different inhibitor concentrations for 1 h prior to receiving UVA irradiation. Appropriate controls which received no UVA exposure were also included. Absolute survival in the absence of any irradiation was calculated relative to untreated controls to determine how inhibition of ATM and ATR affected the repair of endogenous DNA damage. In the absence of UVA exposure, pre-treatment with ATM inhibitor (ATMi) and ATR inhibitor (ATRi) at each concentration was not sufficient to decrease cell survival as indicated in figure 3.2.

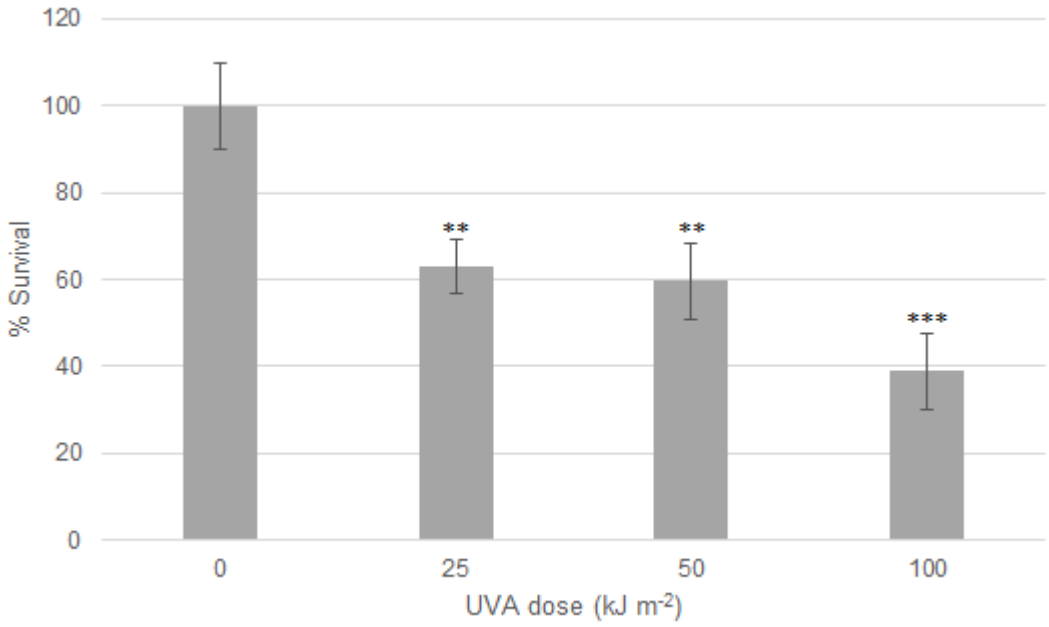

Figure 3.1. The effect of UVA on cell viability

HaCaT keratinocytes were seeded in triplicate at 5000 cells/well to a final volume of 100 μl in 96-well plates and allowed to grow for 24 h at 37ºC and 5% CO_2. Cells were irradiated with various doses of UVA from 0 to 100 kJ m^{-2} and incubated for 24 h. 25 μl activated XTT solution was added to each well and plates incubated for an addition 3 h. 25 μL was used as it provides a broader range of detection in comparison to the use of 50 μL activated reagent, which reaches signal saturation at a lower cell number. Signal absorbance was measured at 490 nm and background signals measured at 630 nm. Percentage survival was calculated relative to control cells that received no irradiation. The data presented indicates the mean survival and SD for three replicate experiments performed. **$p < 0.01$, ***$p < 0.001$ indicate the significant differences between the experimental conditions and the control group which received no UVA irradiation.

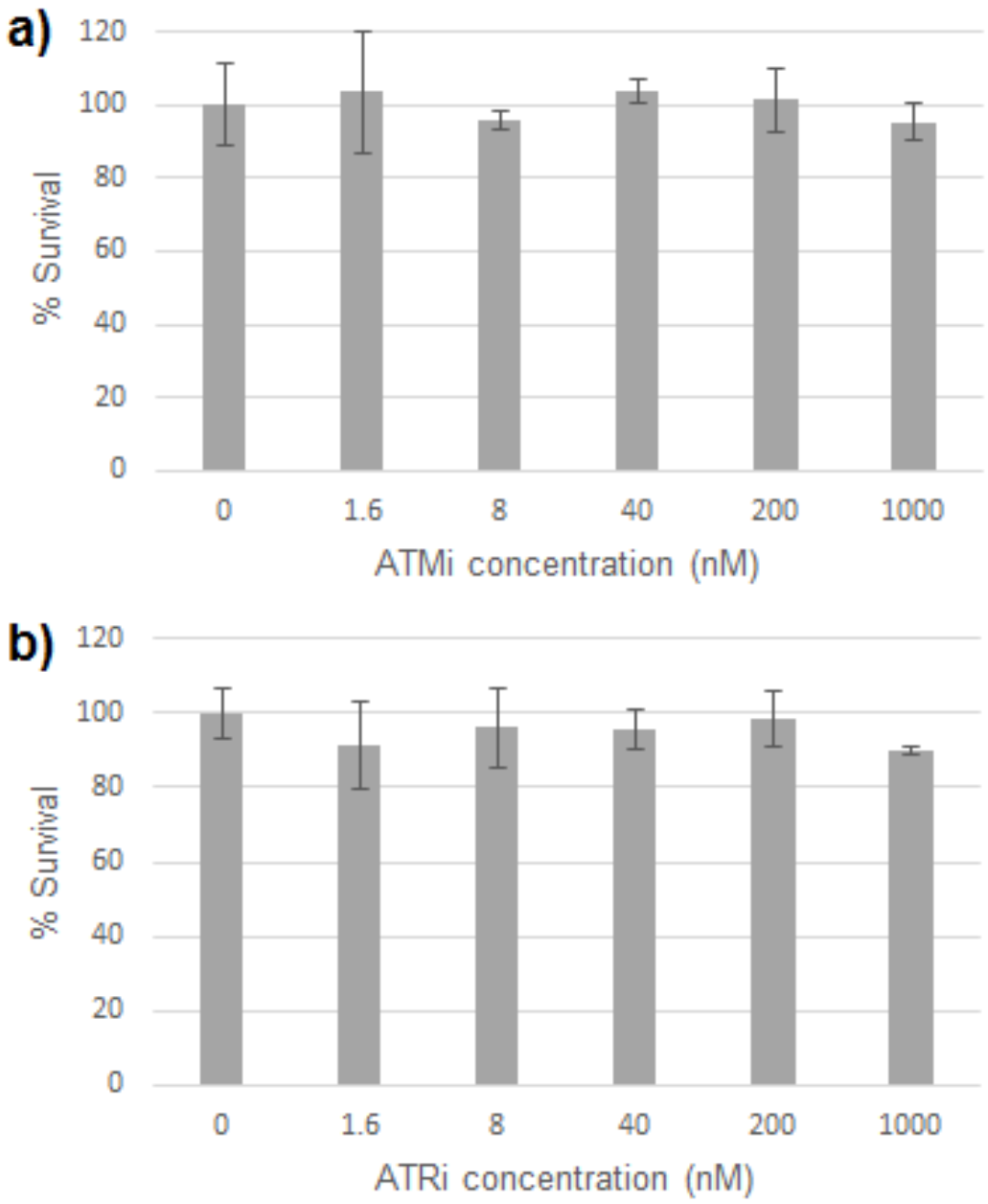

Figure 3.2. Assessment of cell viability following ATM and ATR inhibition at varying concentrations in the absence of UVA irradiation

Cell viability was investigated via MTT cell viability assays whereby cells were seeded in triplicate in 96-well plates at 5000 cells/well and incubated as with figure 3.1. Cells were pre-treated for 1 h with various concentrations of ATMi (a) or ATRi (b). Appropriate controls that received no DDR inhibition were included. Cell growth was detected by MTT assay with DMSO used to dissolve the formazan crystals and absorbance was measured at 540 nm. Cell survival was calculated for each condition in which cells were pre-treated with ATMi or ATRi relative to the untreated control condition. The data shown represents the mean survival and SD for triplicate repeats measured in a single experiment.

Following this, relative cell survival was calculated to determine how the introduction of UVA irradiation following ATM or ATR inhibition affected cell viability. Pre-treatment with ATMi and ATRi at each concentration caused decreased cellular survival following UVA irradiation relative to nonirradiated controls which had been treated with the same concentrations in a dose-dependent manner (Figure 3.3). Pre-treatment with 200 nM ATMi and ATRi followed by UVA exposure caused cell viability to decrease to 56% ($p < 0.05$) and 49% ($p < 0.05$), respectively, at which point the decrease in relative cell survival appeared to plateau, suggesting that 0.2 μM was the point at which saturation was reached for each inhibitor. This concentration was used for subsequent experiments due to its ability to decrease cell survival by approximately 40-50%.

III. Inhibition of ATM and ATR did not decrease cell viability at a higher dose of UVA

In order to investigate cell viability following UVA irradiation and DDR component inhibition further, additional components were inhibited along with ATM and ATR prior to irradiation with a higher dose of UVA than before (100 kJ m^{-2}). Here, pre-treatment with 200 nM ATMi or ATRi was compared to inhibition of PI3K (50 μM PI3Ki) and the MRN complex (100 μM mirin). The XTT assay is a more robust method for measuring cell viability as it bypasses flaws associated with the MTT assay. HaCaT keratinocytes were pre-treated with the relevant inhibitors for 1 h prior to being irradiated with UVA. Again, survival was calculated for the nonirradiated control conditions relative to controls that were completely untreated. Relative survival was then calculated for each irradiated experimental condition relative to the nonirradiated control which received the same inhibitor pre-treatment.

Once again, pre-treatment with 200 nM ATMi and ATRi did not significantly impact cell survival in the absence of UVA exposure and a similar observation was seen for nonirradiated controls pre-treated with PI3Ki and mirin (Figure 3.4). As with Figure 3.1, direct irradiation with 100 kJ m^{-2} UVA caused cell survival to decrease by approximately 60% ($p = 0.002$). With the exception of PI3Ki ($p = 0.184$), the introduction of UVA caused a significant decrease in cell survival for the irradiated conditions relative to the nonirradiated controls pre-treated with the same inhibitors ($p \leq 0.05$). However, unlike in Figure 3.3 where the inclusion of 200 nM ATMi or ATRi caused cell survival to decrease further compared to when cells were treated with 50 kJ m^{-2} UVA only, the same effect was not observed when UVA dose was increased

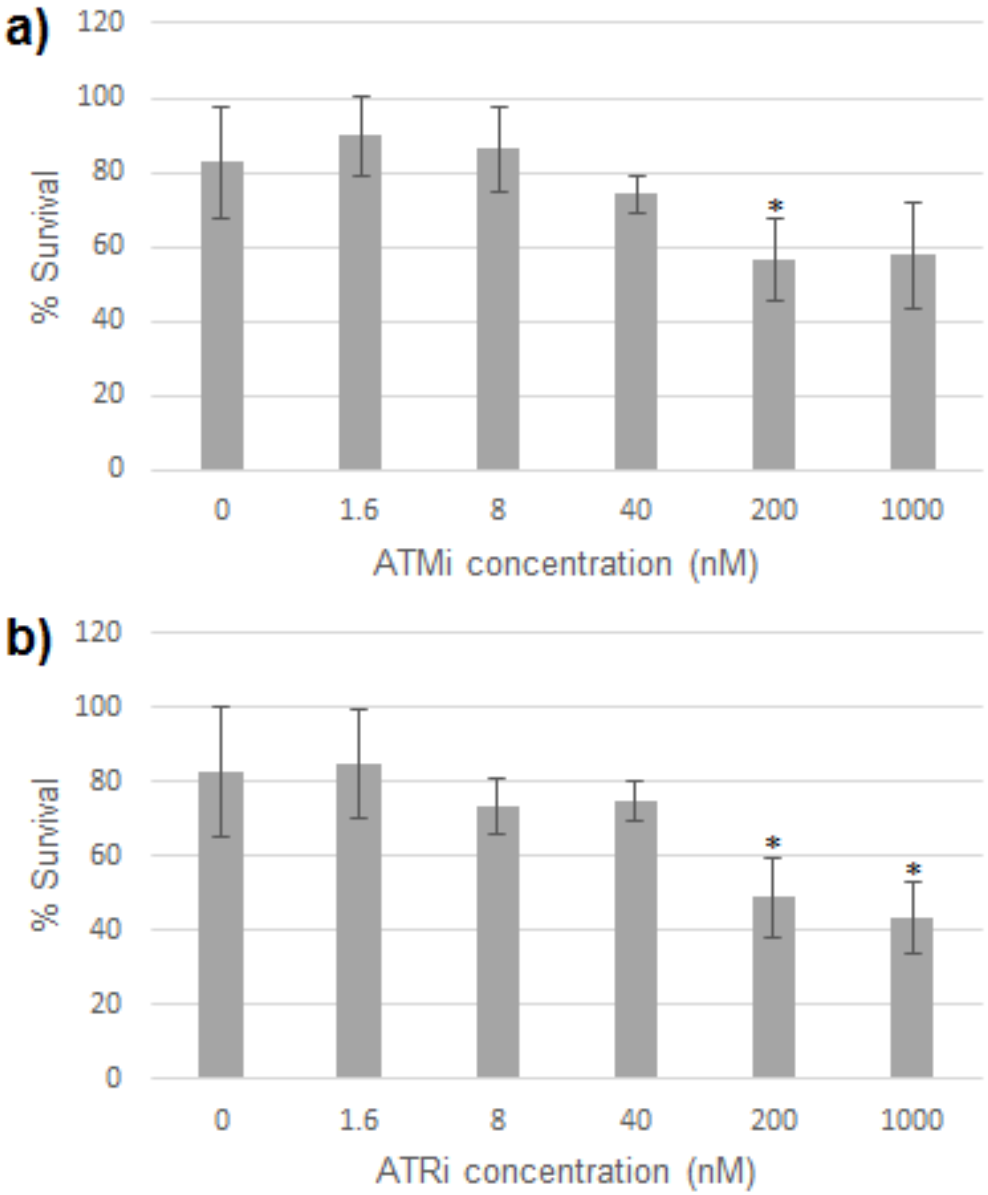

Figure 3.3. Effects of ATM and ATR inhibition on cell viability

Cell viability was again investigated via MTT cell viability assays as with figure 3.2. Cells were pre-treated for 1 h with various concentrations of ATMi (a) or ATRi (b). Following this, cells were exposed to 50 kJ m^{-2} UVA irradiation and incubated for 24 h. Appropriate controls that received no DDR inhibition, no UVA exposure or were completely untreated were included. Cell growth was detected as with Figure 3.2. Cell survival for each condition in which cells were exposed to 50 kJ m^{-2} UVA irradiation following ATMi or ATRi pre-treatment were calculated relative to nonirradiated controls pre-treated with the same inhibitor concentrations (Figure 3.2). The data shown represents the mean survival and SD for triplicate repeats measured in a single experiment. *$p \leq 0.05$ indicates the significant differences between the experimental conditions and the control group which received no UVA irradiation and pre-treatment with the same inhibitor concentration.

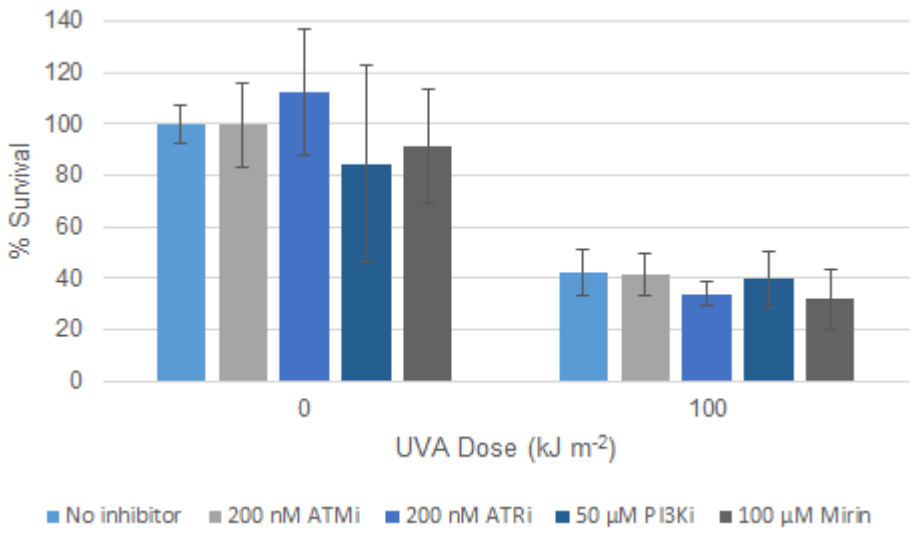

Figure 3.4. Further analysis of the effects of DDR component inhibition on cell survival following UVA exposure

HaCaT keratinocytes were seeded into 96-well plates and grown as before and cell survival determined by XTT assay as performed in figure 3.1. Cells were pre-treated with 200 nM ATMi, 200 nM ATRi, 50 µM PI3Ki or 100 µM mirin for 1 h prior to irradiation with 100 kJ m^{-2} UVA. Absolute survival was again calculated for the control conditions that received no irradiation relative to the untreated control which received no DDR inhibition. Relative cell survival was then calculated for each irradiated experimental condition relative to the corresponding control which received no irradiation. The data shown represents the mean survival and SD from three individual experiments.

to 100 kJ m^{-2}. This was also seen for the instance in which PI3K and the MRN complex were inhibited as cell survival following PI3Ki and mirin pre-treatment prior to irradiation with 100 kJ m^{-2} UVA did not significantly decrease compared to UVA irradiated cells which received no DDR inhibition.

IV. Direct irradiation with UVA and the resulting impact on the DNA damage response

As well as looking at how direct irradiation with various doses of UVA, both in the absence and in the presence of various inhibitors for DDR components, impacted cell viability by MTT and XTT assays, western blot analysis was also conducted. This was done in order to investigate how activation of components of the DDR changes over time following direct UVA exposure. Cells were irradiated with 100 kJ m^{-2} UVA and protein extracts obtained at specific time points post-irradiation. This dose was chosen as it resulted in a 60% decrease in cell survival over the course of an XTT assay (Figure 3.1 and 3.4) and would likely produce a significant number of DNA

damage lesions and therefore a pronounced DNA damage response. A component of the DDR downstream of both ATM and ATR is H2AX, which is phosphorylated by these kinases at Ser139 following DDR activation to generate γH2AX, which has been well-established as an effective biomarker for DNA damage. As indicated by figure 3.5, γH2AX activation changed over the course of the experiment following direct UVA irradiation. Whilst some γH2AX activation was present immediately following UVA exposure, activation continued to increase up until 2 h post-irradiation, where phosphorylation peaked. There was still some γH2AX activation observed at 16 h post-UVA irradiation and was abolished by 24 h, γH2AX activation was completely abolished. Chk2 phosphorylation was also analysed. Phosphorylation of Chk2 is a key event in the DDR and engagement of this diffusible kinase occurs following its phosphorylation by ATM and is responsible for phosphorylating a number of effector proteins to bring about the actions of the DDR. The UVA dose used was found to induce Chk2 phosphorylation, with maximum activity seen immediately following UVA exposure. Chk2 phosphorylation, although at decreased levels, was also present 16 h post-irradiation. Minor Chk2 phosphorylation was also seen in the 24 h untreated control condition in the figure presented but this was absent in the repeat experiments.

As with the cell viability assays, the effect of direct UVA irradiation on the DDR in HaCaT keratinocytes was then investigated further by the inclusion of ATMi. Prior to irradiation with 100 kJ m^{-2} UVA, cells were pre-treated with 0.2 μM ATMi and incubated for 1 h. Once again, DDR component activation was assessed via western blot analysis (Figure 3.6). This analysis indicated that UVA irradiation of cells that have been pre-treated with ATMi increases the time required for H2AX to become phosphorylated at Ser139 to generate γH2AX, as indicated by the delay in peak activation from 1 and 2 h post-irradiation to 4 h, with no activation observed at 1 h post UVA exposure. Interestingly however, whilst the activation of γH2AX changed in the first few hours following UVA exposure once ATM was inhibited, the same effect was not observed for the phosphorylation of Chk2. Phosphorylation of Chk2 again peaked immediately following UVA exposure and gradually decreased over time. It is important to note that due to time constraints, this experiment was only completed twice. An additional repeat is required.

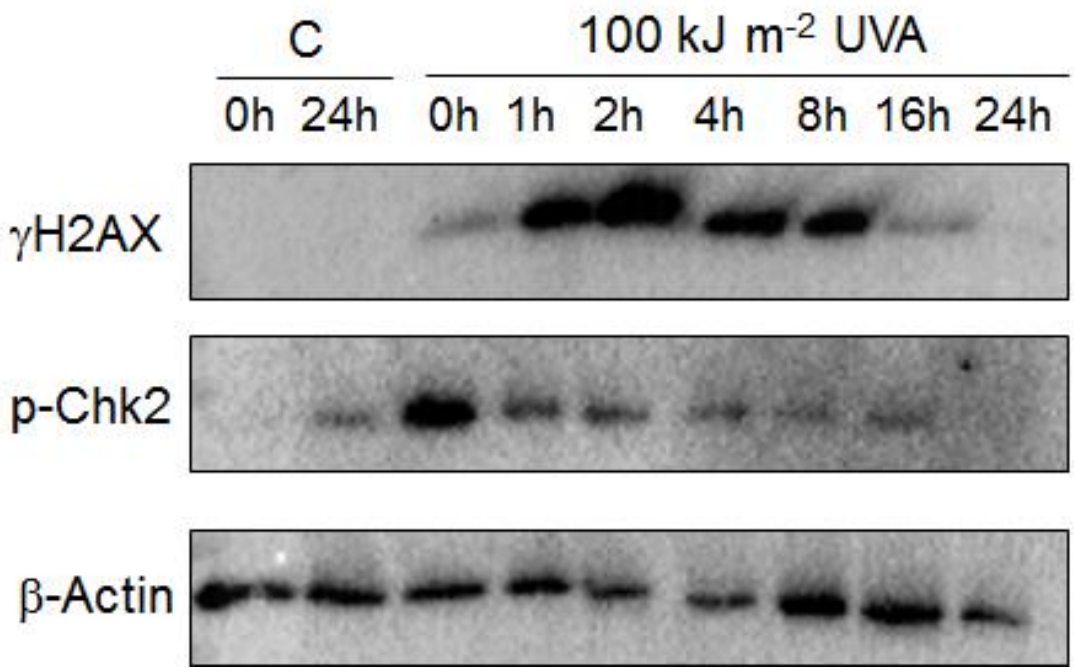

Figure 3.5. DNA damage response component activation following direct UVA exposure

HaCaT keratinocytes were seeded at a density of 3 x 10^6 cells per 60 mm cell culture dish and incubated until attachment. The cells were irradiated with 100 kJ m^{-2} UVA and protein extracts obtained at the indicated times post-irradiation using RIPA supplemented with protease and phosphatase inhibitors. Cellular debris was pelleted and protein concentrations determined via Bradford assay. Samples were ran on a 4-15% gradient TGX gel. Expression levels of γH2AX and p-Chk2 were examined via western blot analysis with β-actin was used as a load control. The data presented is representative of three individual experiments.

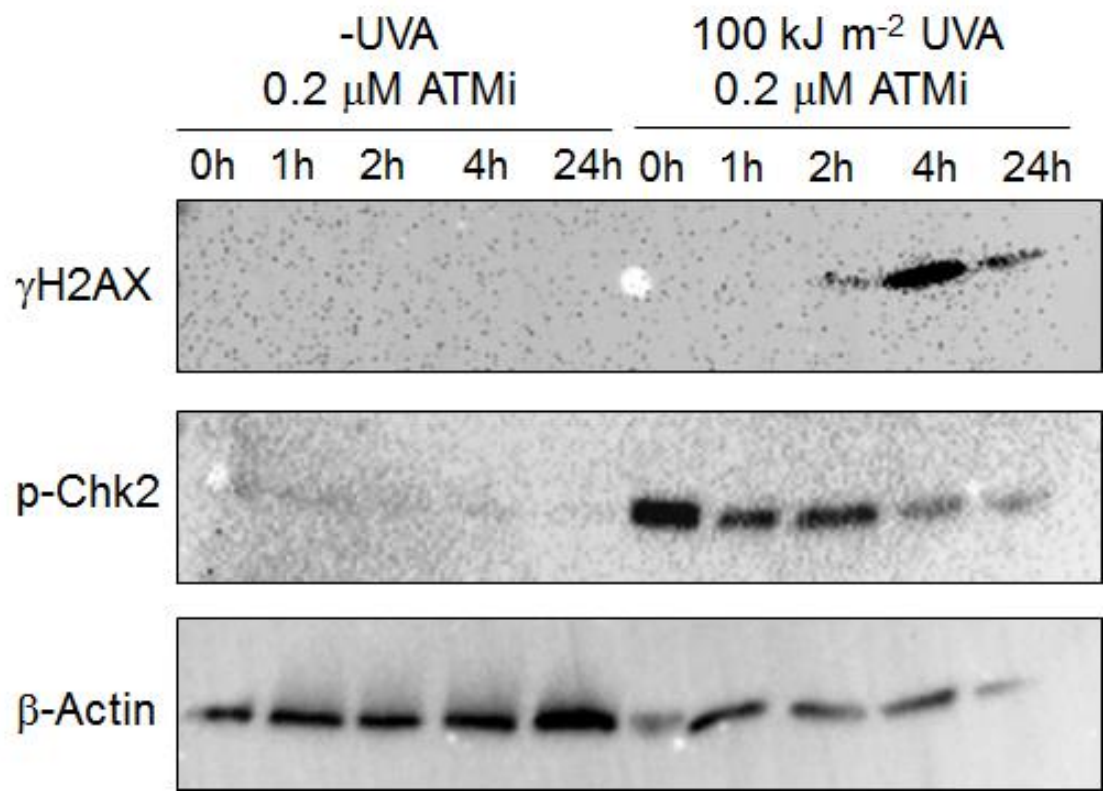

Figure 3.6. DDR component activation of UVA irradiated cells following inhibition of ATM

HaCaTs were seeded at 3 x 10^6 cells per 60 mm cell culture dish and incubated. Cells were pre-treated for 1 h prior to UVA irradiation with 0.2 μM ATMi. Cells within the experimental condition were irradiated with 100 kJ m^{-2} UVA and protein extracts obtained at the given times post-irradiation and analysed by western blot analysis using the same procedure used in Figure 3.4. Expression levels of γH2AX and p-Chk2 were examined and β-actin was used as a load control. The data shown is representative of two individual experiments.

V. Further analysis of H2AX phosphorylation following direct UVA irradiation via immunofluorescence

Immunofluorescence experiments were conducted in order to further investigate the phosphorylation of the histone variant H2AX following direct exposure to the same UVA dose at the same times post-irradiation previously investigated. A conjugated AlexaFluor 488 secondary antibody was used to detect γH2AX activation. Images were taken for each control and experimental condition (Figure 3.7). The generated signal intensity was determined for each condition using the Zen software measure feature. Individual intensity measurements were normalised to the mean intensity for that of the control 0 h condition.

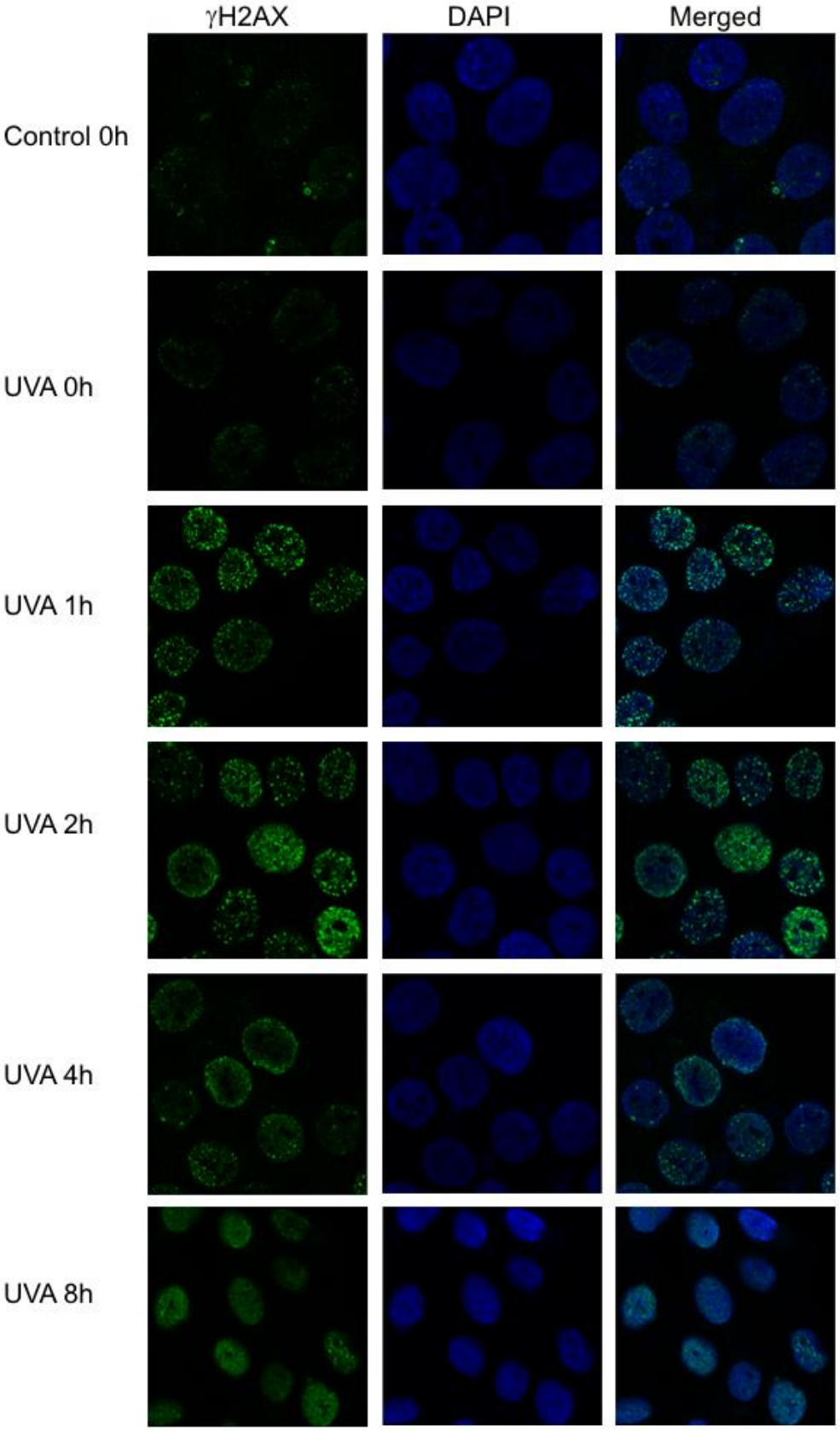
γH2AX
DAPI
Merged
Control 0h
UVA 0h
UVA 1h
UVA 2h
UVA 4h
UVA 8h

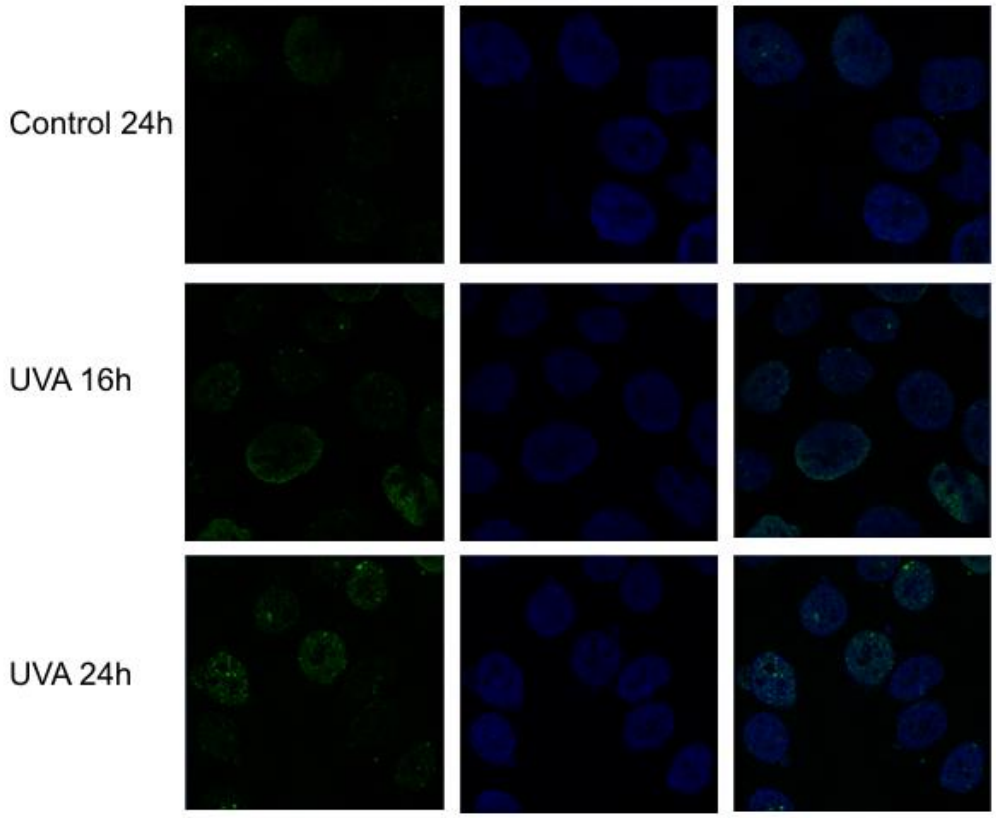

Figure 3.7. γH2AX activation following direct UVA irradiation as analysed by immunofluorescence.

HaCaT keratinocytes were seeded onto coverslips contained within 30 mm culture dishes at a density of 1.5 x 10^5 cells/plate and incubated. The cells were irradiated with 100 kJ m^{-2} UVA and cells fixed at the indicated times. Cells were stained with the appropriate γH2AX primary and AlexaFluor 488 secondary antibodies prior to being mounted using Vectashield which contained DAPI. Cells were visualised via confocal microscopy and images taken using Zen software.

As with the western blot analysis, analysis of fluorescence intensity demonstrated that γH2AX activation increased over the initial few hours following irradiation with 100 kJ m^{-2} UVA with peak intensity seen at 1, 2 and 4 h post-irradiation (Figure 3.8). There was no significant difference between the mean normalised intensities measured between these three time points. There was no significant difference between the two control conditions that received no UVA irradiation ($p = 0.569$) whilst each experimental condition had mean intensities elevated above that of the controls (UVA 0 – 8 h, $p < 0.001$; UVA 16 h, $p = 0.0353$; UVA 24 h, $p = 0.001$). Furthermore, no significant difference was calculated between cells which were fixed immediately following UVA irradiation and those which were fixed 8, 16 and 24 h post-irradiation.

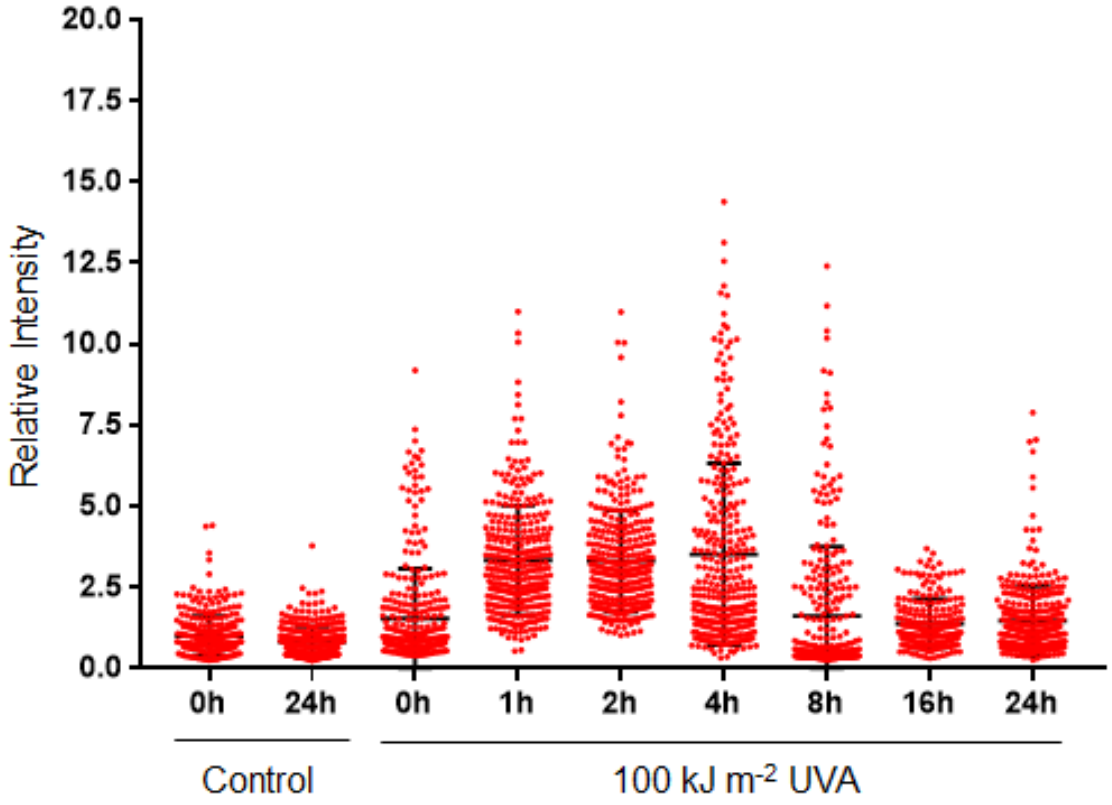

Figure 3.8. Quantification of γH2AX activation via measurement of AlexaFluor 488 signal intensity for cells directly irradiated with 100 kJ m^{-2} UVA relative to untreated controls

AlexaFluor 488 signal intensity was measured using the Zen software measure feature for the cells that were stained via immunofluorescence and visualised through confocal microscopy in Figure 3.7. The mean intensity was calculated for the control condition in which nonirradiated cells were fixed at the same time as the cells which were fixed immediately following UVA exposure. All intensity values for the control and experimental conditions were then normalised against this mean. The data represents the individual normalised values for each condition and the mean normalised intensity and SD represent that for three individual experiments, with the exception of the UVA 16 h condition, for which only two experiments were conducted. The number of cells in each condition was as follows: Control 0 h 334; 24 h 323; UVA 0 h 329, 1 h 323; 2 h 335; 4 h 313; 8 h 311; 16 h 216; 24 h = 332.

In addition to measuring the fluorescent intensities for each experimental and control condition, the type of staining was also recorded. The types of γH2AX staining were divided into three types; pan-nuclear staining, in which a γH2AX signal was distributed over the whole nucleus, γH2AX foci, where the nucleus possessed distinct foci, and negative where by the nucleus did not shown signs of pan-nuclear staining or foci or were not positively stained for γH2AX. Figure 3.9a provides representations of the different stain types recorded.

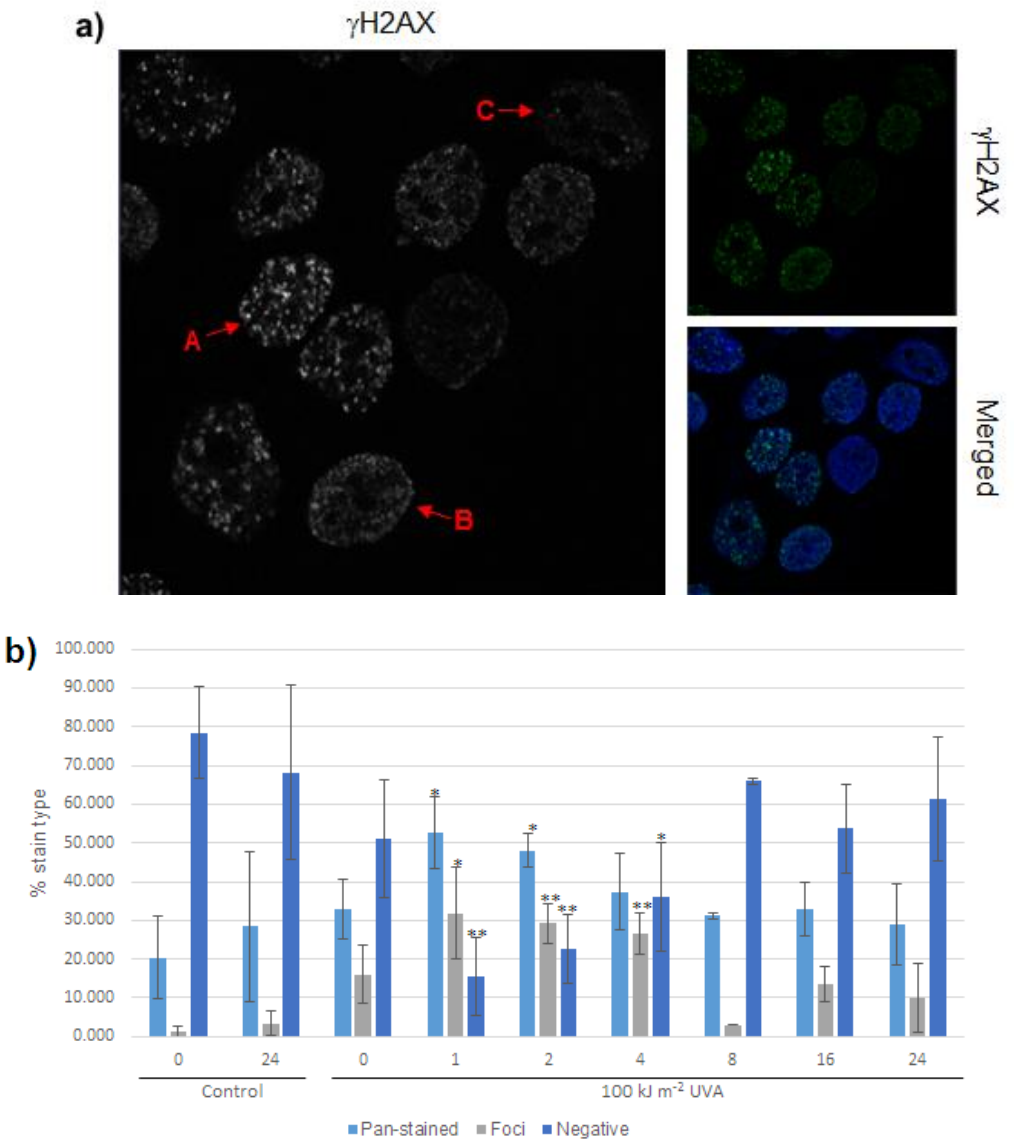

Figure 3.9. The effect of direct UVA irradiation on the type of γH2AX signal produced

The HaCaT keratinocytes that were irradiated with 100 kJ m^{-2} UVA and analysed by immunofluorescence as in figure 3.7 and 3.8 were assessed for the type of γH2AX signal that each cell presented. The types of γH2AX signal were divided into three types, pan-nuclear staining whereby the γH2AX signal was distributed across the whole nucleus, γH2AX foci where the nucleus possessed distinct foci which had a more intense signal, and negative, in which the nucleus did not show signs of pan-nuclear staining or foci or were not positively stained for γH2AX. (a) Representatives of each staining type are indicated by red arrows where (A) depicts γH2AX foci, (B) depicts pan-nuclear staining and (C) shows a negatively stained nucleus. Both black and white and colour images are shown to help distinguish the types of γH2AX staining. (b) The type of γH2AX staining presented by each cell used for data analysis in figure 3.6 was recorded and the percentage for each type of stain for each condition calculated. *$p \leq 0.05$, **$p \leq 0.01$, indicate the significant differences between the experimental conditions and the control group which received no UVA irradiation.

The type of stain presented by each cell that had its γH2AX signal intensity measured was recorded and the percentage type of stain for each condition was calculated (Figure 3.7b). Cells which received no UVA exposure were primarily negatively stained. Following exposure to 100 kJ m^{-2} UVA, the percentage of pan-nuclear stained cells increased with a peak seen for cells fixed 1 h post-irradiation, after which the number of pan-nuclear stained cells decreased. Cells fixed 1, 2 and 4 h post-irradiation had the highest number of cells with γH2AX foci, with significant increases observed relative to nonirradiated controls (UVA 1 h, $p \leq 0.05$, UVA 2, 4 h, $p \leq 0.01$). Additionally, whilst pan-nuclear staining and γH2AX foci generation increased over the initial few hours following UVA exposure, the number of negatively stained cells decreased. By 24 h post-UVA exposure, the number of cells that were neither pan-stained or had no γH2AX foci had nearly returned to the level observed for the nonirradiated controls.

VI. Immunofluorescent analysis of γH2AX activation following ATM inhibition prior to UVA irradiation

After using immunofluorescence to analyse γH2AX activation following direct irradiation with 100 kJ m^{-2} UVA, immunofluorescence was used to quantify the decrease in γH2AX activation following pre-treatment with ATMi prior to UVA irradiation. Confocal microscopy was again used to image the stained cells for each experimental and control condition (Figure 3.10a). Images for the nonirradiated controls that were either pre-treated with ATMi or were not, were excluded as there was no difference in γH2AX activation between the two control conditions and the controls included in figure 3.8 and 3.9. The γH2AX signal intensity was quantified as before and the individual measurements for each control and experimental condition was normalised against the mean value for the control in which cells received no UVA exposure or ATM inhibition and were fixed at the same time as those fixed immediately following UVA exposure.

As before, irradiation with 100 kJ m^{-2} UVA, in the absence of ATM inhibition, caused a marked increase in γH2AX signal intensity relative to untreated controls (Figure 3.10b). Similarly, cells pre-treated with ATMi prior to UVA exposure had significantly increased γH2AX activation compared to controls which received ATM inhibition but no UVA exposure ($p < 0.001$). The ATM inhibitor pre-treatment caused the intensity of the γH2AX signal to significantly decrease

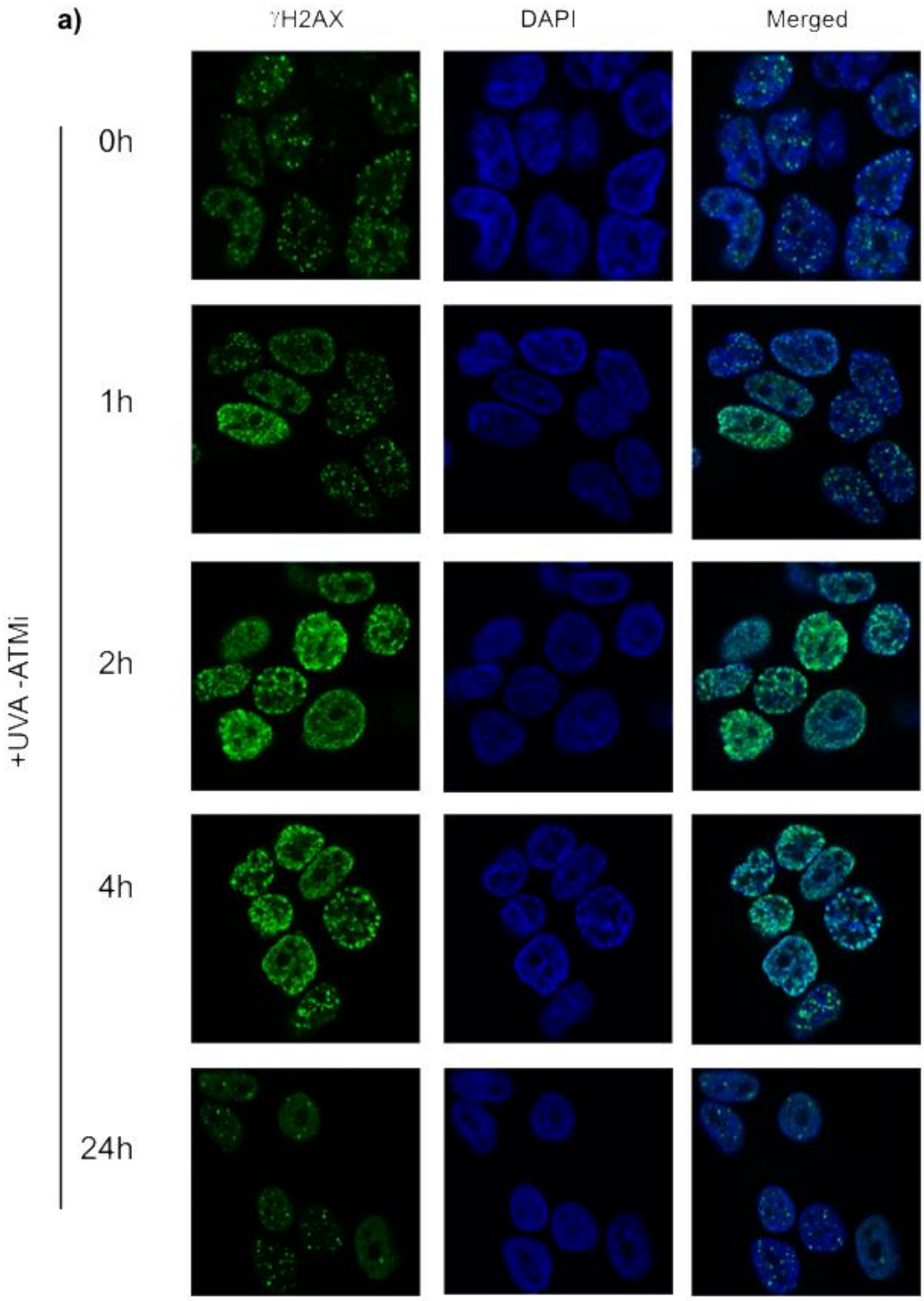
a)
γH2AX
DAPI
Merged
0h
1h
2h
4h
24h
+UVA -ATMi

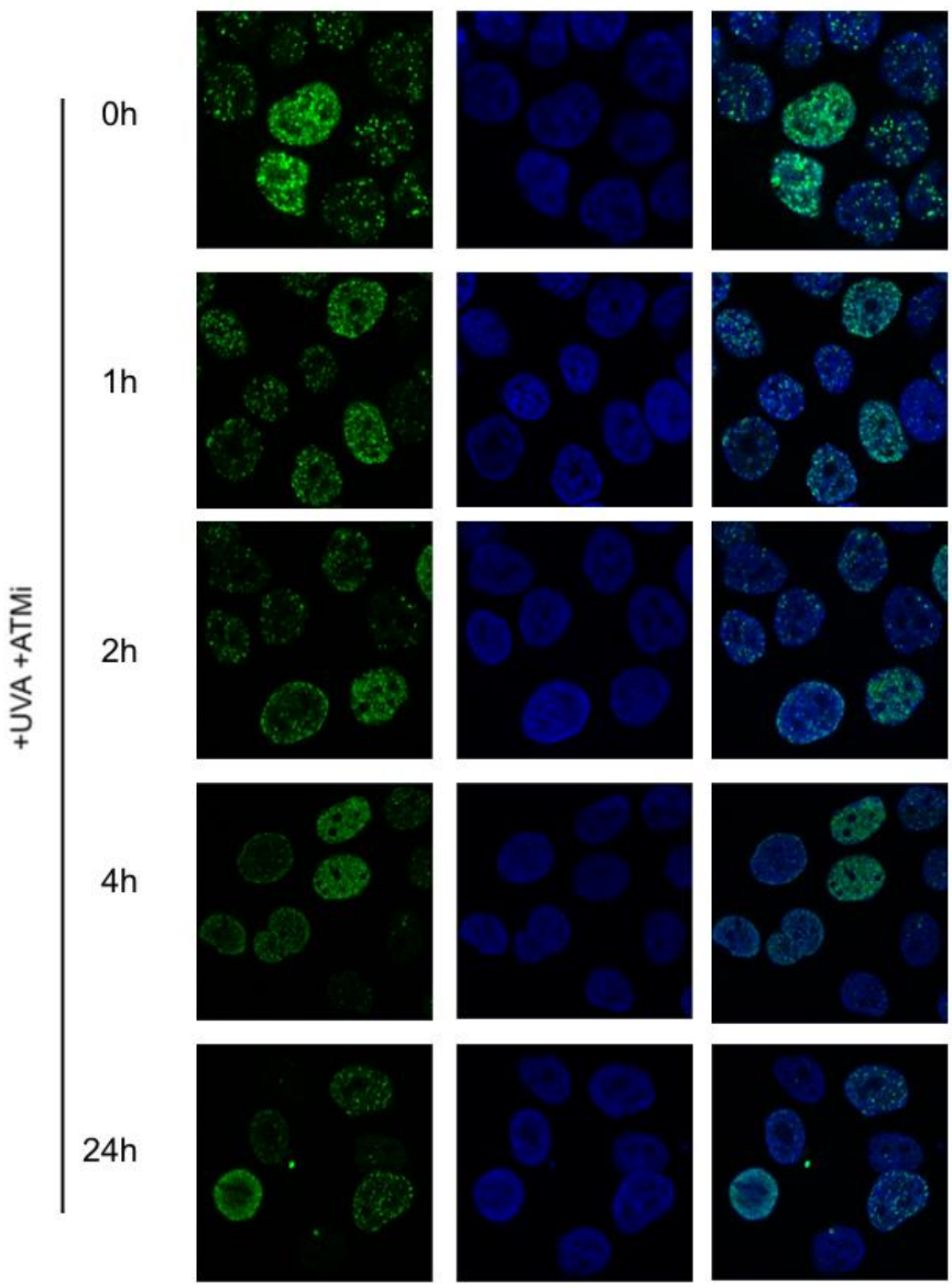
+UVA +ATMi
0h
1h
2h
4h
24h

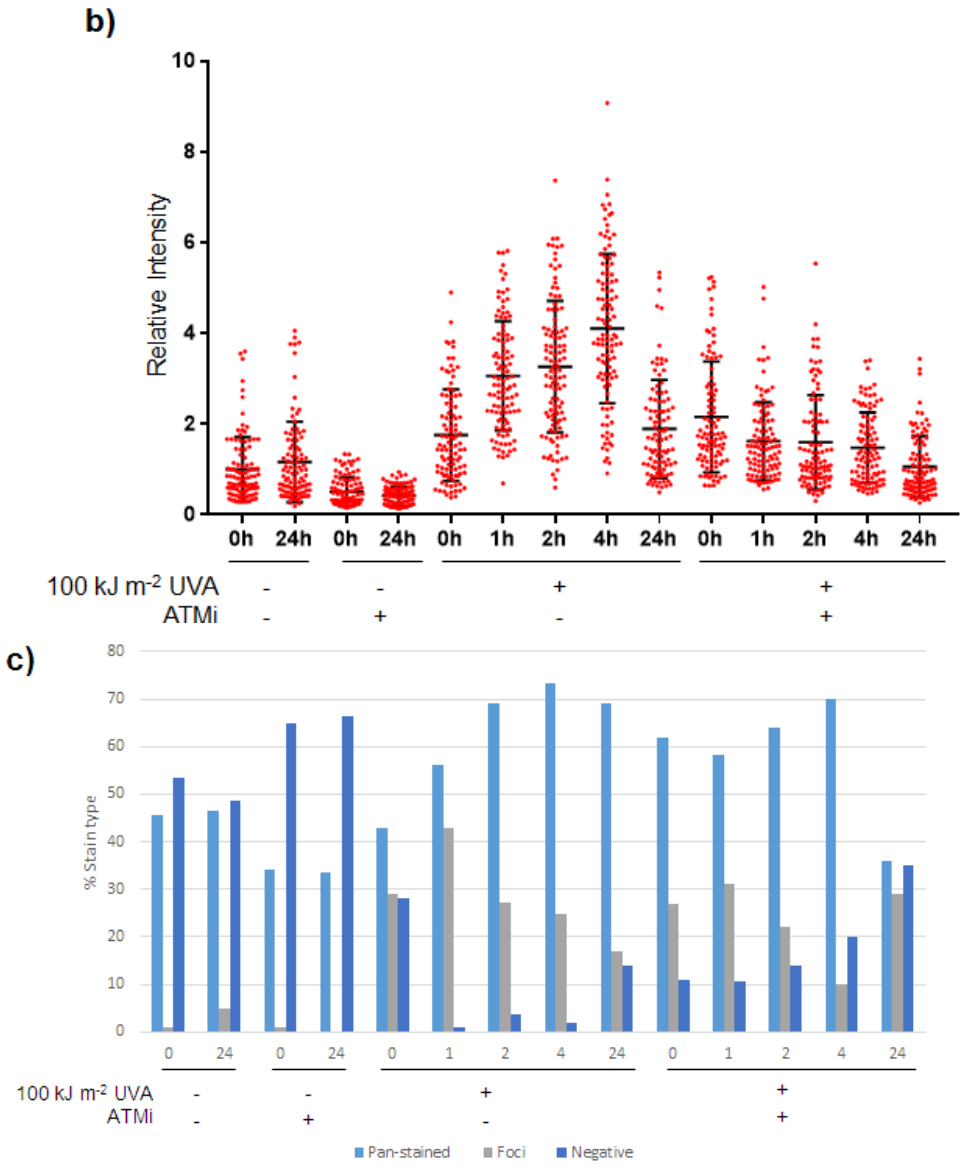

Figure 3.10. Effect of ATM inhibitor pre-treatment on UVA-induced γH2AX activation

HaCaTs were seeded onto coverslips as in figure 3.6. Prior to irradiation with 100 kJ m^{-2} UVA, one experimental group received 1 h pre-treatment with 200 nM ATMi. Cells were fixed at the indicated times following UVA exposure. The appropriate controls which received no ATM inhibition, no UVA irradiation or were completely untreated were included. (a) Cells were visualised via confocal microscopy and images taken using Zen software. Images for control conditions were not included as γH2AX activation did not significantly increase and resembled that seen in Figure 3.6. (b) Signal intensities were determined and normalised to the untreated control as before. The mean normalised intensities and SD values are shown. (c) The type of γH2AX signal observed by the different experimental and control conditions were determined and the percentage of each type of signal calculated. The number of cells in each condition was as follows: -UVA –ATMi: 0 h 105, 24 h 101; +UVA –ATMi: 0 h 100, 1 h 107, 2 h 110, 4 h 109, 8 h 100, 24 h 100; -UVA +ATMi: 0 h 100, 1 h 101, 2 h 101, 4 h 101, 24 h 101; +UVA +ATMi: 0 h 100, 1 h 103, 2 h 100, 4 h 100, 24 h 100.

at each time point investigated relative to those which received no ATM inhibition ($p < 0.001$ for each time). It is important to note that the immunofluorescence data presented in figure 3.10 represents that of a single experiment. No duplicate experiments in which the same confocal microscope laser settings for laser power and gain were used to image both the ATM inhibited and uninhibited UVA experimental conditions were conducted. Consequently, confident and accurate conclusions cannot be made.

The type of γH2AX signal generated was once again investigated, using the same classification system as with figure 3.9a, in order to assess whether ATM inhibition had an impact on the type of staining generated. UVA exposure caused the number of pan-nuclear stained cells and cells with γH2AX foci to increase between cells treated with ATMi but received no irradiation and those which received both ATM inhibition and UVA exposure (Figure 3.10c). However, the inclusion of ATM inhibition did not appear to have an impact on the type of γH2AX signal generated following UVA exposure relative to cells which received irradiation but no inhibition. However, once again, repeat experiments should be conducted.

VII. Analysis of γH2AX activation in bystander cells co-cultured with UVA irradiated cells over time

The radiation-induced bystander effect is a phenomenon in which nonirradiated cells exhibit the characteristics of irradiated cells, such as apoptosis induction, cytogenic damage and DDR activation, as a result of signals received from nearby cells which had been irradiated (Nagawa and Little, 1992). The bystander effect has been well established for ionising radiation (Rzeszowska-Wolny et al., 2009, Prise et al., 2003) and there is also supporting evidence for the ability for both UVB and UVA irradiation to induce a bystander effect in nonirradiated cells (Dahle et al., 2005). Here, a similar methodology of co-culturing nonirradiated and irradiated HaCaTs used in a number of studies was used to analyse γH2AX activation in nonirradiated bystander cells (Whiteside and McMillan., 2009, Widel et al., 2014).

Prior to the commencement of this research project, a PhD student in the lab also investigated the UVA-induced bystander effect by looking at how γH2AX activation changes from 24 to 48 h (Steele., 2016). It was observed that γH2AX activation increased between 24 and 48 h. To investigate this further, an additional co-culture

duration of 72 h was included in the present study. HaCaT keratinocytes which were to be irradiated were seeded into inserts that possessed a 1 μm pore membrane, whilst the nonirradiated bystander cells were seeded into wells of six-well plates (Figure 2.1). Media supplemented with different components were used for the different cell populations. Phenol red can function as a photosensitiser and as a result, phenol red free medium was used for the culturing of the irradiated cells. Phenol red medium was used for the bystander cells as this media was supplemented with antibiotics and would therefore help to prevent infection following extended periods of incubation. Following irradiation with UVA, the inserts were transferred to the six-well plates containing the bystander cells and incubated according to the experimental demands. Immunofluorescence was used to investigate how activation of γH2AX in the bystander cells changes over time following exposure to cells irradiated with 100 kJ m^{-2} UVA.

As with the investigations into the role of direct UVA irradiation on the DDR, immunofluorescence was used to image bystander cells that had been co-cultured with cells that had been irradiated with 100 kJ m^{-2} UVA for 24, 48 and 72 h (Figure 3.11a). As before, the intensity of the γH2AX signal was measured. The individual intensity values were normalised against the mean intensity for the control 24 h condition as before. Co-incubation of bystander cells with feeder cells that had not been irradiated did not increase γH2AX signal intensity with increasing duration of co-incubation up to 72 h (Figure 3.11b). As a result, it can be concluded that any difference seen between the experimental conditions whereby irradiated cells were co-cultured with nonirradiated bystander cells is due to signals received from the irradiated cells, not due to endogenous damage, which may increase with increased co-culture. Whilst γH2AX activation was slightly increased following 24 h co-incubation between irradiated feeder cells and nonirradiated bystander cells, a much greater increase in γH2AX activation was seen following 48 and 72 h co-culture. Signal intensity significantly increased from 24 h to 48 h ($p < 0.001$) for the irradiated experimental groups whilst no difference was seen between 48 and 72 h co-culture ($p = 0.900$). Comparison of signal intensity between each control condition and its corresponding experimental condition showed that γH2AX activation was significantly increased at each time point ($p < 0.001$).

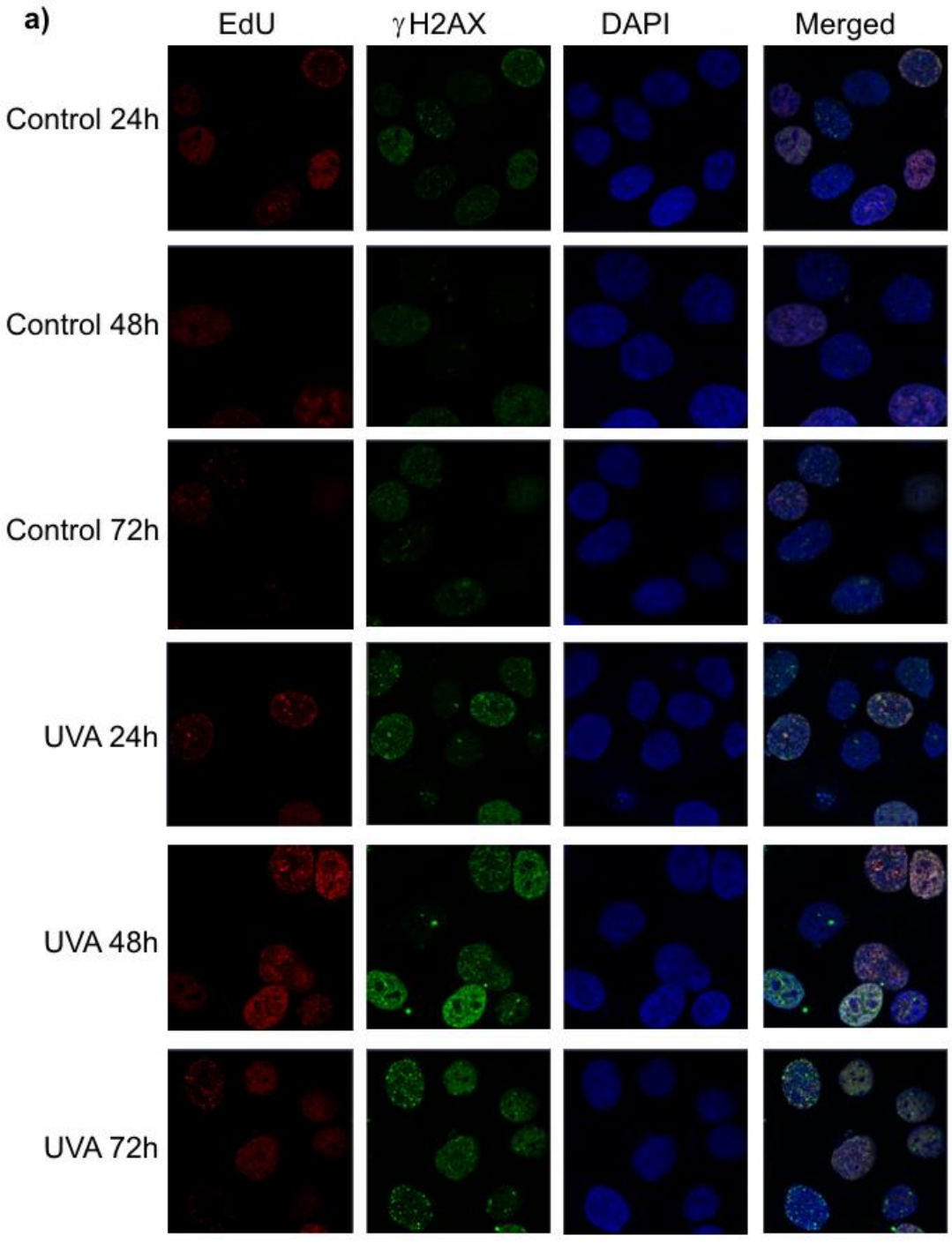
a)
EdU
γH2AX
DAPI
Merged
Control 24h
Control 48h
Control 72h
UVA 24h
UVA 48h
UVA 72h

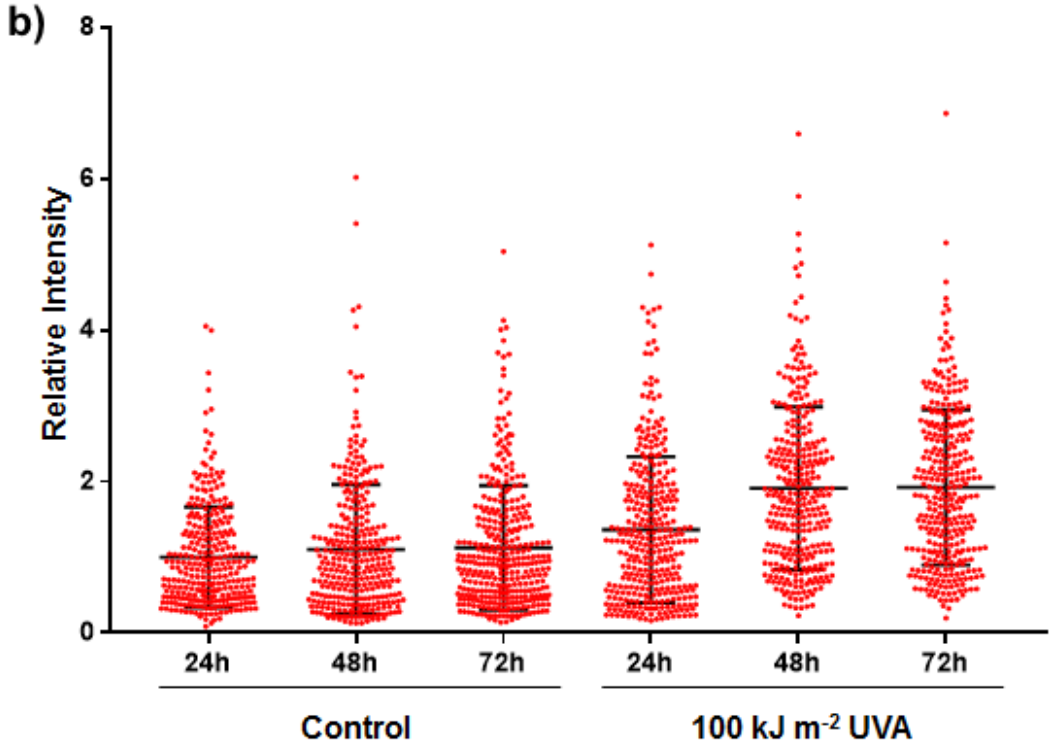
b)
Relative Intensity
8
6
4
2
0
24h
48h
72h
24h
48h
72h
Control
100 kJ m-2 UVA

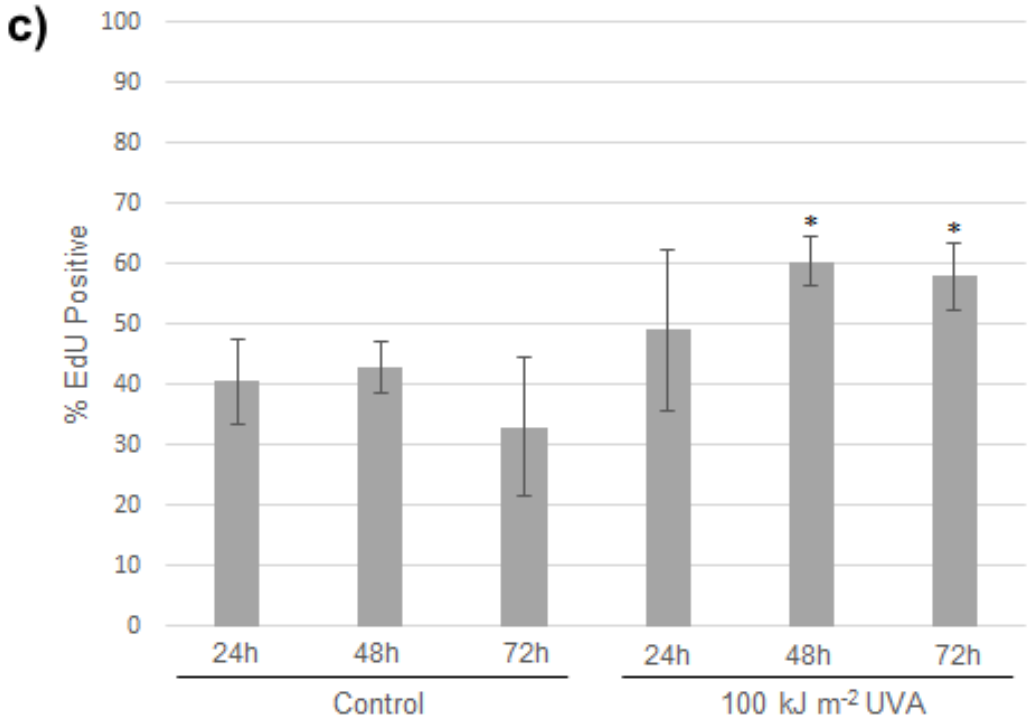
c)
% EdU Positive
100
90
80
70
60
50
40
30
20
10
0
*
*
24h
48h
72h
24h
48h
72h
Control
100 kJ m-2 UVA

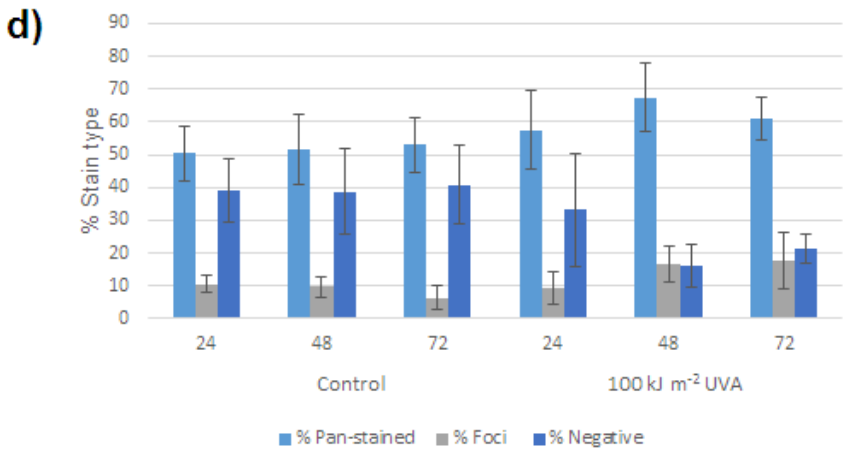

Figure 3.11. Immunofluorescent analysis of γH2AX activation and cell cycle progression in bystander cells co-cultured with UVA irradiated cells.

HaCaT keratinocytes were seeded into the wells of six-well plates containing coverslips at a density of 1 x 10^5 cells/well and into sterile inserts which possess 1 μm pore membranes at a density of 5000 cells/insert. Cells within the inserts were irradiated with 100 kJ m^{-2} UVA and immediately transferred to the wells containing the bystander cells. The appropriate nonirradiated control was included. The irradiated cells and bystander cells were co-cultured and incubated for the indicated lengths of time. Replicating cells were stained by addition of EdU. The bystander cells were fixed and permeabilised as before. (a) Cells were visualised via confocal microscopy and images taken using Zen software. (b) Signal intensity values were measured and normalised against the mean intensity for the control 24 h condition. The data presented represents the mean and SD for three individual experiments. (c) The number of EdU positive cells for the three individual experiments was determined and the overall percentage for each condition calculated. (d) The type of signal produced by each individual cell was recorded and the overall percentage for each type of staining across the three experiments was determined. The number of cells in each condition was as follows: Control 24 h 294; 48 h 312; 72 h 349; UVA 100 kJ m^{-2} 24 h 337; 48 h 313; 72 h 318. *p $\leq$ 0.05, indicates the significant difference between each experimental condition and its corresponding control group in which feeder cells received no UVA irradiation.

In addition to the analysis of γH2AX activation, the proportion of replicating cells in each experimental and control group was also assessed through the use of a Click-iT EdU Alexafluor imaging kit. The number of EdU positive cells was not affected by increased incubation of bystander cells with non-irradiated feeder cells (Figure 3.11c). Similarly, the number of EdU positive cells did not increase as the duration of co- culture of bystander cells with irradiated cells increased. However, comparison of each experimental group with its corresponding control showed that the number of cells in S-phase significantly increased for the bystander cells which were co-cultured with irradiated cells for 48 h ($p = 0.014$) and 72 h ($p = 0.046$). However, no difference

between the number of EdU positive cells was seen for bystander cells co-cultured with nonirradiated cells for 24 h and those which were co-cultured for the same duration with irradiated feeder cells ($p = 0.416$).

The types of γH2AX signal produced by co-incubation of nonirradiated bystander cells with UVA irradiated feeder cells was also assessed. The same classification system as in figure 3.9 was utilised. For each control and experimental condition, the most frequent type of γH2AX signal recorded was that of pan-nuclear staining (Figure 3.11d). Whilst it appeared as though the proportion of negatively stained nuclei decreased with increased co-culture duration with irradiated feeder cells, no significant differences were observed between any of the conditions for this type of signal. The proportion of cell nuclei with γH2AX foci was not significantly affected by the introduction of UVA irradiated feeder cells compared to nonirradiated controls.

VIII. Immunofluorescence analysis of the dose-dependent UVA-induced bystander effect

As well as investigating the effect of the UVA-induced bystander effect over time with a fixed dose of UVA, investigations were carried out to determine whether or not the UVA-induced bystander effect is dose-dependent. The same experimental design as with figure 3.11 was used. Here, feeder cells were irradiated with various doses of UVA up to 100 kJ m^{-2} and were co-cultured with UVA irradiated cells for 48 h before fixation, permeabilisation and staining. This co-incubation duration was chosen as 48 h co-incubation of bystander cells with cells irradiated with 100 kJ m^{-2} UVA represented a significant increase in γH2AX activation from 24 h and there was no significant difference between 48 and 72 h (Figure 3.11b). As before, immunofluorescence was used to image the bystander HaCaTs via confocal microscopy (Figure 3.12a). Signal intensity was measured and the individual intensity values normalised against the mean intensity calculated for the control condition in which feeder cells were not irradiated. The introduction of UVA irradiated feeder cells caused γH2AX activation to increase above that seen for the control condition with significant differences in signal intensity observed for each UVA dose ($p < 0.001$) (Figure 3.12b). This indicates that co-incubation of feeder cells irradiated with 25 kJ m^{-2} UVA is sufficient to activate the DDR in bystander cells as indicated by increased γH2AX activation above the levels observed in the controls. However, no difference was observed between each of the experimental conditions ($p = 0.243$ between the

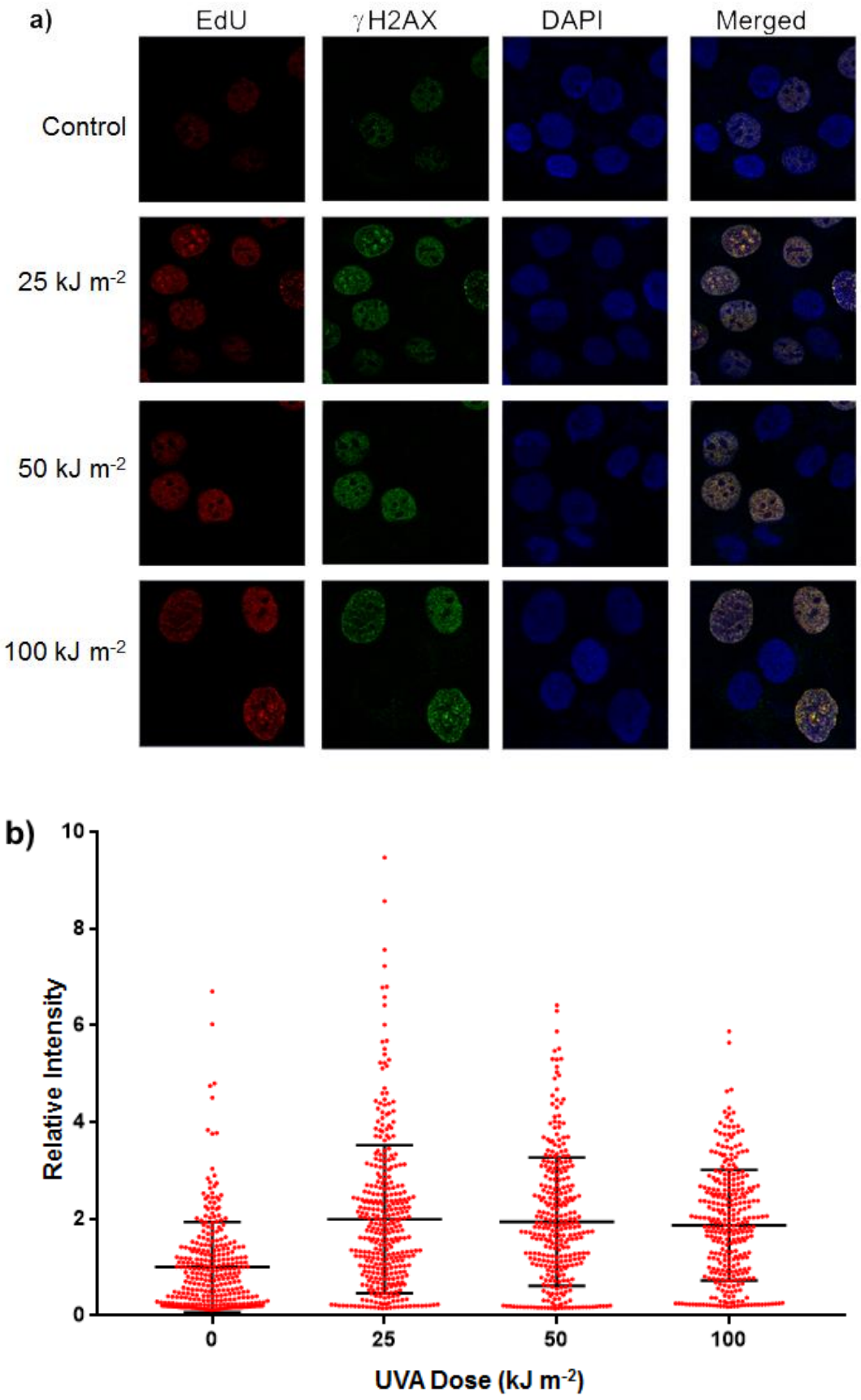
a)
EdU
γH2AX
DAPI
Merged
Control
25 kJ m-2
50 kJ m-2
100 kJ m-2
b)
Relative Intensity
0
2
4
6
8
10
0
25
50
100
UVA Dose (kJ m-2)

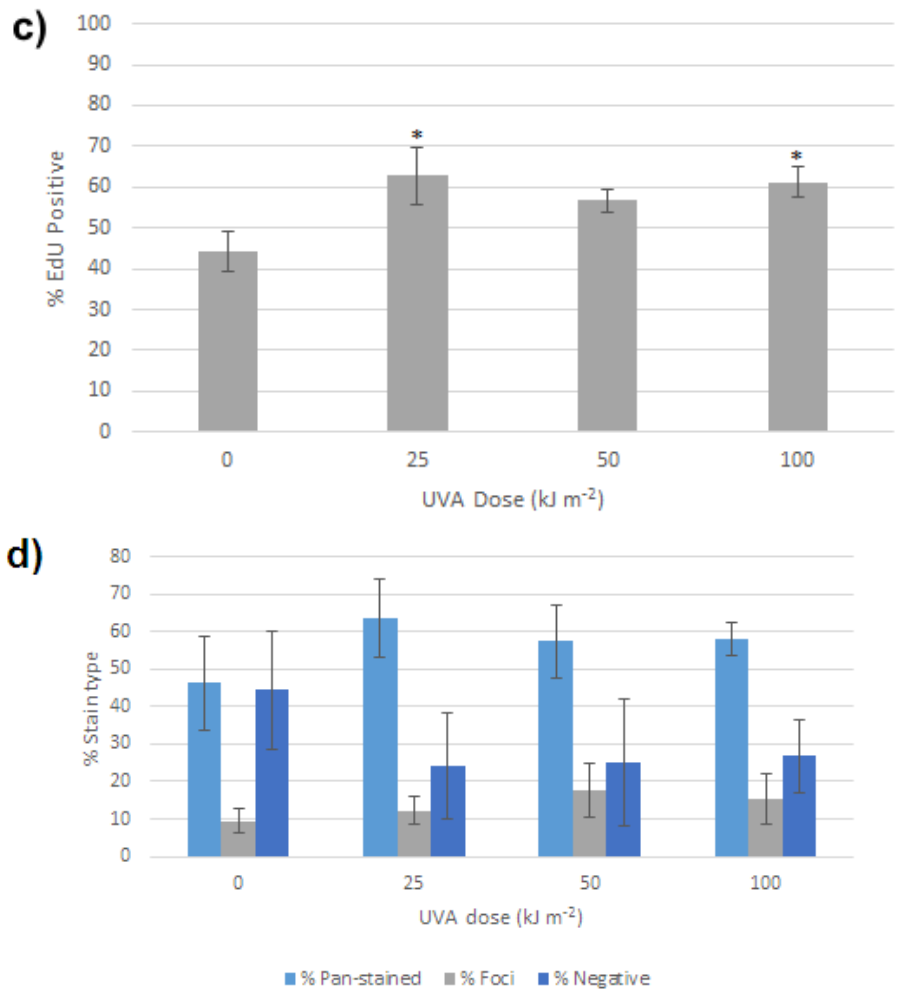

Figure 3.12. Immunofluorescent analysis of γH2AX signalling and cell cycle progression in bystander cells co-cultured with cells irradiated with various dosages of UVA irradiation.

HaCaT cells were seeded into the wells of six-well plates and into thincerts as with figure 3.11. Cells within the inserts were irradiated with the indicated dosages of UVA irradiation and immediately transferred to six-well plates containing nonirradiated bystander cells. They were co-cultured together for 48 h before being stained with EdU, fixed, permabilised, and stained with the appropriate antibodies required for detection of γH2AX as before. (a) Cells were visualised via confocal microscopy and images taken using Zen software. (b) The mean signal intensity for the control bystander cells was calculated and all individual intensity measurements normalised against this value. The mean and SD indicated represent that of three individual experiments. (c) The number of EdU positive cells for the three individual experiments was determined and the overall percentage for each condition calculated. (d) The type of signal produced by each individual cell was recorded and the overall percentage for each type of staining across the three experiments was determined. The number of cells in each condition was as follows: Control 312; UVA 25 kJ m^{-2} 350; 50 kJ m^{-2} 307; 100 kJ m^{-2} 314. *$p \leq 0.05$, indicates the significant difference between each experimental condition and its corresponding control group in which feeder cells received no UVA irradiation.

25 and 100 kJ m^{-2} conditions). This would suggest that the UVA-induced bystander effect is not dose-dependent.

The number of S-phase cells was again determined through the use of a Click-iT EdU AlexaFluor imaging kit. The proportion of EdU positive cells increased between the control bystander cells and those which were co-cultured with feeder cells irradiated with various UVA doses (Figure 3.12c). Significant differences were observed between the control condition and the 25 and 100 kJ m^{-2} UVA conditions ($p = 0.014$ and $p = 0.023$, respectively). However, as with γH2AX signal intensity, increasing the dose of UVA to which the feeder cells were exposed to did not affect the proportion of EdU positive cells ($p = 0.780$ between the 25 and 100 kJ m^{-2} experimental conditions). The number of proliferating bystander cells did not increase in a dose-dependent manner.

Similarly, the type of γH2AX signal generated in nonirradiated bystander cells following co-incubation with UVA feeder cells was unaffected by increasing UVA dose (Figure 3.12d). The proportion of pan-nuclear stained cells, nuclei with γH2AX foci and nuclei which were negatively stained did not change with the introduction of UVA irradiated feeder cells compared to nonirradiated controls or with increased UVA irradiation.

IX. Investigation of the dose-dependent UVA-induced bystander effect with increased co-incubation duration via clonogenic survival assays

Clonogenics survival assays were conducted to further investigate whether or not the UVA-induced bystander effect was dose-dependent. As with the other bystander experiments, the cells to be irradiated were seeded into inserts and transferred immediately following irradiation into the wells of the plates containing the bystander cells, which had been seeded at a density of 200 cells/well.

An additional UVA dose of 12.5 kJ m^{-2} was included to help determine the threshold dose at which the UVA-induced bystander effect is induced as 25 kJ m^{-2} was shown to be sufficient to induce a bystander effect. Following one week co-culture, the number of colonies per well was determined and the mean number of colonies from triplicate samples determined. Percentage survival was calculated for each experimental condition relative to the control condition in which feeder cells were not irradiated. Whilst the previous immunofluorescence experiment suggested that the

UVA-induced bystander effect is not dose-dependent, the results from the clonogenics survival assays inferred the opposite, that the UVA-induced bystander effect is dose-dependent. As UVA dose increased, the survival of the bystander cells relative to the controls decreased (Figure 3.13). Significant decreases in survival relative to the control were observed for bystander cells that were co-cultured with feeder cells irradiated with 25 kJ m^{-2} ($p < 0.05$) and 50 and 100 kJ m^{-2} UVA ($p < 0.01$). Significant differences in survival were also seen between the 12.5 kJ m^{-2} experimental conditions and all other experimental conditions ($p < 0.01$), between 25 and 100 kJ m^{-2} UVA ($p = 0.005$) and between 50 and 100 kJ m^{-2} ($p = 0.033$).

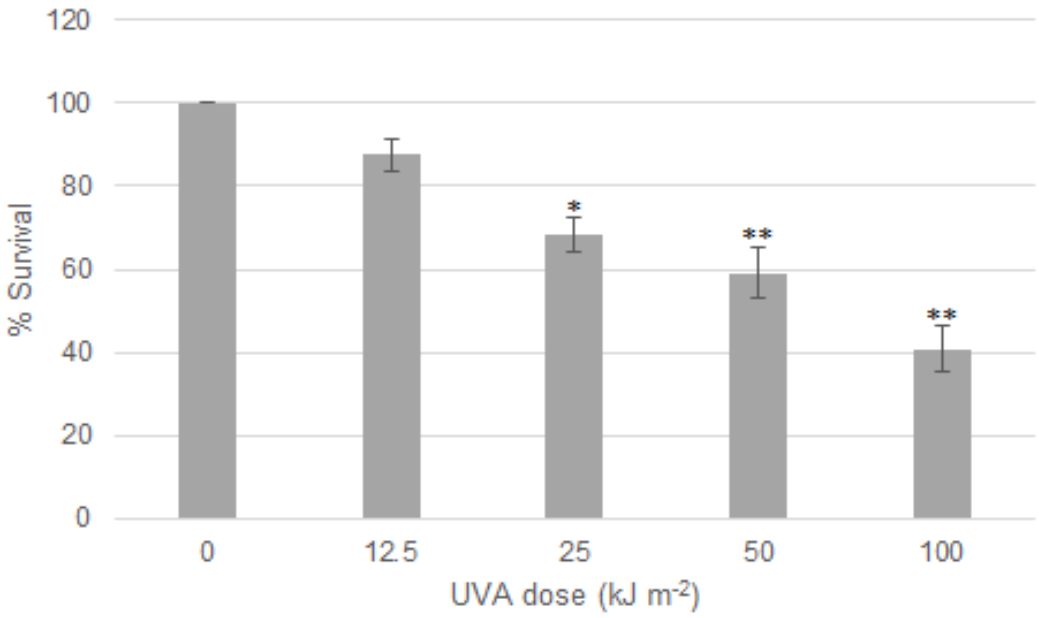

Figure 3.13. Clonogenic survival assay investigating the effect of various dosages of UVA on the UVA-induced bystander effect.

HaCaT keratinocytes were seeded into the wells of six-well plates at a density of 200 cells/well and into thincerts which possess 1 μm pore membranes at a density of 5000 cells/insert. Cells within the inserts were irradiated with various dosages of UVA and immediately transferred to the wells containing the bystander cells. The appropriate nonirradiated control was included. The irradiated cells and bystander cells were co-cultured and incubated for seven days. The resulting colonies were fixed and stained with Giemsa. The mean number of colonies for each treatment from triplicate samples was determined and the mean percentage survival calculated relative to untreated controls. The data shown represents the mean and SD survival from three individual experiments. *$p \leq 0.05$, indicates the significant difference between each experimental condition and the control group in which bystander cells were co-cultured with nonirradiated cells.

4. Discussion

DNA damage surveillance and repair pathways play an important role in protecting skin cells against the carcinogenic effects of ultraviolet radiation. This is exemplified by the thousand fold increased risk of developing skin cancer in patients with the inherited syndrome Xeroderma pigmentosum in which patients have defective nucleotide excision repair. The major source of ultraviolet radiation to which we are exposed to is solar radiation, and whilst UVR is composed of three wavebands, UVC, UVB and UVA, 90-95% of terrestrial UVR that we are exposed to is UVA with the remainder being UVB. This is due to the capacity for the ozone layer to absorb all of the UVC waveband and the vast majority of the UVB waveband. Both UVB and UVA cause damage to DNA, as well as other cellular biomolecules, but the theoretical mechanisms proposed for each differ. Whilst a direct mechanism is accepted for UVB, both indirect and direct mechanisms have been proposed for UVA. Although UVA makes up the majority of the UVR we are exposed to, it is relatively understudied in comparison to UVB. In particular, the impact of UVA exposure on the initiation of the DNA damage response remains to be fully understood. In the present study, the effect of UVA irradiation on the DDR was studied. A number of techniques were employed to analyse the different aspects of the DDR following both direct irradiation with UVA, and also in bystander cells which, although they had not been irradiated themselves, had been co-cultured with feeder cells which had been. The dynamics of the DDR response was studied in terms of how activation of key components of the vital signalling pathway changes over time and how inhibition of certain components impacts the response.

I. UVA irradiation induces a dose-dependent decrease in cell survival in HaCaT keratinocytes

In the past, it was believed that, although making up the majority of terrestrial UVR, that UVA was far less carcinogenic and harmful than UVB irradiation. This is exemplified by the majority of sunbeds in the past emitting less UVB and therefore more UVA, as the dangers of UVA were understudied (WWW, WHO | Sunbeds). However, as the amount of research into the harmful effects of UVA increased, it became increasingly apparent that exposure to UVA alone can generate the same mutational fingerprint consisting of pyrimidine dimers as UVB (Ikehata et al., 2008). Consequently, in 2009, the full spectrum of UVR was categorised as being carcinogenic to humans (El Ghissassi et al., 2009). In this present study, the first experiment conducted confirmed the detrimental effects of UVA on cell viability.

HaCaT keratinocytes exposed to UVA (up to 100 kJ m^{-2}) experienced decreased cell survival in a dose-dependent manner (Figure 3.1). This observation was consistent with a number of previous reports (He et al., 2016, Hwang et al., 2011). The dose-dependent decrease in cell viability is unsurprising as numerous studies have described different types of lesions that can be generated by UVA. Although the mechanisms by which they arise are unclear, UVA has been shown to be able to generate CPDs, which lead to the generation of oxidised bases and DSBs (Mouret et al., 2005, Cadet et al., 2015, Rapp and Greulich, 2004). Each of these lesions are detected by DNA damage sensors, which consequently leads to the activation of the DDR, which ultimately, through the propagation of a signalling cascade, brings about cell cycle arrest so that repair of these lesions can take place. In the event that the damage cannot be repaired, cells are directed to enter senescence or undergo apoptosis. It would therefore be expected that as UVA exposure increases, so do the number of generated lesions and as a result, increased numbers of cells enter apoptosis to avoid replication with a modified genome.

II. Inhibition of ATM and ATR caused decreased cell viability following irradiation with 50 kJ m^{-2} UVA

Different types of lesions generated by genotoxic agents, including UVA, are detected by different DNA damage sensors. Whilst the MRN complex recognises DSBs, the 9-1-1 complex and RPA cooperate to detect stalled replication forks. Activation of these damage sensors leads to the recruitment and activation of the apical kinases ATM and ATR, respectively, which propagate the DNA damage signal to bring about the actions of the DDR. The different arms of the DDR were evaluated in context of UVA irradiation by the independent inhibition of ATM and ATR. The apical kinase inhibitors used, KU-60019 (ATMi) and VE-821 (ATRi), have been shown to be highly selective and specific for their targets with minimal cross-reactivity against related PIKKs, which include each other, DNA-PK, mTOR and PI3K. VE-821 had very little cross-reactivity with these related PIKKs at the concentrations used and KU-60019 is an improved inhibitor for ATM in comparison to KU-55933 and too has very little activity against similar PIKKs at the concentrations used in the present study (Reaper et al., 2011, Golding et al., 2009). A UVA irradiation dosage of 50 kJ m^{-2} was used as this caused a cell loss of approximately 50% in the absence of any inhibition.

In the absence of irradiation with UVA, pre-treatment with ATMi and ATRi at each concentration did not decrease cell survival (Figure 3.2). However, independent inhibition of ATM and ATR both caused decreased cell survival in a dose-dependent manner in conjunction with exposure to 50 kJ m^{-2} UVA (Figure 3.3). This would suggest that both ATM and ATR and their downstream targets are required in processing lesions generated by UVA. This is consistent with evidence that Chk2 and Chk1 are phosphorylated by ATM and ATR, respectively, following exposure to UVA irradiation (Di Siena et al., 2013, Girard et al., 2008, Zhang et al., 2002). The importance of both ATM and ATR in responding to damage generated following UVA irradiation is also consistent with evidence that both apical kinases are required for DDR activation following exposure to ionising radiation (Cui et al., 2014).

Inhibition of ATR prevents phosphorylation of Chk1 following the detection of stalled replication forks and therefore prevents the activation of CDC25 and other downstream effectors. ATR is recruited to stalled replication forks at regions of ssDNA, which are subsequently coated in RPA. ATR is recruited to ssDNA regions generated during the processing of bulky lesions such as CPDs and 64PPs (Batista et al., 2009). It has been demonstrated that ATM and the nuclease activity of the Mre11 component of the MRN complex are required for the processing of DSBs to generate regions of ssDNA that can then be coated with RPA to allow for the recruitment of ATR (Jazayeri et al., 2006). Although ATM is inhibited (Figure 3.3a), the MRN complex is able to generate ssDNA regions that can be recognised by the ATR arm of the DDR. The importance of ATR in bringing about checkpoint arrest and cell survival following DNA damage is highlighted by the fact that multiple tumour types frequently possess an ATM deficiency through ATM mutations or epigenetic downregulation (Greenman et al., 2007).

ATR inhibition caused a dose-dependent decrease in combination with exposure to 50 kJ m^{-2} UVA, with no significant differences seen in cell survival between cells pre-treated with 0.2 and 1 μM ATRi (Figure 3.3b). However, even at the highest concentration used, there was still over 40% survival. This may be due to the fact that ATM is still available to propagate the DNA damage signal from the activated MRN complex to numerous downstream effectors so that repair can occur. UVA has been shown to be able to generate DSBs with the proposed mechanism being through the repair of clustered oxidative DNA damage (Rapp and Greulich, 2004, Greinert et al. 2012). As a result, ATM-mediated repair following its activation by the MRN complex following recognition of DSBs would explain why ATR inhibition does not result in the complete loss of repair of UVA-induced lesions.

III. Inhibition of ATM, ATR and other DNA damage response components did not decrease cell viability at a higher dose of UVA

In order to investigate the role of other DDR components in responding to UVA-induced DNA damage, additional cell viability assays were conducted. The more robust XTT cell viability assay was used to investigate how inhibition of additional components of the DDR affected cell viability following UVA exposure. During the process of performing the MTT assay, prior to the addition of DMSO in order to dissolve the formazan crystal within each well, the media is carefully removed. This can cause issues as the removal of the media can displace crystals and lead to the resulting readings being lower than they should be, providing false negative results. The XTT cell viability assay presents a more robust method for measuring cell survival as this assay skips the requirement of carefully removing the media prior to detection.

Using the XTT assay, the inhibition of additional components was investigated in relation to cell survival following exposure to UVA irradiation. These inhibitors included a PI3K inhibitor (PI3Ki) and a MRN inhibitor (mirin). Mirin was included to investigate how preventing detection of DSBs impacted cell viability following UVA exposure. PI3Ks regulate cellular signalling networks involved in processes such as survival, growth, and cell cycle regulation as part of the PI3K/AKT/mTOR pathway (Gharbi et al., 2007). This pathway is linked with protecting cells from apoptosis and UVA has been demonstrated to, although not as effectively as UVB, lead to increased expression of PI3Kp85, a regulatory subunit of PI3K (Syed et al., 2012). It would therefore be expected that inhibition of this pathway would lead to decreased cell survival.

In this experiment, the UVA dose was increased to 100 kJ m^{-2} in order to better reflect UVA exposure that is environmentally relevant. This dose reflects an hour's exposure in subtropical regions in the summer months (Whiteside and McMillan, 2009). There was consistency with the previous MTT assays in that DDR component inhibition did not impact cell survival in the absence of UVA irradiation. However, the synergy between UVA and independent inhibition of ATM or ATR were not reproduced. Whilst pre-treatment with 200 nM ATMi and ATRi caused a significant decrease in cell survival following exposure to 50 kJ m^{-2} UVA, the same decrease did not occur once the UVA dose increased (Figure 3.4).

Similarly, PI3K inhibition and MRN inhibition did not decrease cell survival relative to the irradiated, uninhibited control. This may have occurred as a result of increasing

the dose of UVA to which the cells were exposed to. As shown in the absence of any inhibition, an increase of 50 to 100 kJ m^{-2} UVA resulted in a significant decrease in cell survival, likely as a result of increased lesions generation. Perhaps exposure to 50 kJ m^{-2} in the absence of DDR component inhibition generated lesions that could be repaired efficiently without the requirement of apoptosis induction. Inhibition of ATM or ATR may then have prevented these lesions from being repaired efficiently, resulting in decreased cell survival. Conversely, the increased lesions generated following exposure to 100 kJ m^{-2} in the absence of DDR component inhibition may have been unrepairable and as a result the DDR induced apoptosis and senescence. Possible supporting evidence for this explanation was provided by a PhD student working in the same lab in which the present study was completed. Here, changes in mitochondrial membrane potential were measured in order to study apoptosis induction following UVA irradiation. Mitochondrial membrane depolarisation was seen within 1 h of irradiation with 100 kJ m^{-2} UVA, a duration which is not long enough for the p53 axis of the DDR to exert its effect (Steel, 2016). This could potentially explain why DDR inhibition was then unable to decrease cell viability above that seen in the absence of inhibition. An appropriate future experiment would be to therefore investigate how varying the UVA dose to which cells are exposed to following pre-treatment with inhibitors against DDR components impacts cell survival.

Cui et al. (2014) demonstrated that ATM and ATR are both required for responding to damage induced by ionising radiation as, while depletion of one apical kinase alone had little effect on cell cycle arrest, depletion of ATR in ATM-deficient cells caused severe G2/M checkpoint attenuation and increased lethality. Consequently, similar studies should be carried out to investigate how inhibition of both ATM and ATR impacts cell survival following UVA irradiation and to provide further insight into the involvement of other PIKKs such as DNA-PKcs and the involvement of PI3K in DDR activation following UVA exposure. Additionally, future experiments should also investigate how different combinations of inhibition impact cell survival. For example, it has been demonstrated that the Mre11 component of the MRN complex possesses nuclease activity which can generate ssDNA regions that can then be coated by RPA, allowing for the recruitment and activation of ATR. It would be interesting to see how inhibition of the MRN complex and ATR at the same time impacts the DDR following UVA exposure.

Both cell viability assays used in the present study work by measuring the reduction of tetrazolium salts (Abe and Matsuki, 2000, Roehm et al., 1991). The two colorimetric assays both measure cell viability and proliferation by measuring the

capacity of mitochondrial enzymes present in living cells to reduce the salts. The amount of formazan product can then be measured using a spectrophotometer. The use of metabolic activity as a surrogate for cell viability incurs problems as resting cells may have low metabolic activity, leading to an underestimation of cell survival, whilst dying cells may still possess some activity, leading to an overestimation. Future work investigating the role of DDR component inhibition in the context of UVA should also consider using alternative methods for assessing cell viability, such as methods that measure rates of apoptosis, including TUNEL assays to measure DNA fragmentation and using Annexin V to measure phosphatidyl serine externalisation. In particular, future experiments should assess how inhibiting both ATM and ATR impacts cell viability as data in the present study suggests that both are involved in responding to damage generated following UVA irradiation.

In addition to investigating the role of direct UVA exposure on cell viability, the effect of direct UVA irradiation was further analysed by western blot and immunofluorescence to assess how activation of different components of the DDR change over time following irradiation. Once again, 100 kJ m^{-2} UVA was used as it is an environmentally relevant dose.

IV. Western blot analysis found γH2AX activation to peak at 1 and 2 h following irradiation with 100 kJ m^{-2} UVA

γH2AX has been well-established as an effective biomarker for DNA damage and has also been shown to be an accurate biomarker for detecting damage generated by UVA exposure both in vitro in both keratinocyte cell culture and within an artificial epidermis and also in vivo in human skin (Cleaver, 2011, Kuo et al., 2008, Barnes et al., 2010). There is also controversy in past research regarding the ability of UVA to induce H2AX phosphorylation at Ser139 to yield γH2AX. For example, Rizzo et al. (2011) studied DSB-formation in primary skin fibroblasts following exposure to various dosages of UVA and found that UVA irradiation did not cause γH2AX nuclear foci formation. Similarly, UVA up to 50 kJ m^{-2} alone was found to be incapable of inducing γH2AX activation, although treatment with the photosensitiser 8-methoxypsoralen (8-MOP) in combination with UVA exposure was able to induce the production of γH2AX (Toyooka et al., 2011). However, numerous other studies have found that UVA irradiation can induce γH2AX formation (Lu et al., 2006, Rapp and Greulich, 2004). The data in the present study are consistent with these latter studies

as irradiation with 100 kJ m^{-2} UVA resulted in γH2AX activation, as indicated by both western blot analysis and immunofluorescence.

In conjunction with this study, another study undertaken in the lab looked at γH2AX activation at 0, 1, 3 and 24 h post-irradiation, where activation peaked at 1 h, remained present at 3 h and was abrogated by 24 h (Steel, 2016). However, there is a large window of 21 h unaccounted for. Here, additional time points were investigated including 2, 4, 8 and 16 h post-exposure, with peak activation seen between 1 and 2 h post exposure to UVA (Figure 3.5). Western blot data indicated that γH2AX was still present 16 h following irradiation. The increased γH2AX activation over this period of time is likely as a result of the positive feedback loop that is generated in order to extend H2AX phosphorylation to the megabase chromatin region flanking the lesion (Rogakou et al., 1999). This provides a docking site for DNA repair factors and forms visible γH2AX immunofluorescent foci. The positive feedback loop arises as a result of MDC1 recruitment following initial phosphorylation of γH2AX. MDC1 is then phosphorylated by casein kinase 2 (CK2), which promotes phosphorylation-dependent interactions with NBS1, which is a component of the MRN complex. This leads to increased activation of the MRN complex, which results in increased ATM activation and therefore increased H2AX phosphorylation (Kinner et al., 2008). In the data presented in Figure 3.5, γH2AX activation was also observed in the wildtype control condition at 24 h, in which the cells received no irradiation. This observation was absent in the repeat experiments.

V. Immunofluorescence was used to further quantify γH2AX activation following irradiation with 100 kJ m^{-2} UVA

Immunofluorescent analysis of γH2AX signalling was utilised to quantify γH2AX activation over time following UVA exposure and served to support the evidence provided by western blot. Here, γH2AX activation was again elevated at 1 and 2 h post UVA exposure but similar levels of γH2AX activation were also present at 4 h post irradiation (Figure 3.8). In addition to providing information on the amount of H2AX phosphorylation, immunofluorescence was used to record the type of γH2AX signal generated. Three types of signal were recorded, pan-nuclear staining, γH2AX foci and negative, in which nuclei were neither pan-stained nor presented foci (Figure 3.9a). Direct UVA irradiation resulted in increased pan-nuclear staining and increased numbers of nuclei with γH2AX foci (figure 3.9b). Pan-nuclear staining

peaked at 1 and 2 h post-irradiation whilst foci generation peaks at 1, 2 and 4 h post-irradiation. As mentioned previously, an aspect of the DDR is a positive feedback loop to amplify H2AX phosphorylation to megabase regions of chromatin to provide a region for repair factors to interact with. This process has been shown by numerous studies to produce immunofluorescent foci in mammals following induction of DNA damage from a number of sources. It is therefore highly likely that the increase in γH2AX foci seen between 1 and 4 h post-irradiation is a result of this positive feedback loop, generated to provide a platform for repair factors to repair lesions generated by UVA exposure.

Similarly, the induction of pan-nuclear γH2AX signals have been demonstrated for numerous DNA damaging agents, including IR and UVR (Ding et al., 2016, Meyer et al., 2013). Meyer et al. (2013) suggest that pan-nuclear staining occurs as a result of H2AX phosphorylation in undamaged chromatin over the entire nucleus and does not elicit a full pan-nuclear DDR. They found that the pan-nuclear γH2AX signal is mediated by the kinases ATM and DNA-PK and they suggest that the pan-nuclear response depends on the amount of DNA damage. Ding et al. (2016) provided further insight into the role of pan-nuclear γH2AX staining, suggesting that the pan-nuclear response represents an apoptotic signal, again triggered by ATM and DNA-PKcs activation. Conversely, pan-nuclear γH2AX signalling has also been shown to have no effect on cell survival following UV irradiation (Revet et al., 2011).

The use of additional time points allows for the investigation of how phosphorylation of H2AX to generate γH2AX changes over time and may provide insight into the types of damage UVA induces as γH2AX activation is regarded as an early event following the production of DSBs (Barnes et al., 2010). The increase up to 1 and 2 h post-irradiation with 100 kJ m^{-2} was inconsistent with results generated by Lu et al. (2006) in which treatment with 80 kJ m^{-2} UVA caused increased phosphorylation of H2AX at Ser139 in a time-dependent manner with γH2AX levels increasing up to 6 h post-irradiation. A similar dynamic in γH2AX activation to the present study was seen following UVB exposure that caused increased levels of γH2AX in the initial couple of hours following irradiation, with peak activation 0.5 h following irradiation (which was not investigated here) (Scarpato et al., 2013). However, in this study, basal levels of γH2AX were restored 5 h post-UVB exposure, not 24 h as with UVA here. UVB irradiation leads to the generation of pyrimidine dimers and UVA has been shown to generate CPDs, although not 64PPs and irradiation with 100 kJ m^{-2} UVA has been shown to induce similar levels of CPDs as high doses of UVB (0.6 kJ m^{-2}) (Murray et

al., 2016). It is therefore possible that the persistence of γH2AX activation is due to increased time required to repair UVA induced damage, such as DSBs and oxidative damage. The role of UVA-induced CPDs in initiating the DDR and leading to γH2AX activation cannot be ignored however as areas positive for CPDs have been shown to co-localised with γH2AX (Oh et al., 2011). Additionally, UVA-induced DSB formation and ROS-mediated damage as a result of UVA exposure have also both been shown to result in γH2AX activation (Calo et al., 2015, Greinert et al., 2012). Further investigations into how repair of the different types of lesions that UVA has been shown to generate should be conducted to provide insight into how the different pathways of the DDR cooperate to repair the different lesions.

VI. Phosphorylation of Chk2 peaked immediately following UVA exposure and was unchanged following the introduction of ATM inhibition

Western blot analysis was also used to investigate how Chk2 phosphorylation changes over time following direct UVA irradiation. Chk2 phosphorylation peaks at 0 h and gradually decreases from there (figure 3.5). Chk2 is phosphorylated and activated by ATM following activation of the apical kinase by the MRN complex. This finding is indicative that repair of UVA damage, is, at least in part, ATM dependent. This is consistent with the cell viability data in the present study and with previous studies that UVA irradiation produces damage that is repaired following ATM activation. A similar peak in Chk2 phosphorylation was reported by Girard et al. (2008) following exposure of MRC5Vi cells to 80 kJ m^{-2} UVA.

Following this, the dynamics of γH2AX and p-Chk2 activation were assessed with the addition of an ATMi pre-treatment. The impact of ATM inhibition on H2AX and Chk2 phosphorylation was studied by both western blot and immunofluorescence. Cells were pre-treated with 200 nM ATMi as the compound has very little cross-reactivity with other PIKKs at this concentration and was far and above the IC_{50} for the compound. As before, 100 kJ m^{-2} UVA was used to induce DNA damage and DDR activation measured at different times post-irradiation. γH2AX activation shifted with decreased levels seen at 1 h and increased activation levels now at 2 and 4 h post-irradiation (Figure 3.6). However, Chk2 is a downstream target of ATM and so it would be expected that ATM inhibition would too cause decreased phosphorylation of this target. Girard et al. (2008) investigated Chk2 phosphorylation in ATM deficient cells and found that activation of this target did not occur at 2 h post-irradiation with

80 kJ m^{-2} UVA. Although this is also seen in the present study, the study did not investigate activation immediately following irradiation. The result therefore suggests that UVA-induced p-Chk2 activation may not be entirely ATM-dependent and so the role of other DDR components such as ATR and PI3K needs to be considered.

Crosstalk between the ATM-Chk2 and ATR-Chk1 pathways is limited but it has been demonstrated that Chk2 can function as a target for ATR in response to ionising and ultraviolet irradiation (Wang et al., 2006). Additional replicates should be completed as only two sets of data showed this delay in γH2AX activation whilst p-Chk2 activation was unaffected.

ATM and ATR are both PI-3 Kinase-related kinase (PIKK) family members, which have sequence similarity to phosphatidylinositol-3 kinases (PI3Ks) (Falck et al., 2005). Another member of this family includes DNA-dependent protein kinase catalytic subunit (DNA-PKcs) and this has also been shown to be able to phosphorylate Chk2 (Zannini et al., 2014, Li and Stern, 2005). DNA-PKcs plays an important role in DSB repair, particularly in NHEJ (Shrivastav et al., 2008). ATM deficient cells have been shown to display strong dependence on DNA-PKcs to repair DSBs and pharmacological or genetic abrogation of DNA-PKcs in ATM-defective cells has been shown to lead to the accumulation of DSBs and subsequent generation of ssDNA regions that are subsequently repaired by the RPA/ATR/Chk1 axis of the DDR (Riabinska et al., 2013). Perhaps the lack of a delay in p-Chk2 activation is due to DNA-PKcs compensating for the loss of ATM following the introduction of DNA lesions by UVA irradiation? The apparent temporal decoupling of H2AX and Chk2 phosphorylation following UVA exposure should be further investigated in future research through the use of pan-PIKK inhibitors as well as individual inhibition of ATM, ATR and DNA-PKcs and combined treatments where different combinations are inhibited. This would allow investigation into how the DDR is initiated following UVA exposure and may provide insight into the different types of lesion generated by UVA are repaired.

VII. γH2AX activation decreased following ATM inhibition in UVA irradiated HaCaTs

γH2AX activation following ATM inhibition was assessed via immunofluorescence. The delay in peak γH2AX activation seen in the western blot analysis (Figure 3.6) was not seen following immunofluorescence analysis, but reduced γH2AX activation

relative to that seen for uninhibited, UVA irradiated cells was observed (Figure 3.10). This would be expected for the similar reasons as mentioned previously. As ATM is inhibited, one of the pathways within the DDR is downregulated and so there is reduced repair of the UVA-induced lesions, as indicated by the reduced γH2AX activation. However, ATR remains active and so γH2AX can still be generated and ssDNA regions generated by the MRN complex can be repaired in an ATR-dependent manner (Di Siena et al., 2013). The discrepancy in γH2AX activation seen between the Western blot analysis and immunofluorescence data needs to be considered. The intensity data presented in figure 3.10 represents that of a single experiment. Due to time limitations, no duplicate experiments in which the same confocal microscope laser settings for laser power and gain were used to image both the ATM inhibited and uninhibited UVA experimental conditions were conducted. Additional experiments must be completed to further determine how γH2AX activation changes following ATM inhibition of UVA irradiated cells and to help determine why the shift in γH2AX activation was not seen for the immunofluorescence data.

The type of γH2AX signal produced was also investigated in the context of ATM inhibition. As mentioned previously, γH2AX foci over megabase regions arise from a positive feedback loop in which MDC1 recruited to the area interacts with NBS1 of the MRN complex in a CK2-dependent manner. This results in increased ATM activation, leading to increase H2AX phosphorylation at Ser139. It would therefore be expected that as ATM is downregulated by pre-treatment with ATMi, that the number of cells with γH2AX foci would be decreased. In this investigation, the highest proportion of cells with γH2AX foci was seen for cells that were not pre-treated with ATMi and were fixed 1 h following UVA exposure. Populations fixed 1 h post-irradiation that received ATM inhibition had decreased numbers of cells positive for γH2AX foci as would be expected and similar effects were seen between the two experimental conditions at 2 and 4 h post-irradiation. Interestingly, the number of foci-positive cells was elevated for the ATM inhibited condition that were fixed 24 h post-irradiation. However, the data presented only came from one individual experiment in which images were taken for both the uninhibited and ATMi pre-treated experimental conditions with the same confocal microscope settings. Consequently, confident conclusion cannot be reached and additional repeats are required to assess whether this data is reliable and if the differences seen are significant.

Furthermore, pan-nuclear γH2AX signalling has been shown to be ATM and DNA-PKcs dependent (Meyer et al. 2013). As a result, it would be anticipated that DNA-

PKcs-mediated pan-nuclear staining would be able to compensate for the loss of ATM. Whilst the proportion of cells that were pan-stained appeared to be similar for each experimental condition at each time point, additional repeats would again be required.

The impact of direct UVA irradiation on DDR initiation was only investigated in the context of how inhibition of ATM impacts the repair process. Whilst it was expected that the observed decrease in γH2AX activation would occur following ATM inhibition, additional research should be completed to investigate why a shift in peak activation was observed when Western blot analysis was carried out. Furthermore, ATM inhibition did not cause a delay in p-Chk2 activation. Whilst it is possible that this occurred due to DNA-PKcs activity, there is no direct supporting evidence for its involvement in Chk2 phosphorylation following UVA exposure. As a result, research should be conducted to assess how DNA-PKcs inhibition compares and how inhibition of both DNA-PKcs and ATM contributes to Chk2 phosphorylation. Activation of other DDR pathway components should be investigated in the context of UVA irradiation both in the absence of inhibition and with individual and combined inhibition of different DDR components. In particular, there is evidence that UVA induced lesions detected by the MRN complex can be processed into ssDNA regions by the Mre11 component. Investigations should be conducted to see how ATR-dependent phosphorylation of H2AX and Chk1 occurs following direct UVA irradiation. The impact of inhibiting various components both independently and together on γH2AX foci generation should also be investigated. One of the outcomes of the DDR is to bring about cell cycle arrest. Therefore, cell cycle progression following UVA irradiation should be studied in order to analyse the stage of the cell cycle in which progression is stalled. This could be done by immunofluorescence via labelling techniques such as with EdU as in the bystander portion of the present study, or alternatively through flow cytometry. Alternatively, western blot analysis could be used to monitor the expression levels of different cyclins.

VIII. γH2AX activation increases in bystander cells co-cultured with UVA irradiated HaCaTs

The radiation-induced bystander effect has been well-established for ionising radiation (Rzeszowska-Wolny et al., 2009, Prise et al., 2003) and there is also evidence that UVB and UVA can too induce a bystander effect (Whiteside and McMillan, 2009). In the past, the UVA-induced bystander effect has been studied

using models that involve co-culturing irradiated feeder cells with nonirradiated bystander cells in a two-chamber system, as in the present study, or through culturing bystander cells with medium from which irradiated feeder cells had previously been cultured (Redmond et al., 2014, Nishiura et al., 2012, Whiteside et al., 2011, Whiteside and McMillan, 2009). This allowed for the study of interactions between the differentially treated cell populations in the absence of direct cell-to-cell contact. The diffusible species released by the irradiated cells are able to traverse the membrane of the transwell insert (Chakraborty et al., 2009). The inclusion of appropriate controls whereby feeder cells received no irradiation prior to co-incubation with the bystander cells demonstrates this as these bystander cells experienced no increase in DDR activation as opposed to those co-cultured with irradiated cells. Whilst previous studies investigating the UVA-induced bystander effect used clonogenic survival assays and techniques to measure ROS generation in the bystander cells, the present study assessed the effect via assessment of γH2AX activation to analyse DDR initiation, which has not previously been conducted. Using this method, it was once again confirmed that UVA can induce a bystander effect.

Immunofluorescence was used to assess DDR initation in bystander cells following co-cultured incubation with irradiated feeder cells. The UVA-induced bystander effect was investigated in terms of how DDR initiation changes over time following irradiation of feeder cells with 100 kJ m^{-2} UVA, which has previously been demonstrated to be able to induce the bystander effect (Whiteside and McMillan, 2009). Co-incubation of bystander cells with feeder cells that had not been irradiated with UVA did not increase γH2AX intensity with increasing duration of co-incubation up to 72 h (Figure 3.11b). Consequently, any difference between the experimental groups in which nonirradiated bystander cells were co-cultured with irradiated cells and the control conditions is due to signals received from the irradiated cells, not due to endogenous damage, which may increase with increased co-culture duration. The experiment conducted in the present study follows on from that conducted by Steel (2016), where γH2AX activation in the context of the UVA induced bystander effect was investigated at 24 and 48 h. The present study investigated the same co-culture durations as well as an addition duration of 72 h. Activation of γH2AX increased at each time point for the experimental groups relative to their corresponding untreated controls (24, 48, 72 h) as determined by signal intensity normalised to the mean of the control 24 h condition. The increase seen at 24 and 48 h was consistent with that seen by Steel (2016). Only a slight increase in γH2AX signal intensity was seen

following 24 h co-incubation between irradiated feeder cells and nonirradiated bystander cells. A much greater increase was seen following 48 and 72 h co-incubation. Whilst a significant increase was seen between the 24 and 48 h experimental conditions, no differences was seen between 48 and 72 h.

Using a similar co-culture model, Whiteside et al. (2011) investigated the timeframes of UVA-induced bystander effects using clonogenic survival assays. Here, they reported that UVA irradiated cells do not release signals that induce a bystander effect immediately and that there is a time lag of over 24 h before levels are sufficient to induce an effect. This may account for the lower, although increased activation of γH2AX. Although the signals released at 24 h are sufficient to cause an increase in DNA damage and induce the bystander effect, signals are continuously released from the irradiated cells after this point. This would explain why γH2AX activation continues to increase until 48 h, as more signals are being released. This has significant importance as cells directly irradiated with 100 kJ m^{-2} UVA show a return to basal levels of γH2AX activation 24 h following irradiation, suggesting that repair of generated lesions has taken place. Despite this, data presented here and in previous studies indicate that a single exposure to UVA can exert an effect for several days following UVA irradiation with the same dosage, therefore amplifying the deleterious effects of UVA exposure. A possible avenue for future research could be to investigate how the rate at which signals are released from the irradiation changes over time. For example, following the initial 24 h lag, does signal release increase for a set period of time or not? Consequently, an investigation could be designed to compare the bystander effect following 24 and 48 h co-culture with 24 h co-culture of bystander cells followed by 24 h in the absence of co-incubation with the irradiated cells. Furthermore, Whiteside et al. (2011) demonstrated that signals released by the UVA irradiated cells persists for a minimum of three days. Therefore, future experiments could assess DDR activation passed the 72 h examined in this study.

The effect of the UVA-induced bystander effect on S-phase entry was also investigated. The duration of co-incubation with UVA irradiated cells had no effect on the number of EdU positive cells but the number of EdU positive cells at each time did increase for the bystander cells co-cultured with irradiated cells in comparison to those which had not been irradiated (Figure 3.11b). One possibility as to why bystander cells exposed to damaging signals released by UVA irradiated cells has increased EdU incorporation is that the received signals cause slowed progression through S-phase. Dardalhon et al. (2008), using *Schizosaccharomyces pombe* as a model organism, found that UVA irradiation of S phase cells slows down DNA

replication in a checkpoint independent manner. It is important to consider that this study focused on direct irradiation rather than the UV-induced bystander effect. Furthermore, the ability to apply the findings for *S. pombe* to mammalian cell types is unclear. Alternative possibilities as to why there was increased numbers of EdU positive cells for the experimental bystander groups could be that the damaging signals received by the bystander cells caused decreased exiting from S-phase or increased entry. It would be interesting to see how the number of EdU positive cells changes within a synchronised population of bystander cells. The increase in the number of EdU positive cells seen in the UVA-induced bystander effect should be compared to the effect of direct UVA irradiation.

The type of γH2AX signal generated by the UVA-induced bystander effect was also studied. Pan-nuclear staining was the predominant type of γH2AX signal for both the control and UVA conditions (Figure 3.11d). Whilst it appeared as though γH2AX foci numbers were increasing as co-culture duration increased, no significant differences were seen among the experimental groups and between the UVA treated conditions and their corresponding control groups. Meyer et al. (2013) found that pan-nuclear γH2AX signalling is dependent on the amount of induced DNA damage. As the proportion of pan-nuclear stained bystander cells co-cultured with irradiated cells appeared to increase for 48 h co-incubation in comparison to 24 h, it is possible that the bystander cells fixed after 48 h possess more lesions. This theory would be consistent with the elevation of γH2AX activation seen via analysis of signal intensity.

IX. The UVA induced bystander effect is not dose-dependent following 48 h co-culture incubation

In addition to investigating how the UVA induced bystander effect changes over time, the effect of different doses of UVA were also studied. Here, feeder cells were irradiated with various doses of UVA up to 100 kJ m^{-2} and co-incubated with nonirradiated bystander cells for 48 h. This duration was chosen as it produced the largest increase in γH2AX activation in the previous experiment. The present study has demonstrated that direct UVA irradiation causes dose-dependent toxicity and this observation has been supported by numerous studies, including Redmond et al. (2014) who demonstrated this in primary human melanoncytes, fibroblasts and keratinocytes. However, past research has found that the ionising radiation-induced bystander effect does not follow a dose-dependent response (Kadhim et al., 2013, Rzeszowska-Wolny et al., 2009, Belyakov et al., 2001). Similar to these findings, the

present study found that the UVA-induced bystander effect is not dose-dependent following 48 h co-culture incubation (Figure 3.12b).

The lack of a dose-dependent increase in the UVA-bystander effect following 48 h co-incubation could be due to there being a maximum amount of signals that can be released from the UVA irradiated cells. 25 kJ m^{-2} UVA could be sufficient to produce damage in the feeder cells that results in the same volume of signals being released from the feeder cells as when they are irradiated with 100 kJ m^{-2} UVA.

X. Clonogenic survival assays demonstrated that the UVA-induced bystander effect is dose-dependent following 1 week co-culture

In order to further investigate whether the UVA-induced bystander effect is dose-dependent or not and to assess whether 25 kJ m^{-2} UVA was the lowest dose sufficient to induce the effect, clonogenic survival assays were completed using the previous doses and an additional dose of 12.5 kJ m^{-2} UVA. Bystander cells were fixed and stained with giemsa following one week co-culture with UVA irradiated cells. It was found that the number of colonies decreased with increasing UVA dose, suggesting that there is a dose-dependent bystander effect created by UVA (Figure 3.11). Whiteside et al. (2011), using a similar co-culture experimental design as the present study, showed that UVA-irradiated feeder cells release signals for a minimum of three days following irradiation. Perhaps the lack of a dose-dependent effect seen at 48 h is due to the implemented doses of UVA releasing similar amounts of signals for this duration, but as the duration of the co-incubation increases, the amount of signals released by cells exposed to lower doses of UVA begins to decrease. As a result, increased co-culture duration and increased UVA exposure causes more signals to be received by the bystander cells with increased damage leading to the DDR-mediated loss of viability. This could explain the dose-dependent decrease in survival following one week co-incubation in comparison to 48 h. A future experiment could test this by irradiating the feeder cells with the same UVA doses as the present study and co-culturing these with nonirradiated bystander cells for 48 h. Following this, the inserts could be transferred to the wells of six-well plates containing nonirradiated bystander cells. This would allow comparison between nonirradiated cells which received signals released by feeder cells up to 48 h and those which received signals from 48 h up to 1 week. Alternative durations could be investigated to further investigate the dynamics of signal release from the irradiated cells.

Alternatively, it is possible that the composition of signals released by the irradiated cells varies and changes with increased incubation. As a result, it is possible that the dose-dependent decrease in cell survival seen following one week co-incubation is due to activation of a different pathway other than the DDR (Banerjee et al., 2005). Future research should therefore assess how the dose-dependent UVA-induced bystander effect changes with varying durations of co-incubation and should also assess both DDR initiation and clonogenic survival. If similar immunofluorescent techniques were to be used in future research to assess DDR activation, the optimal density at which bystander cells should be seeded would need to be determined in order to prevent issues with contact inhibition as co-culture duration increases.

Another possible explanation as to why a dose-dependent response was observed at 1 week could be through dose-dependent activation of alternative pathways, other than the DDR. This may lead to apoptosis induction and therefore decreased colonies at higher UVA doses.

XI. Using immunofluorescence to further analyse the dose-dependent UVA-induced bystander effect

As well as assessing S-phase entry in relation to co-incubation duration, UVA dose and its effect on bystander cell proliferation was also examined. The proportion of EdU positive cells increased between control bystander cells and those that were co-cultured with UVA irradiated cells. However, the number of EdU positive bystander cells did not increase in a dose-dependent manner. As 25 kJ m^{-2} UVA was found to be sufficient to induce a bystander effect following 48 h co-culture, as determined by increased γH2AX activation, it is highly probable the increased number of cells in S- and G_2 phase is a result of the same factor as with 100 kJ m^{-2} UVA. It would be interesting to see if the number of EdU positive bystander cells decreased in a dose-dependent manner with increased duration of co-incubation, similar to how a dose-dependent bystander effect was observed following seven days co-incubation. Would there be fewer EdU positive cells as the amount of replication stress decreased?

Additionally, the type of γH2AX signal produced was also investigated in the context of varying the dose of UVA to which feeder cells are exposed to. The proportion of pan-nuclear stained cells was slightly elevated for the bystander cells co-cultured with UVA irradiated cells in comparison to control bystander cells, although the increase was not significant. No difference was seen between the different UVA

doses. As mentioned above, Meyer et al. (2013) suggest that pan-nuclear staining is dependent on the amount of DNA damage the cell possesses. The lack of a dose-dependent increase in the number of pan-nuclear stained cells supports the idea that at 48 h, the same amount of damage signals are released from the feeder cells, regardless of the UVA dose to which they were exposed.

Although the present study provides some insight into the UVA-induced bystander effect in terms of how H2AX phosphorylation changes over time, how various UVA doses affect the bystander effect and how cell cycle progression is impacted, the data do not provide any further insight into the source of the lesions in the bystander cells. This is important as the DDR is initiated following detection of different types of lesions and γH2AX activation is common to numerous arms of the DDR.

In 2014, Widel et al. investigated the roles of ROS and interleukins in the UVA-induced bystander effect. Here, they found increased levels of ROS and IL-6 within the bystander cells and within the media of the irradiated cells, suggesting that these may be the signals released from the irradiated cells. Remond et al. (2014) supported the suggestion for the involvement of ROS in the UVA-induced bystander effect when investigating the interplay in the bystander effect between different cell types. Steel (2016) used antioxidants to investigate the role of ROS in the UVA-induced bystander effect and found that the number of EdU positive cells was reduced. Future research should be conducted to investigate the role of other factors, such as IL-6, in increasing the number of EdU positive cells, as they may also have an effect.

IL-6 inhibitors should also be investigated in the context of the UVA-induced bystander effect to investigate the findings of Widel et al. (2014) further. There is an abundance of evidence that ROS generation following direct UVA exposure occurs via type I and II photosensitisation reactions. Although it is likely that ROS generated via the UVA-induced bystander effect occurs through this mechanism, there is some evidence for the involvement of dermal extracellular matrix proteins such as keratin, collagen and elastin (Wondrak et al. 2003). Another possible avenue for future research when investigating the source of the lesions in the bystander cells is to investigate the mechanism by which the released ROS induce their damaging outcomes in the bystander cells.

An important aspect that needs to be considered when investigating the radiation-induced bystander effect is that the skin is a complex organ harbouring a rich array of different cell types, which together carry out a number of diverse functions including

protection from insults, infection and dehydration and also enabling thermoregulation and sensory perception. It is therefore important to consider how one cell type that received direct irradiation, whether it is due to UVA or not, and how it exerts a bystander effect to nearby cells that are the same type as itself, but also that are different. For example, does the UVA-induced bystander effect produce a different outcome when signals are released from keratinocytes and taken up by melanocytes than when signals are received by keratinocytes following their release from a UVA-irradiated fibroblast?

Redmond et al. (2014) investigated this in vitro using a co-culture model similar to that in the present study. The UVA-induced bystander effect was observed between all three cutaneous cell types (melanocytes, keratinocytes and fibroblasts). The significant finding was that melanocytes appeared to be more resistant to direct UVA effects compared to the other cell types studied and that melanocytes were more susceptible to bystander oxidative signalling. CPDs have been demonstrated as being the predominant lesions generated following direct UVA irradiation. In many cell types, CPDs occur at rates of approximately 5-fold higher than 8-oxoG, the main lesion generated from oxidative damage. Interestingly, however, when comparing the ratio of CPDs to 8-oxoG in melanocytes, Mouret et al. (2012) found that the ratio decreased to 1.4 in melanocytes. Together, these studies suggest that melanocytes are more susceptible to oxidative damage. UVA is able to penetrate deeper into the skin than UVB, which is rapidly attenuated with increasing depth. UVA lesion generation has been found to increase with increasing skin depth (Tewari et al. 2013). Consequently, the role of the UVA-induced bystander effect in melanomagenesis needs to be considered. Deciphering the role of UVA in melanomagenesis would have huge clinical implications and would help shed light on conflicting arguments within the literature in regards to whether UVA can or cannot induce melanomagenesis (Noonan et al., 2012, De Fabo et al., 2004). One method by which this could be analysed could be to implement next-generation sequencing to compare the mutation spectra between cells directly irradiated with UVA and bystander cells co-cultured with UVA exposed cells.

Additionally, investigations into the UVA-induced bystander effect use two chamber models to investigate how co-culturing differentially treated cell populations affects nonirradiated bystander cells. However, this only takes into account signalling that occurs through a permeable membrane that separates the two populations and does not consider signalling through intercellular connections such as gap junctions. In vivo, not every cell will absorb UVA and other forms of irradiation directly and so the

signals released through intercellular connections to neighbouring cells also need to be considered in addition to signals released and taken up by cells that are not in direct contact with the directly irradiated cell. A number of studies have considered the involvement of gap junctions in the radiation-induced bystander effect using methods that involve inhibition of gap junction intercellular communication, with mixed results observed for different types of radiation (Gerashchenko and Howell, 2003, Azzam et al., 1998, Mothersill and Seymour, 1998).

XII. Future work

In addition to the suggestions made in regards to future work for specific areas involving the outcomes of UVA irradiation (e.g. the UVA-induced bystander effect), a number of other general areas of research could possibly be explored in future research into UVA and the DDR. Firstly, the DDR components investigated in the present study are limited as, at most, only γH2AX and p-Chk2 activation were analysed. It would therefore make sense to analyse how activation of other components within the different pathways of the DDR change following both direct and indirect UVA irradiation, and how inhibition of various DNA damage sensors and kinases such as ATM and ATR impact these. For example, p53-binding protein 1 (53BP1) can be phosphorylated by ATM and together with mediator of DNA damage checkpoint 1 (MDC1) forms a positive feedback loop to enhance ATM activation and result in sustained DDR signalling (Lou et al., 2003). There is evidence for the accumulation of 53BP1 to sites of DNA damage and γH2AX foci formation (Stixova et al., 2014). In the present study, p-Chk2 activation did not change following ATM inhibition. Therefore, it would be interesting to see how 53BP1 activation and accumulation is affected by similar levels of ATM inhibition and to also assess if MRN complex inhibition affects 53BP1 activation differently. Additionally, activation of DDR components that are downstream of ATR should also be investigated in the context of both direct and indirect UVA exposure and both in the absence and presence of DDR component inhibitors. In particular, p-Chk1 activation should be assessed at various times following direct UVA irradiation in the absence of any inhibition and following individual and combined inhibition of ATM, MRN and ATR.

The methods used in the present study to investigate the role of UVA on DDR initiation failed to provide any insight into how different lesions generated by direct and indirect UVA irradiation activated the different pathways within the DDR. Whilst UVA irradiation resulted in increased γH2AX activation, this can occur via H2AX

phosphorylation by either ATM or ATR. ATM inhibition caused decreased γH2AX activation but activation levels remained above basal levels present in untreated cells. Although it is possible that DSBs generated by UVA resulted in the generation of ssDNA regions available for detection by RPA and the 9-1-1 complex, the available data only allows for speculation based on previous research. Activation of the DDR and its various components, including how their activation changes over time should be investigated alongside investigations assessing the different types of DNA lesion generated. In particular, how does inhibition of various components impact the spectra of generated lesions? Due to the fact that ATM, ATR and DNA-PKcs have been implemented as being involved in the repair of DNA lesions generated following UVA exposure, it would be interesting to see how the use of a pan-PIKK inhibitor impacted DDR component activation and how this was reflected in the types of lesion generated and the resulting mutational spectrum.

As mentioned previously, skin is composed of a diverse array of cell types including keratinocytes, melanocytes and fibroblasts. The consequences of direct and indirect UVA exposure on DDR initiation, cell viability and the types of lesions generated need to be investigated in the context of models that reflect human skin. Additionally, whilst terrestrial UVR to which we are exposed to consist of 90-95% UVA, a small proportion of this still consists of UVB. As a result, the cooperative role of UVB and UVA on the DNA damage response needs to be considered. Both wavebands, regardless of the proportion of terrestrial UVR they make up, are able to produce DNA damage and contribute to mutagenesis and carcinogenesis. This is of particular importance in relation to malignant melanoma, which, due to its high potential for metastasis, is the most dangerous form of skin cancer.

At present, very little is known about the comparative action of UVA and UVB irradiation on the DNA damage response in melanocytes, with the available literature consisting of only one paper to date describing γH2AX activation using a UV source consisting of non-terrestrial ratios of UVA to UVB (Swope et al., 2014). Understanding how melanocytes respond to DNA damage caused by environmentally relevant doses of UVA and UVB may provide important insight into understanding the underlying process of UV carcinogenesis. Not only should the comparative role of direct irradiation with UVB and UVA on the DDR of melanocytes be investigated but the difference in DDR activation between primary melanocytes from both light skinned and dark skinned neonates should also be considered, given the important role that melanin plays. Also, the comparative role of UVA and UVB on

DDR activation in bystander melanocytes as a result of signals received from cells of the same type and cell of a different should also be taken into account.

5. References

1. ABE, K. & MATSUKI, N. 2000. Measurement of cellular 3-(4,5-dimethylthiazol-2-yl)-2,5-diphenyltetrazolium bromide (MTT) reduction activity and lactate dehydrogenase release using MTT. *Neurosci Res,* 38**,** 325-9.
2. ABRAHAM, R. T. 2002. Checkpoint signalling: focusing on 53BP1. *Nat Cell Biol,* 4**,** E277-E279.
3. AGAR, N. S., HALLIDAY, G. M., BARNETSON, R. S., ANANTHASWAMY, H. N., WHEELER, M. & JONES, A. M. 2004. The basal layer in human squamous tumors harbors more UVA than UVB fingerprint mutations: A role for UVA in human skin carcinogenesis. *Proceedings of the National Academy of Sciences of the United States of America,* 101**,** 4954-4959.
4. AZZAM, E. I., DE TOLEDO, S. M., GOODING, T. & LITTLE, J. B. 1998. Intercellular communication is involved in the bystander regulation of gene expression in human cells exposed to very low fluences of alpha particles. *Radiat Res,* 150**,** 497-504.
5. BANERJEE, G., GUPTA, N., KAPOOR, A. & RAMAN, G. 2005. UV induced bystander signaling leading to apoptosis. *Cancer Lett,* 223**,** 275-84.
6. BANIN, S., MOYAL, L., SHIEH, S., TAYA, Y., ANDERSON, C. W., CHESSA, L., SMORODINSKY, N. I., PRIVES, C., REISS, Y., SHILOH, Y. & ZIV, Y. 1998. Enhanced phosphorylation of p53 by ATM in response to DNA damage. *Science,* 281**,** 1674-7.
7. BARNES, L., DUMAS, M., JUAN, M., NOBLESSE, E., TESNIERE, A., SCHNEBERT, S., GUILLOT, B. & MOLES, J. P. 2010. GammaH2AX, an accurate marker that analyzes UV genotoxic effects on human keratinocytes and on human skin. *Photochem Photobiol,* 86**,** 933-41.
8. BARRY, S. P., TOWNSEND, P. A., KNIGHT, R. A., SCARABELLI, T. M., LATCHMAN, D. S. & STEPHANOU, A. 2010. STAT3 modulates the DNA damage response pathway. *International Journal of Experimental Pathology,* 91**,** 506-514.
9. BATISTA, L. F., KAINA, B., MENEGHINI, R. & MENCK, C. F. 2009. How DNA lesions are turned into powerful killing structures: insights from UV-induced apoptosis. *Mutat Res,* 681**,** 197-208.
10. BATTIE, C., JITSUKAWA, S., BERNERD, F., DEL BINO, S., MARIONNET, C. & VERSCHOORE, M. 2014. New insights in photoaging, UVA induced damage and skin types. *Experimental Dermatology,* 23**,** 7-12.
11. BATTY, D. P. & WOOD, R. D. 2000. Damage recognition in nucleotide excision repair of DNA. *Gene,* 241**,** 193-204.
12. BELYAKOV, O. V., MALCOLMSON, A. M., FOLKARD, M., PRISE, K. M. & MICHAEL, B. D. 2001. Direct evidence for a bystander effect of ionizing radiation in primary human fibroblasts. *British Journal of Cancer,* 84**,** 674-679.
13. BERGER, M. F., HODIS, E., HEFFERNAN, T. P., DERIBE, Y. L., LAWRENCE, M. S., PROTOPOPOV, A., IVANOVA, E., WATSON, I. R., NICKERSON, E., GHOSH, P., ZHANG, H., ZEID, R., REN, X., CIBULSKIS, K., SIVACHENKO, A. Y., WAGLE, N., SUCKER, A., SOUGNEZ, C., ONOFRIO, R., AMBROGIO, L., AUCLAIR, D., FENNELL, T., CARTER, S. L., DRIER, Y., STOJANOV, P., SINGER, M. A., VOET, D., JING, R., SAKSENA, G., BARRETINA, J., RAMOS, A. H., PUGH, T. J., STRANSKY, N., PARKIN, M., WINCKLER, W., MAHAN, S., ARDLIE, K., BALDWIN, J., WARGO, J., SCHADENDORF, D., MEYERSON, M., GABRIEL, S. B., GOLUB, T. R., WAGNER, S. N., LANDER, E. S., GETZ, G., CHIN, L. & GARRAWAY, L. A. 2012. Melanoma genome sequencing reveals frequent PREX2 mutations. *Nature,* 485**,** 502-6.
14. BESARATINIA, A., SYNOLD, T. W., XI, B. & PFEIFER, G. P. 2004. G-to-T transversions and small tandem base deletions are the hallmark of mutations induced by ultraviolet a radiation in mammalian cells. *Biochemistry,* 43**,** 8169-77.
15. BEUKERS, R. & BERENDS, W. 1960. ISOLATION AND IDENTIFICATION OF THE IRRADIATION PRODUCT OF THYMINE. *Biochimica Et Biophysica Acta,* 41**,** 550-551.

16. BIERTUMPFEL, C., ZHAO, Y., KONDO, Y., RAMON-MAIQUES, S., GREGORY, M., LEE, J. Y., MASUTANI, C., LEHMANN, A. R., HANAOKA, F. & YANG, W. 2010. Structure and mechanism of human DNA polymerase eta. *Nature,* 465**,** 1044-U102.
17. BOUKAMP, P. 2005. Non-melanoma skin cancer: what drives tumor development and progression? *Carcinogenesis,* 26**,** 1657-67.
18. BRASH, D. E. 2015. UV Signature Mutations. *Photochemistry and Photobiology,* 91**,** 15-26.
19. BRASH, D. E., RUDOLPH, J. A., SIMON, J. A., LIN, A., MCKENNA, G. J., BADEN, H. P., HALPERIN, A. J. & PONTEN, J. 1991. A role for sunlight in skin cancer: UV-induced p53 mutations in squamous cell carcinoma. *Proc Natl Acad Sci U S A,* 88**,** 10124-8.
20. BURREN, R., SCALETTA, C., FRENK, E., PANIZZON, R. G. & APPLEGATE, L. A. 1998. Sunlight and carcinogenesis: expression of p53 and pyrimidine dimers in human skin following UVA I, UVA I + II and solar simulating radiations. *Int J Cancer,* 76**,** 201-6.
21. CADET, J., DELATOUR, T., DOUKI, T., GASPARUTTO, D., POUGET, J. P., RAVANAT, J. L. & SAUVAIGO, S. 1999. Hydroxyl radicals and DNA base damage. *Mutat Res,* 424**,** 9-21.
22. CADET, J., DOUKI, T. & RAVANAT, J. L. 2015. Oxidatively generated damage to cellular DNA by UVB and UVA radiation. *Photochem Photobiol,* 91**,** 140-55.
23. CADET, J., MOURET, S., RAVANAT, J. L. & DOUKI, T. 2012. Photoinduced Damage to Cellular DNA: Direct and Photosensitized Reactions. *Photochemistry and Photobiology,* 88**,** 1048-1065.
24. CALO, R., VISONE, C. M. & MARABINI, L. 2015. Thymol and Thymus Vulgaris L. activity against UVA- and UVB-induced damage in NCTC 2544 cell line. *Mutation Research-Genetic Toxicology and Environmental Mutagenesis,* 791**,** 30-37.
25. CAMPALANS, A., AMOUROUX, R., BRAVARD, A., EPE, B. & RADICELLA, J. P. 2007. UVA irradiation induces relocalisation of the DNA repair protein hOGG1 to nuclear speckles. *J Cell Sci,* 120**,** 23-32.
26. CHAKRABORTY, A., HELD, K. D., PRISE, K. M., LIBER, H. L. & REDMOND, R. W. 2009. Bystander Effects Induced by Diffusing Mediators after Photodynamic Stress. *Radiation research,* 172**,** 74-81.
27. CLEAVER, J. E. 1968. Defective repair replication of DNA in xeroderma pigmentosum. *Nature,* 218**,** 652-6.
28. CLEAVER, J. E. 2011. gammaH2Ax: biomarker of damage or functional participant in DNA repair "all that glitters is not gold!". *Photochem Photobiol,* 87**,** 1230-9.
29. CLEAVER, J. E., FEENEY, L. & REVET, I. 2011. Phosphorylated H2Ax is not an unambiguous marker for DNA double-strand breaks. *Cell Cycle,* 10**,** 3223-4.
30. CORTAT, B., GARCIA, C. C., QUINET, A., SCHUCH, A. P., DE LIMA-BESSA, K. M. & MENCK, C. F. 2013. The relative roles of DNA damage induced by UVA irradiation in human cells. *Photochem Photobiol Sci,* 12**,** 1483-95.
31. CORTEZ, D., GUNTUKU, S., QIN, J. & ELLEDGE, S. J. 2001. ATR and ATRIP: partners in checkpoint signaling. *Science,* 294**,** 1713-6.
32. COURDAVAULT, S., BAUDOUIN, C., CHARVERON, M., CANGUILHEM, B., FAVIER, A., CADET, J. & DOUKI, T. 2005. Repair of the three main types of bipyrimidine DNA photoproducts in human keratinocytes exposed to UVB and UVA radiations. *DNA Repair (Amst),* 4**,** 836-44.
33. COURDAVAULT, S., BAUDOUIN, C., CHARVERON, M., FAVIER, A., CADET, J. & DOUKI, T. 2004. Larger yield of cyclobutane dimers than 8-oxo-7,8-dihydroguanine in the DNA of UVA-irradiated human skin cells. *Mutat Res,* 556**,** 135-42.
34. CUI, Y., PALII, S. S., INNES, C. L. & PAULES, R. S. 2014. Depletion of ATR selectively sensitizes ATM-deficient human mammary epithelial cells to ionizing radiation and DNA-damaging agents. *Cell Cycle,* 13**,** 3541-50.

35. D'ADDA DI FAGAGNA, F. 2008. Living on a break: cellular senescence as a DNA-damage response. *Nat Rev Cancer,* 8**,** 512-522.
36. DAHLE, J., KAALHUS, O., STOKKE, T. & KVAM, E. 2005. Bystander effects may modulate ultraviolet A and B radiation-induced delayed mutagenesis. *Radiation Research,* 163**,** 289-295.
37. DARDALHON, D., REYNAUD-ANGELIN, A., BALDACCI, G., SAGE, E. & FRANCESCONI, S. 2008. Unconventional effects of UVA radiation on cell cycle progression in S. pombe. *Cell Cycle,* 7, 611-622.
38. DAVIES, H., BIGNELL, G. R., COX, C., STEPHENS, P., EDKINS, S., CLEGG, S., TEAGUE, J., WOFFENDIN, H., GARNETT, M. J., BOTTOMLEY, W., DAVIS, N., DICKS, E., EWING, R., FLOYD, Y., GRAY, K., HALL, S., HAWES, R., HUGHES, J., KOSMIDOU, V., MENZIES, A., MOULD, C., PARKER, A., STEVENS, C., WATT, S., HOOPER, S., WILSON, R., JAYATILAKE, H., GUSTERSON, B. A., COOPER, C., SHIPLEY, J., HARGRAVE, D., PRITCHARD-JONES, K., MAITLAND, N., CHENEVIX-TRENCH, G., RIGGINS, G. J., BIGNER, D. D., PALMIERI, G., COSSU, A., FLANAGAN, A., NICHOLSON, A., HO, J. W. C., LEUNG, S. Y., YUEN, S. T., WEBER, B. L., SEIGLER, H. F., DARROW, T. L., PATERSON, H., MARAIS, R., MARSHALL, C. J., WOOSTER, R., STRATTON, M. R. & FUTREAL, P. A. 2002. Mutations of the BRAF gene in human cancer. *Nature,* 417**,** 949-954.
39. DE FABO, E. C., NOONAN, F. P., FEARS, T. & MERLINO, G. 2004. Ultraviolet B but not ultraviolet A radiation initiates melanoma. *Cancer Res,* 64**,** 6372-6.
40. DE JAGER, M., VAN NOORT, J., VAN GENT, D. C., DEKKER, C., KANAAR, R. & WYMAN, C. 2001. Human Rad50/Mre11 is a flexible complex that can tether DNA ends. *Mol Cell,* 8**,** 1129-35.
41. DENG, C., ZHANG, P., HARPER, J. W., ELLEDGE, S. J. & LEDER, P. 1995. Mice lacking p21CIP1/WAF1 undergo normal development, but are defective in G1 checkpoint control. *Cell,* 82**,** 675-84.
42. DI SIENA, S., CAMPOLO, F., ROSSI, P., JANNINI, E. A., DOLCI, S. & PELLEGRINI, M. 2013. UV and genotoxic stress induce ATR relocalization in mouse spermatocytes. *Int J Dev Biol,* 57**,** 281-7.
43. DING, D., ZHANG, Y., WANG, J., ZHANG, X., GAO, Y., YIN, L., LI, Q., LI, J. & CHEN, H. 2016. Induction and inhibition of the pan-nuclear gamma-H2AX response in resting human peripheral blood lymphocytes after X-ray irradiation. *Cell Death Discovery,* 2**,** 16011.
44. DOUKI, T. & CADET, J. 2001. Individual determination of the yield of the main UV-induced dimeric pyrimidine photoproducts in DNA suggests a high mutagenicity of CC photolesions. *Biochemistry,* 40**,** 2495-2501.
45. DOUKI, T., PERDIZ, D., GROF, P., KULUNCSICS, Z., MOUSTACCHI, E., CADET, J. & SAGE, E. 1999. Oxidation of guanine in cellular DNA by solar UV radiation: biological role. *Photochem Photobiol,* 70**,** 184-90.
46. DOUKI, T., REYNAUD-ANGELIN, A., CADET, J. & SAGE, E. 2003. Bipyrimidine photoproducts rather than oxidative lesions are the main type of DNA damage involved in the genotoxic effect of solar UVA radiation. *Biochemistry,* 42**,** 9221-6.
47. DOWNEY, M. & DUROCHER, D. 2006. gammaH2AX as a checkpoint maintenance signal. *Cell Cycle,* 5**,** 1376-81.
48. DROGE, W. 2002. Free radicals in the physiological control of cell function. *Physiological Reviews,* 82, 47-95.
49. DUBAS, L. E. & INGRAFFEA, A. 2013. Nonmelanoma skin cancer. *Facial Plast Surg Clin North Am,* 21**,** 43-53.
50. EIBERGER, W., VOLKMER, B., AMOUROUX, R., DHERIN, C., RADICELLA, J. P. & EPE, B. 2008. Oxidative stress impairs the repair of oxidative DNA base modifications in human skin fibroblasts and melanoma cells. *DNA Repair,* 7**,** 912-921.

51. EL GHISSASSI, F., BAAN, R., STRAIF, K., GROSSE, Y., SECRETAN, B., BOUVARD, V., BENBRAHIM-TALLAA, L., GUHA, N., FREEMAN, C., GALICHET, L., COGLIANO, V. & WO, W. H. O. I. A. R. C. M. 2009. A review of human carcinogens - Part D: radiation. *Lancet Oncology,* 10**,** 751-752.
52. FALCK, J., COATES, J. & JACKSON, S. P. 2005. Conserved modes of recruitment of ATM, ATR and DNA-PKcs to sites of DNA damage. *Nature,* 434**,** 605-11.
53. FALCK, J., PETRINI, J. H., WILLIAMS, B. R., LUKAS, J. & BARTEK, J. 2002. The DNA damage-dependent intra-S phase checkpoint is regulated by parallel pathways. *Nat Genet,* 30**,** 290-4.
54. FELL, L. J., PAUL, N. D. & MCMILLAN, T. J. 2002. Role for non-homologous end-joining in the repair of UVA-induced DNA damage. *Int J Radiat Biol,* 78**,** 1023-7.
55. FERLAY, J., SOERJOMATARAM, I., DIKSHIT, R., ESER, S., MATHERS, C., REBELO, M., PARKIN, D. M., FORMAN, D. & BRAY, F. 2015. Cancer incidence and mortality worldwide: sources, methods and major patterns in GLOBOCAN 2012. *Int J Cancer,* 136**,** E359-86.
56. FINKEL, T. & HOLBROOK, N. J. 2000. Oxidants, oxidative stress and the biology of ageing. *Nature,* 408**,** 239-247.
57. FREEMAN, S. E., GANGE, R. W., MATZINGER, E. A. & SUTHERLAND, B. M. 1986. HIGHER PYRIMIDINE DIMER YIELDS IN SKIN OF NORMAL HUMANS WITH HIGHER UVB SENSITIVITY. *Journal of Investigative Dermatology,* 86**,** 34-36.
58. FREEMAN, S. E., GANGE, R. W., SUTHERLAND, J. C., MATZINGER, E. A. & SUTHERLAND, B. M. 1987. Production of pyrimidine dimers in DNA of human skin exposed in situ to UVA radiation. *J Invest Dermatol,* 88**,** 430-3.
59. FREEMAN, S. E., HACHAM, H., GANGE, R. W., MAYTUM, D. J., SUTHERLAND, J. C. & SUTHERLAND, B. M. 1989. Wavelength dependence of pyrimidine dimer formation in DNA of human skin irradiated in situ with ultraviolet light. *Proceedings of the National Academy of Sciences of the United States of America,* 86**,** 5605-5609.
60. GARINIS, G. A., MITCHELL, J. R., MOORHOUSE, M. J., HANADA, K., DE WAARD, H., VANDEPUTTE, D., JANS, J., BRAND, K., SMID, M., VAN DER SPEK, P. J., HOEIJMAKERS, J. H., KANAAR, R. & VAN DER HORST, G. T. 2005. Transcriptome analysis reveals cyclobutane pyrimidine dimers as a major source of UV-induced DNA breaks. *Embo j,* 24**,** 3952-62.
61. GERASHCHENKO, B. I. & HOWELL, R. W. 2003. Cell proximity is a prerequisite for the proliferative response of bystander cells co-cultured with cells irradiated with gamma-rays. *Cytometry A,* 56**,** 71-80.
62. GHARBI, S. I., ZVELEBIL, M. J., SHUTTLEWORTH, S. J., HANCOX, T., SAGHIR, N., TIMMS, J. F. & WATERFIELD, M. D. 2007. Exploring the specificity of the PI3K family inhibitor LY294002. *Biochem J,* 404**,** 15-21.
63. GIRARD, P. M., POZZEBON, M., DELACOTE, F., DOUKI, T., SMIRNOVA, V. & SAGE, E. 2008. Inhibition of S-phase progression triggered by UVA-induced ROS does not require a functional DNA damage checkpoint response in mammalian cells. *DNA Repair,* 7**,** 1500-1516.
64. GOLDING, S. E., ROSENBERG, E., VALERIE, N., HUSSAINI, I., FRIGERIO, M., COCKCROFT, X. F., CHONG, W. Y., HUMMERSONE, M., RIGOREAU, L., MENEAR, K. A., O'CONNOR, M. J., POVIRK, L. F., VAN METER, T. & VALERIE, K. 2009. Improved ATM kinase inhibitor KU-60019 radiosensitizes glioma cells, compromises insulin, AKT and ERK prosurvival signaling, and inhibits migration and invasion. *Mol Cancer Ther,* 8**,** 2894-902.
65. GREENMAN, C., STEPHENS, P., SMITH, R., DALGLIESH, G. L., HUNTER, C., BIGNELL, G., DAVIES, H., TEAGUE, J., BUTLER, A., STEVENS, C., EDKINS, S., O'MEARA, S., VASTRIK, I., SCHMIDT, E. E., AVIS, T., BARTHORPE, S., BHAMRA, G., BUCK, G., CHOUDHURY, B.,

CLEMENTS, J., COLE, J., DICKS, E., FORBES, S., GRAY, K., HALLIDAY, K., HARRISON, R., HILLS, K., HINTON, J., JENKINSON, A., JONES, D., MENZIES, A., MIRONENKO, T., PERRY, J., RAINE, K., RICHARDSON, D., SHEPHERD, R., SMALL, A., TOFTS, C., VARIAN, J., WEBB, T., WEST, S., WIDAA, S., YATES, A., CAHILL, D. P., LOUIS, D. N., GOLDSTRAW, P., NICHOLSON, A. G., BRASSEUR, F., LOOIJENGA, L., WEBER, B. L., CHIEW, Y. E., DEFAZIO, A., GREAVES, M. F., GREEN, A. R., CAMPBELL, P., BIRNEY, E., EASTON, D. F., CHENEVIX-TRENCH, G., TAN, M. H., KHOO, S. K., TEH, B. T., YUEN, S. T., LEUNG, S. Y., WOOSTER, R., FUTREAL, P. A. & STRATTON, M. R. 2007. Patterns of somatic mutation in human cancer genomes. *Nature,* 446**,** 153-8.

66. GREER, A. 2006. Christopher Foote's discovery of the role of singlet oxygen [1O2 (1Delta g)] in photosensitized oxidation reactions. *Acc Chem Res,* 39**,** 797-804.
67. GREINERT, R., VOLKMER, B., HENNING, S., BREITBART, E. W., GREULICH, K. O., CARDOSO, M. C. & RAPP, A. 2012. UVA-induced DNA double-strand breaks result from the repair of clustered oxidative DNA damages. *Nucleic Acids Research,* 40**,** 10263-10273.
68. GRIEWANK, K. G., MURALI, R., SCHILLING, B., SCHIMMING, T., MOLLER, I., MOLL, I., SCHWAMBORN, M., SUCKER, A., ZIMMER, L., SCHADENDORF, D. & HILLEN, U. 2013. TERT promoter mutations are frequent in cutaneous basal cell carcinoma and squamous cell carcinoma. *PLoS One,* 8**,** e80354.
69. GULSTON, M., DE LARA, C., JENNER, T., DAVIS, E. & O'NEILL, P. 2004. Processing of clustered DNA damage generates additional double-strand breaks in mammalian cells post-irradiation. *Nucleic Acids Res,* 32**,** 1602-9.
70. HALLIDAY, G. M., BYRNE, S. N. & DAMIAN, D. L. 2011. Ultraviolet A Radiation: Its Role in Immunosuppression and Carcinogenesis. *Seminars in Cutaneous Medicine and Surgery,* 30**,** 214-221.
71. HANAHAN, D. & WEINBERG, R. A. 2011. Hallmarks of Cancer: The Next Generation. *Cell,* 144**,** 646-674.
72. HE, Z., ZHANG, L., ZHUO, C., JIN, F. & WANG, Y. 2016. Apoptosis inhibition effect of Dihydromyricetin against UVA-exposed human keratinocyte cell line. *Journal of Photochemistry and Photobiology B: Biology,* 161**,** 40-49.
73. HORN, S., FIGL, A., RACHAKONDA, P. S., FISCHER, C., SUCKER, A., GAST, A., KADEL, S., MOLL, I., NAGORE, E., HEMMINKI, K., SCHADENDORF, D. & KUMAR, R. 2013. TERT Promoter Mutations in Familial and Sporadic Melanoma. *Science,* 339**,** 959-961.
74. HORSFALL, M. J. & LAWRENCE, C. W. 1994. Accuracy of replication past the T-C (6-4) adduct. *J Mol Biol,* 235**,** 465-71.
75. HUANG, X. X., BERNERD, F. & HALLIDAY, G. M. 2009. Ultraviolet A within sunlight induces mutations in the epidermal basal layer of engineered human skin. *American Journal of Pathology,* 174, 1534-1543.
76. HUHN, D., BOLCK, H. A. & SARTORI, A. A. 2013. Targeting DNA double-strand break signalling and repair: recent advances in cancer therapy. *Swiss Med Wkly,* 143**,** w13837.
77. HWANG, Y. P., OH, K. N., YUN, H. J. & JEONG, H. G. 2011. The flavonoids apigenin and luteolin suppress ultraviolet A-induced matrix metalloproteinase-1 expression via MAPKs and AP-1-dependent signaling in HaCaT cells. *J Dermatol Sci,* 61**,** 23-31.
78. IKEHATA, H., KAWAI, K., KOMURA, J.-I., SAKATSUME, K., WANG, L., IMAI, M., HIGASHI, S., NIKAIDO, O., YAMAMOTO, K., HIEDA, K., WATANABE, M., KASAI, H. & ONO, T. 2008. UVA1 Genotoxicity Is Mediated Not by Oxidative Damage but by Cyclobutane Pyrimidine Dimers in Normal Mouse Skin. *Journal of Investigative Dermatology,* 128**,** 2289-2296.
79. IKEHATA, H. & ONO, T. 2011. The Mechanisms of UV Mutagenesis. *Journal of Radiation Research,* 52**,** 115-125.

80. JACKSON, S. P. & BARTEK, J. 2009. The DNA-damage response in human biology and disease. *Nature,* 461**,** 1071-1078.
81. JANS, J., SCHUL, W., SERT, Y. G., RIJKSEN, Y., REBEL, H., EKER, A. P., NAKAJIMA, S., VAN STEEG, H., DE GRUIJL, F. R., YASUI, A., HOEIJMAKERS, J. H. & VAN DER HORST, G. T. 2005. Powerful skin cancer protection by a CPD-photolyase transgene. *Curr Biol,* 15**,** 105-15.
82. JAVERI, A., HUANG, X. X., BERNERD, F., MASON, R. S. & HALLIDAY, G. M. 2008. Human 8-oxoguanine-DNA glycosylase 1 protein and gene are expressed more abundantly in the superficial than basal layer of human epidermis. *DNA Repair (Amst),* 7**,** 1542-50.
83. JAZAYERI, A., FALCK, J., LUKAS, C., BARTEK, J., SMITH, G. C., LUKAS, J. & JACKSON, S. P. 2006. ATM- and cell cycle-dependent regulation of ATR in response to DNA double-strand breaks. *Nat Cell Biol,* 8**,** 37-45.
84. JIANG, W., ANANTHASWAMY, H. N., MULLER, H. K. & KRIPKE, M. L. 1999. p53 protects against skin cancer induction by UV-B radiation. *Oncogene,* 18**,** 4247-53.
85. JIANG, Y., RABBI, M., KIM, M., KE, C. H., LEE, W., CLARK, R. L., MIECZKOWSKI, P. A. & MARSZALEK, P. E. 2009. UVA Generates Pyrimidine Dimers in DNA Directly. *Biophysical Journal,* 96**,** 1151-1158.
86. KADHIM, M., SALOMAA, S., WRIGHT, E., HILDEBRANDT, G., BELYAKOV, O. V., PRISE, K. M. & LITTLE, M. P. 2013. Non-targeted effects of ionizing radiation–implications for low dose risk. *Mutation research,* 752**,** 84-98.
87. KIELBASSA, C., ROZA, L. & EPE, B. 1997. Wavelength dependence of oxidative DNA damage induced by UV and visible light. *Carcinogenesis,* 18**,** 811-816.
88. KIM, Y. J. & WILSON, D. M., 3RD 2012. Overview of base excision repair biochemistry. *Curr Mol Pharmacol,* 5**,** 3-13.
89. KIMONIS, V. E., GOLDSTEIN, A. M., PASTAKIA, B., YANG, M. L., KASE, R., DIGIOVANNA, J. J., BALE, A. E. & BALE, S. J. 1997. Clinical manifestations in 105 persons with nevoid basal cell carcinoma syndrome. *American Journal of Medical Genetics,* 69**,** 299-308.
90. KINNER, A., WU, W., STAUDT, C. & ILIAKIS, G. 2008. γ-H2AX in recognition and signaling of DNA double-strand breaks in the context of chromatin. *Nucleic Acids Research,* 36**,** 5678-5694.
91. KOZMIN, S., SLEZAK, G., REYNAUD-ANGELIN, A., ELIE, C., DE RYCKE, Y., BOITEUX, S. & SAGE, E. 2005. UVA radiation is highly mutagenic in cells that are unable to repair 7,8-dihydro-8-oxoguanine in Saccharomyces cerevisiae. *Proceedings of the National Academy of Sciences of the United States of America,* 102**,** 13538-13543.
92. KRAEMER, A., CHEN, I. P., HENNING, S., FAUST, A., VOLKMER, B., ATKINSON, M. J., MOERTL, S. & GREINERT, R. 2013. UVA and UVB irradiation differentially regulate microRNA expression in human primary keratinocytes. *PLoS One,* 8**,** e83392.
93. KULUNCSICS, Z., PERDIZ, D., BRULAY, E., MUEL, B. & SAGE, E. 1999. Wavelength dependence of ultraviolet-induced DNA damage distribution: involvement of direct or indirect mechanisms and possible artefacts. *J Photochem Photobiol B,* 49**,** 71-80.
94. KUO, L. J. & YANG, L. X. 2008. Gamma-H2AX - a novel biomarker for DNA double-strand breaks. *In Vivo,* 22**,** 305-9.
95. KVAM, E. & TYRRELL, R. M. 1997. Induction of oxidative DNA base damage in human skin cells by UV and near visible radiation. *Carcinogenesis,* 18**,** 2379-2384.
96. LAVIN, M. F. 2007. ATM and the Mre11 complex combine to recognize and signal DNA double-strand breaks. *Oncogene,* 26**,** 7749-58.
97. LAVKER, R. & KAIDBEY, K. 1997. The spectral dependence for UVA-induced cumulative damage in human skin. *J Invest Dermatol,* 108**,** 17-21.

98. LEE, J. H., BAE, S. H. & CHOI, B. S. 2000. The Dewar photoproduct of thymidylyl(3'-->5')- thymidine (Dewar product) exhibits mutagenic behavior in accordance with the "A rule". *Proc Natl Acad Sci U S A,* 97**,** 4591-6.
99. LI, J. & STERN, D. F. 2005. Regulation of CHK2 by DNA-dependent protein kinase. *J Biol Chem,* 280**,** 12041-50.
100. LIAO, X.-H., ZHENG, L., HE, H.-P., ZHENG, D.-L., WEI, Z.-Q., WANG, N., DONG, J., MA, W.-J. & ZHANG, T.-C. 2015. STAT3 regulated ATR via microRNA-383 to control DNA damage to affect apoptosis in A431 cells. *Cellular Signalling,* 27**,** 2285-2295.
101. LO, J. A. & FISHER, D. E. 2014. The melanoma revolution: From UV carcinogenesis to a new era in therapeutics. *Science,* 346**,** 945-949.
102. LOMAS, A., LEONARDI-BEE, J. & BATH-HEXTALL, F. 2012. A systematic review of worldwide incidence of nonmelanoma skin cancer. *British Journal of Dermatology,* 166**,** 1069-1080.
103. LORD, C. J. & ASHWORTH, A. 2012. The DNA damage response and cancer therapy. *Nature,* 481**,** 287-294.
104. LOU, Z., MINTER-DYKHOUSE, K., WU, X. & CHEN, J. 2003. MDC1 is coupled to activated CHK2 in mammalian DNA damage response pathways. *Nature,* 421**,** 957-61.
105. LU, C., ZHU, F., CHO, Y. Y., TANG, F., ZYKOVA, T., MA, W. Y., BODE, A. M. & DONG, Z. 2006. Cell apoptosis: requirement of H2AX in DNA ladder formation, but not for the activation of caspase-3. *Mol Cell,* 23**,** 121-32.
106. LUO, C., SHENG, J., HU, M. G., HALUSKA, F. G., CUI, R., XU, Z., TSICHLIS, P. N., HU, G. F. & HINDS, P. W. 2013. Loss of ARF sensitizes transgenic BRAFV600E mice to UV-induced melanoma via suppression of XPC. *Cancer Res,* 73**,** 4337-48.
107. LYNCH, H. T., FUSARO, R. M. & JOHNSON, J. A. 1984. XERODERMA PIGMENTOSUM - COMPLEMENTATION GROUP-C AND MALIGNANT-MELANOMA. *Archives of Dermatology,* 120**,** 175-179.
108. MASUTANI, C., KUSUMOTO, R., IWAI, S. & HANAOKA, F. 2000. Mechanisms of accurate translesion synthesis by human DNA polymerase η. *The EMBO Journal,* 19**,** 3100-3109.
109. MENCK, C. F. M. & MUNFORD, V. 2014. DNA repair diseases: What do they tell us about cancer and aging? *Genetics and Molecular Biology,* 37**,** 220-233.
110. MENENDEZ, D., INGA, A. & RESNICK, M. A. 2009. The expanding universe of p53 targets. *Nat Rev Cancer,* 9**,** 724-37.
111. MEYER, B., VOSS, K. O., TOBIAS, F., JAKOB, B., DURANTE, M. & TAUCHER-SCHOLZ, G. 2013. Clustered DNA damage induces pan-nuclear H2AX phosphorylation mediated by ATM and DNA-PK. *Nucleic Acids Res,* 41**,** 6109-18.
112. MIRZOEVA, O. K. & PETRINI, J. H. 2001. DNA damage-dependent nuclear dynamics of the Mre11 complex. *Mol Cell Biol,* 21**,** 281-8.
113. MITCHELL, D. L., FERNANDEZ, A. A., NAIRN, R. S., GARCIA, R., PANIKER, L., TRONO, D., THAMES, H. D. & GIMENEZ-CONTI, I. 2010. Ultraviolet A does not induce melanomas in a Xiphophorus hybrid fish model. *Proc Natl Acad Sci U S A,* 107**,** 9329-34.
114. MOTHERSILL, C. & SEYMOUR, C. B. 1998. Cell-cell contact during gamma irradiation is not required to induce a bystander effect in normal human keratinocytes: evidence for release during irradiation of a signal controlling survival into the medium. *Radiat Res,* 149**,** 256-62.
115. MOURET, S., BAUDOUIN, C., CHARVERON, M., FAVIER, A., CADET, J. & DOUKI, T. 2006a. Cyclobutane pyrimidine dimers are predominant DNA lesions in whole human skin exposed to UVA radiation. *Proceedings of the National Academy of Sciences of the United States of America,* 103**,** 13765-13770.

116. MOURET, S., BAUDOUIN, C., CHARVERON, M., FAVIER, A., CADET, J. & DOUKI, T. 2006b. Cyclobutane pyrimidine dimers are predominant DNA lesions in whole human skin exposed to UVA radiation. *Proc Natl Acad Sci U S A,* 103**,** 13765-70.
117. MOURET, S., FORESTIER, A. & DOUKI, T. 2012. The specificity of UVA-induced DNA damage in human melanocytes. *Photochemical & Photobiological Sciences,* 11**,** 155-162.
118. MOURET, S., PHILIPPE, C., GRACIA-CHANTEGREL, J., BANYASZ, A., KARPATI, S., MARKOVITSI, D. & DOUKI, T. 2010. UVA-induced cyclobutane pyrimidine dimers in DNA: a direct photochemical mechanism? *Organic & Biomolecular Chemistry,* 8**,** 1706-1711.
119. MURRAY, H. C., MALTBY, V. E., SMITH, D. W. & BOWDEN, N. A. 2016. Nucleotide excision repair deficiency in melanoma in response to UVA. *Experimental Hematolgy & Oncology,* 5**,** 11.
120. NARAYANAN, D. L., SALADI, R. N. & FOX, J. L. 2010. Ultraviolet radiation and skin cancer. *International Journal of Dermatology,* 49**,** 978-986.
121. NIKOLAOU, V., STRATIGOS, A. J. & TSAO, H. 2012. Hereditary Nonmelanoma Skin Cancer. *Seminars in cutaneous medicine and surgery,* 31**,** 204-210.
122. NILSEN, L. T. N., HANNEVIK, M. & VEIEROD, M. B. 2016. Ultraviolet exposure from indoor tanning devices: a systematic review. *British Journal of Dermatology,* 174**,** 730-740.
123. NISHIURA, H., KUMAGAI, J., KASHINO, G., OKADA, T., TANO, K. & WATANABE, M. 2012. The Bystander Effect is a Novel Mechanism of UVA-Induced Melanogenesis. *Photochemistry and Photobiology,* 88**,** 389-397.
124. NOONAN, F. P., ZAIDI, M. R., WOLNICKA-GLUBISZ, A., ANVER, M. R., BAHN, J., WIELGUS, A., CADET, J., DOUKI, T., MOURET, S., TUCKER, M. A., POPRATILOFF, A., MERLINO, G. & DE FABO, E. C. 2012. Melanoma induction by ultraviolet A but not ultraviolet B radiation requires melanin pigment. *Nat Commun,* 3**,** 884.
125. OH, K.-S., BUSTIN, M., MAZUR, S. J., APPELLA, E. & KRAEMER, K. H. 2011. UV-induced histone H2AX phosphorylation and DNA damage related proteins accumulate and persist in nucleotide excision repair-deficient XP-B cells. *DNA repair,* 10**,** 5-15.
126. OLIVIER, M., HOLLSTEIN, M. & HAINAUT, P. 2010. TP53 Mutations in Human Cancers: Origins, Consequences, and Clinical Use. *Cold Spring Harbor Perspectives in Biology,* 2**,** a001008.
127. PARSONS, W. B., JR., WATKINS, C. H., PEASE, G. L. & CHILDS, D. S., JR. 1954. Changes in sternal marrow following roentgen-ray therapy to the spleen in chronic granulocytic leukemia. *Cancer,* 7**,** 179-89.
128. PATTON, E. E., WIDLUND, H. R., KUTOK, J. L., KOPANI, K. R., AMATRUDA, J. F., MURPHEY, R. D., BERGHMANS, S., MAYHALL, E. A., TRAVER, D., FLETCHER, C. D., ASTER, J. C., GRANTER, S. R., LOOK, A. T., LEE, C., FISHER, D. E. & ZON, L. I. 2005. BRAF mutations are sufficient to promote nevi formation and cooperate with p53 in the genesis of melanoma. *Curr Biol,* 15**,** 249-54.
129. PEDERSEN, M., VIROS, A., COOK, M. & MARAIS, R. 2014. (G12D) NRAS and kinase-dead BRAF cooperate to drive naevogenesis and melanomagenesis. *Pigment Cell Melanoma Res,* 27**,** 1162-6.
130. PLEASANCE, E. D., CHEETHAM, R. K., STEPHENS, P. J., MCBRIDE, D. J., HUMPHRAY, S. J., GREENMAN, C. D., VARELA, I., LIN, M. L., ORDONEZ, G. R., BIGNELL, G. R., YE, K., ALIPAZ, J., BAUER, M. J., BEARE, D., BUTLER, A., CARTER, R. J., CHEN, L. N., COX, A. J., EDKINS, S., KOKKO-GONZALES, P. I., GORMLEY, N. A., GROCOCK, R. J., HAUDENSCHILD, C. D., HIMS, M. M., JAMES, T., JIA, M. M., KINGSBURY, Z., LEROY, C., MARSHALL, J., MENZIES, A., MUDIE, L. J., NING, Z. M., ROYCE, T., SCHULZ-TRIEGLAFF, O. B., SPIRIDOU, A., STEBBINGS, L. A., SZAJKOWSKI, L., TEAGUE, J., WILLIAMSON, D.,

CHIN, L., ROSS, M. T., CAMPBELL, P. J., BENTLEY, D. R., FUTREAL, P. A. & STRATTON, M. R. 2010. A comprehensive catalogue of somatic mutations from a human cancer genome. *Nature,* 463**,** 191-U73.

131. POLO, S. E. & JACKSON, S. P. 2011. Dynamics of DNA damage response proteins at DNA breaks: a focus on protein modifications. *Genes Dev,* 25**,** 409-33.
132. POTHOF, J., VERKAIK, N. S., VAN, I. W., WIEMER, E. A., TA, V. T., VAN DER HORST, G. T., JASPERS, N. G., VAN GENT, D. C., HOEIJMAKERS, J. H. & PERSENGIEV, S. P. 2009. MicroRNA-mediated gene silencing modulates the UV-induced DNA-damage response. *Embo j,* 28**,** 2090-9.
133. PREMI, S., WALLISCH, S., MANO, C. M., WEINER, A. B., BACCHIOCCHI, A., WAKAMATSU, K., BECHARA, E. J., HALABAN, R., DOUKI, T. & BRASH, D. E. 2015. Photochemistry. Chemiexcitation of melanin derivatives induces DNA photoproducts long after UV exposure. *Science,* 347**,** 842-7.
134. PRIOR, I. A., LEWIS, P. D. & MATTOS, C. 2012. A comprehensive survey of Ras mutations in cancer. *Cancer Res,* 72**,** 2457-67.
135. PRISE, K. M., FOLKARD, M. & MICHAEL, B. D. 2003. Bystander responses induced by low LET radiation. *Oncogene,* 22**,** 7043-7049.
136. RADY, P., SCINICARIELLO, F., WAGNER, R. F., JR. & TYRING, S. K. 1992. p53 mutations in basal cell carcinomas. *Cancer Res,* 52**,** 3804-6.
137. RAPP, A. & GREULICH, K. O. 2004. After double-strand break induction by UV-A, homologous recombination and nonhomologous end joining cooperate at the same DSB if both systems are available. *J Cell Sci,* 117**,** 4935-45.
138. RAVANAT, J. L., DI MASCIO, P., MARTINEZ, G. R. & MEDEIROS, M. H. 2001a. Singlet oxygen induces oxidation of cellular DNA. *J Biol Chem,* 276**,** 40601-4.
139. RAVANAT, J. L., DOUKI, T. & CADET, J. 2001b. Direct and indirect effects of UV radiation on DNA and its components. *Journal of Photochemistry and Photobiology B-Biology,* 63**,** 88-102.
140. RAY, A., BLEVINS, C., WANI, G. & WANI, A. A. 2016. ATR- and ATM-Mediated DNA Damage Response Is Dependent on Excision Repair Assembly during G1 but Not in S Phase of Cell Cycle. *PLoS One,* 11**,** e0159344.
141. REAPER, P. M., GRIFFITHS, M. R., LONG, J. M., CHARRIER, J. D., MACCORMICK, S., CHARLTON, P. A., GOLEC, J. M. & POLLARD, J. R. 2011. Selective killing of ATM- or p53-deficient cancer cells through inhibition of ATR. *Nat Chem Biol,* 7**,** 428-30.
142. REDMOND, R. W., RAJADURAI, A., UDAYAKUMAR, D., SVIDERSKAYA, E. V. & TSAO, H. 2014. Melanocytes are selectively vulnerable to UVA-mediated bystander oxidative signaling. *J Invest Dermatol,* 134**,** 1083-90.
143. REVET, I., FEENEY, L., BRUGUERA, S., WILSON, W., DONG, T. K., OH, D. H., DANKORT, D. & CLEAVER, J. E. 2011. Functional relevance of the histone gammaH2Ax in the response to DNA damaging agents. *Proc Natl Acad Sci U S A,* 108**,** 8663-7.
144. RIABINSKA, A., DAHEIM, M., HERTER-SPRIE, G. S., WINKLER, J., FRITZ, C., HALLEK, M., THOMAS, R. K., KREUZER, K. A., FRENZEL, L. P., MONFARED, P., MARTINS-BOUCAS, J., CHEN, S. & REINHARDT, H. C. 2013. Therapeutic targeting of a robust non-oncogene addiction to PRKDC in ATM-defective tumors. *Sci Transl Med,* 5**,** 189ra78.
145. RIZZO, J. L., DUNN, J., REES, A. & RUNGER, T. M. 2011. No formation of DNA double-strand breaks and no activation of recombination repair with UVA. *J Invest Dermatol,* 131**,** 1139-48.
146. ROBERT, C., MUEL, B., BENOIT, A., DUBERTRET, L., SARASIN, A. & STARY, A. 1996. Cell survival and shuttle vector mutagenesis induced by ultraviolet A and ultraviolet B radiation in a human cell line. *J Invest Dermatol,* 106**,** 721-8.
147. ROCHETTE, P. J., THERRIEN, J. P., DROUIN, R., PERDIZ, D., BASTIEN, N., DROBETSKY, E. A. & SAGE, E. 2003. UVA-induced cyclobutane pyrimidine dimers form

predominantly at thymine-thymine dipyrimidines and correlate with the mutation spectrum in rodent cells. *Nucleic Acids Research,* 31**,** 2786-2794.
148. ROEHM, N. W., RODGERS, G. H., HATFIELD, S. M. & GLASEBROOK, A. L. 1991. An improved colorimetric assay for cell proliferation and viability utilizing the tetrazolium salt XTT. *J Immunol Methods,* 142**,** 257-65.
149. ROGAKOU, E. P., BOON, C., REDON, C. & BONNER, W. M. 1999. Megabase chromatin domains involved in DNA double-strand breaks in vivo. *J Cell Biol,* 146**,** 905-16.
150. ROSEN, J. E., PRAHALAD, A. K. & WILLIAMS, G. M. 1996. 8-Oxodeoxyguanosine formation in the DNA of cultured cells after exposure to H2O2 alone or with UVB or UVA irradiation. *Photochem Photobiol,* 64**,** 117-22.
151. RUNGER, T. M., FARAHVASH, B., HATVANI, Z. & REES, A. 2012. Comparison of DNA damage responses following equimutagenic doses of UVA and UVB: A less effective cell cycle arrest with UVA may render UVA-induced pyrimidine dimers more mutagenic than UVB-induced ones. *Photochemical & Photobiological Sciences,* 11**,** 207-215.
152. RUNGER, T. M. & KAPPES, U. P. 2008. Mechanisms of mutation formation with long-wave ultraviolet light (UVA). *Photodermatology Photoimmunology & Photomedicine,* 24**,** 2-10.
153. RYAN, K. M., PHILLIPS, A. C. & VOUSDEN, K. H. 2001. Regulation and function of the p53 tumor suppressor protein. *Curr Opin Cell Biol,* 13**,** 332-7.
154. RZESZOWSKA-WOLNY, J., PRZYBYSZEWSKI, W. M. & WIDEL, M. 2009. Ionizing radiation-induced bystander effects, potential targets for modulation of radiotherapy. *European Journal of Pharmacology,* 625**,** 156-164.
155. SADIKOVIC, B., AL-ROMAIH, K., SQUIRE, J. A. & ZIELENSKA, M. 2008. Cause and consequences of genetic and epigenetic alterations in human cancer. *Current Genomics,* 9, 394-408.
156. SAGE, E., LAMOLET, B., BRULAY, E., MOUSTACCHI, E., CHTEAUNEUF, A. & DROBETSKY, E. A. 1996. Mutagenic specificity of solar UV light in nucleotide excision repair-deficient rodent cells. *Proceedings of the National Academy of Sciences of the United States of America,* 93**,** 176-180.
157. SATOKATA, I., TANAKA, K., MIURA, N., NARITA, M., MIMAKI, T., SATOH, Y., KONDO, S. & OKADA, Y. 1992. Three nonsense mutations responsible for group A xeroderma pigmentosum. *Mutat Res,* 273**,** 193-202.
158. SCARPATO, R., CASTAGNA, S., ALIOTTA, R., AZZARA, A., GHETTI, F., FILOMENI, E., GIOVANNINI, C., PIRILLO, C., TESTI, S., LOMBARDI, S. & TOMEI, A. 2013. Kinetics of nuclear phosphorylation (gamma-H2AX) in human lymphocytes treated in vitro with UVB, bleomycin and mitomycin C. *Mutagenesis,* 28**,** 465-73.
159. SCHREIER, W. J., SCHRADER, T. E., KOLLER, F. O., GILCH, P., CRESPO-HERNANDEZ, C. E., SWAMINATHAN, V. N., CARELL, T., ZINTH, W. & KOHLER, B. 2007. Thymine dimerization in DNA is an ultrafast photoreaction. *Science,* 315**,** 625-9.
160. SETLOW, R. B. 1974. The Wavelengths in Sunlight Effective in Producing Skin Cancer: A Theoretical Analysis. *Proceedings of the National Academy of Sciences of the United States of America,* 71**,** 3363-3366.
161. SETLOW, R. B., GRIST, E., THOMPSON, K. & WOODHEAD, A. D. 1993. Wavelengths effective in induction of malignant melanoma. *Proc Natl Acad Sci U S A,* 90**,** 6666-70.
162. SHARPLESS, E. & CHIN, L. 2003. The INK4a/ARF locus and melanoma. *Oncogene,* 22**,** 3092-8.
163. SHEU, C., KANG, P., KHAN, S. & FOOTE, C. S. 2002. Low-temperature photosensitized oxidation of a guanosine derivative and formation of an imidazole ring-opened product. *J Am Chem Soc,* 124**,** 3905-13.

164. SHORROCKS, J., PAUL, N. D. & MCMILLAN, T. J. 2008. The dose rate of UVA treatment influences the cellular response of HaCaT keratinocytes. *Journal of Investigative Dermatology,* 128**,** 685-693.
165. SHRIVASTAV, M., DE HARO, L. P. & NICKOLOFF, J. A. 2008. Regulation of DNA double-strand break repair pathway choice. *Cell Research,* 18**,** 134-147.
166. SINHA, R. P. & HADER, D. P. 2002. UV-induced DNA damage and repair: a review. *Photochemical & Photobiological Sciences,* 1**,** 225-236.
167. Steel, H.L. 2016. Characterisation of the cellular response to ultraviolet radiation, with a particular focus on the DNA damage response (PhD thesis), Lancaster University
168. STEENKEN, S. & JOVANOVIC, S. V. 1997. How Easily Oxidizable Is DNA? One-Electron Reduction Potentials of Adenosine and Guanosine Radicals in Aqueous Solution. *Journal of the American Chemical Society,* 119**,** 617-618.
169. STIXOVA, L., HRUSKOVA, T., SEHNALOVA, P., LEGARTOVA, S., SVIDENSKA, S., KOZUBEK, S. & BARTOVA, B. 2014. Advanced Microscopy Techniques Used for Comparison of UVA- and gamma-Irradiation-Induced DNA Damage in the Cell Nucleus and Nucleolus. *Folia Biologica,* 60**,** 76-84.
170. STOYANOVA, T., ROY, N., KOPANJA, D., BAGCHI, S. & RAYCHAUDHURI, P. 2009. DDB2 decides cell fate following DNA damage. *Proc Natl Acad Sci U S A,* 106**,** 10690-5.
171. SULLI, G., DI MICCO, R. & DI FAGAGNA, F. D. A. 2012. Crosstalk between chromatin state and DNA damage response in cellular senescence and cancer. *Nat Rev Cancer,* 12**,** 709-720.
172. SUTHERLAND, B. M., HARBER, L. C. & KOCHEVAR, I. E. 1980. Pyrimidine dimer formation and repair in human skin. *Cancer Res,* 40**,** 3181-5.
173. SUTHERLAND, J. C. & GRIFFIN, K. P. 1981. Absorption spectrum of DNA for wavelengths greater than 300 nm. *Radiat Res,* 86**,** 399-409.
174. SVOBODOVÁ, A. R., GALANDÁKOVÁ, A., ŠIANSKÁ, J., DOLEŽAL, D., LICHNOVSKÁ, R., ULRICHOVÁ, J. & VOSTÁLOVÁ, J. 2012. DNA damage after acute exposure of mice skin to physiological doses of UVB and UVA light. *Archives of Dermatological Research,* 304**,** 407-412.
175. SWOPE, V., ALEXANDER, C., STARNER, R., SCHWEMBERGER, S., BABCOCK, G. & ABDEL-MALEK, Z. A. 2014. Significance of the melanocortin 1 receptor in the DNA damage response of human melanocytes to ultraviolet radiation. *Pigment Cell Melanoma Res,* 27**,** 601-10.
176. SYED, D. N., AFAQ, F. & MUKHTAR, H. 2012. Differential Activation of Signaling Pathways by UVA and UVB Radiation in Normal Human Epidermal Keratinocytes. *Photochemistry and photobiology,* 88**,** 1184-1190.
177. TAKEUCHI, S., ZHANG, W., WAKAMATSU, K., ITO, S., HEARING, V. J., KRAEMER, K. H. & BRASH, D. E. 2004. Melanin acts as a potent UVB photosensitizer to cause an atypical mode of cell death in murine skin. *Proceedings of the National Academy of Sciences of the United States of America,* 101**,** 15076-15081.
178. TEWARI, A., GRAGE, M. M. L., HARRISON, G. I., SARKANY, R. & YOUNG, A. R. 2013. UVA1 is skin deep: molecular and clinical implications. *Photochemical & Photobiological Sciences,* 12**,** 95-103.
179. TEWARI, A., SARKANY, R. P. & YOUNG, A. R. 2012. UVA1 Induces Cyclobutane Pyrimidine Dimers but Not 6-4 Photoproducts in Human Skin In Vivo. *Journal of Investigative Dermatology,* 132**,** 394-400.
180. THOMAS, N. E., ALEXANDER, A., EDMISTON, S. N., PARRISH, E., MILLIKAN, R. C., BERWICK, M., GROBEN, P., OLLILA, D. W., MATTINGLY, D. & CONWAY, K. 2004. Tandem BRAF mutations in primary invasive melanomas. *J Invest Dermatol,* 122**,** 1245-50.

181. TIERNEY, P., DE GRUIJL, F. R., IBBOTSON, S. & MOSELEY, H. 2015. Predicted increased risk of squamous cell carcinoma induction associated with sunbed exposure habits. *British Journal of Dermatology,* 173**,** 201-208.
182. TIERNEY, P., FERGUSON, J., IBBOTSON, S., DAWE, R., EADIE, E. & MOSELEY, H. 2013. Nine out of 10 sunbeds in England emit ultraviolet radiation levels that exceed current safety limits. *Br J Dermatol,* 168**,** 602-8.
183. TORNALETTI, S. & PFEIFER, G. P. 1995. Complete and tissue-independent methylation of CpG sites in the p53 gene: implications for mutations in human cancers. *Oncogene,* 10**,** 1493-9.
184. TOYOOKA, T., ISHIHAMA, M. & IBUKI, Y. 2011. Phosphorylation of histone H2AX is a powerful tool for detecting chemical photogenotoxicity. *J Invest Dermatol,* 131**,** 1313-21.
185. TYRRELL, R. M. 1973. Induction of pyrimidine dimers in bacterial DNA by 365 nm radiation. *Photochem Photobiol,* 17**,** 69-73.
186. VAN DEN BOSCH, M., BREE, R. T. & LOWNDES, N. F. 2003. The MRN complex: coordinating and mediating the response to broken chromosomes. *EMBO Rep,* 4**,** 844-9.
187. VIROS, A., SANCHEZ-LAORDEN, B., PEDERSEN, M., FURNEY, S. J., RAE, J., HOGAN, K., EJIAMA, S., GIROTTI, M. R., COOK, M., DHOMEN, N. & MARAIS, R. 2014. Ultraviolet radiation accelerates BRAF-driven melanomagenesis by targeting TP53. *Nature,* 511**,** 478-82.
188. WANG, H.-T., CHOI, B. & TANG, M.-S. 2010. Melanocytes are deficient in repair of oxidative DNA damage and UV-induced photoproducts. *Proceedings of the National Academy of Sciences of the United States of America,* 107**,** 12180-12185.
189. WANG, X. Q., REDPATH, J. L., FAN, S. T. & STANBRIDGE, E. J. 2006. ATR dependent activation of Chk2. *J Cell Physiol,* 208**,** 613-9.
190. WATERS, L. S., MINESINGER, B. K., WILTROUT, M. E., D'SOUZA, S., WOODRUFF, R. V. & WALKER, G. C. 2009. Eukaryotic Translesion Polymerases and Their Roles and Regulation in DNA Damage Tolerance. *Microbiology and Molecular Biology Reviews : MMBR,* 73**,** 134-154.
191. Wehner, M. R., Chren, M. M., Nameth, D., Choudhry, A., Gaskins, M., Nead, K. T., Boscardin, W. J. & Linos, E. 2014. International prevalence of indoor tanning: a systematic review and meta-analysis. *JAMA dermatology*, 150, 390-400.
192. WHITESIDE, J. R., ALLINSON, S. L. & MCMILLAN, T. J. 2011. Timeframes of UVA-induced Bystander Effects in Human Keratinocytes. *Photochemistry and Photobiology,* 87**,** 435-440.
193. WHITESIDE, J. R. & MCMILLAN, T. J. 2009. A Bystander Effect is Induced in Human Cells Treated with UVA Radiation but Not UVB Radiation. *Radiation Research,* 171**,** 204-211.
194. WHO | Climate change and human health - risks and responses. Summary. http://www.who.int/globalchange/summary/en/index7.html
195. WHO | Sunbeds http://www.who.int/uv/faq/sunbeds/en/
196. WIDEL, M., KRZYWON, A., GAJDA, K., SKONIECZNA, M. & RZESZOWSKA-WOLNY, J. 2014. Induction of bystander effects by UVA, UVB, and UVC radiation in human fibroblasts and the implication of reactive oxygen species. *Free Radical Biology and Medicine,* 68**,** 278-287.
197. WISCHERMANN, K., POPP, S., MOSHIR, S., SCHARFETTER-KOCHANEK, K., WLASCHEK, M., DE GRUIJL, F., HARTSCHUH, W., GREINERT, R., VOLKMER, B., FAUST, A., RAPP, A., SCHMEZER, P. & BOUKAMP, P. 2008. UVA radiation causes DNA strand breaks,

chromosomal aberrations and tumorigenic transformation in HaCaT skin keratinocytes. *Oncogene,* 27**,** 4269-80.
198. WITKOP, C. J. 1989. Albinism. *Clinics in Dermatology,* 7**,** 80-91.
199. WONDRAK, G. T., JACOBSON, M. K. & JACOBSON, E. L. 2006. Endogenous UVA-photosensitizers: mediators of skin photodamage and novel targets for skin photoprotection. *Photochemical & Photobiological Sciences,* 5**,** 215-237.
200. WONDRAK, G. T., ROBERTS, M. J., CERVANTES-LAUREAN, D., JACOBSON, M. K. & JACOBSON, E. L. 2003. Proteins of the extracellular matrix are sensitizers of photo-oxidative stress in human skin cells. *J Invest Dermatol,* 121**,** 578-86.
201. YANG, G., CURLEY, D., BOSENBERG, M. W. & TSAO, H. 2007. Loss of Xeroderma pigmentosum C (Xpc) enhances melanoma photocarcinogenesis in Ink4a-Arf-deficient mice. *Cancer Research,* 67**,** 5649-5657.
202. YASUI, M., KANEMARU, Y., KAMOSHITA, N., SUZUKI, T., ARAKAWA, T. & HONMA, M. 2014. Tracing the fates of site-specifically introduced DNA adducts in the human genome. *DNA Repair (Amst),* 15**,** 11-20.
203. YOU, Y. H., LEE, D. H., YOON, J. H., NAKAJIMA, S., YASUI, A. & PFEIFER, G. P. 2001. Cyclobutane pyrimidine dimers are responsible for the vast majority of mutations induced by UVB irradiation in mammalian cells. *J Biol Chem,* 276**,** 44688-94.
204. ZANNINI, L., DELIA, D. & BUSCEMI, G. 2014. CHK2 kinase in the DNA damage response and beyond. *Journal of Molecular Cell Biology,* 6**,** 442-457.
205. ZHANG, Y., MA, W. Y., KAJI, A., BODE, A. M. & DONG, Z. 2002. Requirement of ATM in UVA-induced signaling and apoptosis. *J Biol Chem,* 277**,** 3124-31.